

**Plant wax alkanes and alkan-1-ols in ocean
sediments as indicators of continental climate
change – validation of a molecular proxy**

**Wachsalkane und -alkohole in Ozeansedimenten als
Indikatoren kontinentaler Klimaveränderungen –
Validierung eines molekularen Parameters**

Der

Fakultät für Mathematik und Naturwissenschaften

der

Carl von Ossietzky Universität Oldenburg

zur Erlangung des Grades und Titels eines

Doktors der Naturwissenschaften

- Dr. rer. nat. -

angenommene

Dissertation

von

Frau Angela Vogts

geboren am 22. März 1978 in Westerstede

Gutachter: Prof. Dr. Jürgen Rullkötter
Zweitgutachter: Prof. Geoffrey Eglinton, FRS

Eingereicht am: 15.02.2011

Tag der Disputation: 28.03.2011

Parts of this thesis were presented at meetings and conferences:

(oral and poster presentations; presenter underlined)

Vogts, A., Moossen, H., Rommerskirchen, F., and Rullkötter, J., 2007.
Long-chain *n*-alkanes and *n*-alcohols as palaeo-environmental proxies in tropical Africa. 4th North German Organic Geochemistry Meeting, MARUM, Research Center Ocean Margins (RCOM), Bremen, Germany, oral presentation.

Vogts, A., Moossen, H., Rommerskirchen, F., and Rullkötter, J., 2007.
Molecular $\delta^{13}\text{C}$ values of leaf wax components from plants growing in different tropical habitats. 17th Goldschmidt Conference, Cologne, Germany, poster presentation.

Vogts, A., Moossen, H., Rommerskirchen, F., and Rullkötter, J., 2007.
Molecular isotopic composition and distribution patterns of long-chain *n*-alkanes and *n*-alcohols growing in different tropical habitats. 23rd International Meeting on Organic Geochemistry (IMOG), Torquay, United Kingdom, poster presentation.

Vogts, A., Moossen, H., Rommerskirchen, F., and Rullkötter, J., 2007.
Molecular isotopic composition and distribution patterns of long-chain *n*-alkanes and *n*-alcohols growing in different tropical habitats. International Conference and 97th Annual Meeting of the Geologische Vereinigung e.V., Bremen, Germany, poster presentation, (3rd place award for student poster presentation).

Vogts, A., Moossen, H., Rommerskirchen, F., and Rullkötter, J., 2008.
Characteristics of wax lipids from tropical and subtropical plants and their use in palaeoclimatic studies. Werkbesprekingen Leerstoelgroep Biosystematiek, Wageningen University, The Netherlands, oral presentation.

Vogts, A. and Rullkötter, J., 2009.
Palaeoenvironmental changes in Southwest Africa revealed by organic geochemical analysis of a sediment core recovered off Angola. 24th International Meeting on Organic Geochemistry (IMOG), Bremen, Germany, oral presentation.

Eglinton, G. and Vogts, A., 2010.
Biomolecular Palaeobotany - Molecular records of continental vegetation in the Quaternary. Third International Paleontological Congress, London, United Kingdom, plenary lecture.

Badewien, T., Schefuß, E., Vogts, A. and Rullkötter, J., 2010.

Rain forest and savanna: What marine sediments tell about African vegetation. Jahrestagung der Afrikagruppe deutscher Geowissenschaftler (AdG), Frankfurt, Germany, oral presentation.

Badewien, T., Schefuß, E., Vogts, A. and Rullkötter, J., 2010.

Leaf wax components in recent sediments from the SW-African continental slope: Conclusions about terrestrial vegetation. 6th North German Organic Geochemistry Meeting, Hamburg, Germany, oral presentation.

The following parts of this thesis have been published, submitted or prepared for publication:

Chapter 2

Vogts, A., Moossen, H., Rommerskirchen, F., and Rullkötter, J., 2009.
Distribution patterns and stable carbon isotopic composition of alkanes and alkan-1-ols from plant waxes of African rain forest and savanna C₃ species. *Organic Geochemistry* 40, 1037-1054,
doi:10.1016/j.orggeochem.2009.07.011.

Chapter 3

Vogts, A., Schefuß, E., Badewien, T., and Rullkötter, J., 2010.
n-Alkane parameters derived from a deep-sea sediment transect off southwest Africa reflect continental vegetation and climate conditions. *Organic Geochemistry*, submitted.

Chapter 4

Vogts, A., Schefuß, E., Badewien, T., and Rullkötter, J.
Stable hydrogen isotopic compositions of land plant-derived *n*-alkanes in marine sediments reflect δD values of continental precipitation. Prepared for submission to *Geochimica et Cosmochimica Acta*.

Abstract

This study validates the significance of long-chain *n*-alkanes and *n*-alkan-1-ols as proxies for the contribution of terrestrial plant material to geological archives. It focuses on the distribution patterns as well as the molecular stable carbon and hydrogen isotope signatures of these plant wax biomarkers and corroborates and expands their potential as proxies for changes of terrestrial vegetation, climate, and hydrology. The study area selected for this approach is southwest Africa due to the climate-sensitive latitudinal pattern of its vegetation zones and the abundance of plants employing different metabolic pathways (C_3/C_4).

In the first part of the thesis analytical results for long-chain leaf wax lipids of 69 C_3 plants from rain forest and savanna regions in Africa are presented with respect to their growth form (herb, shrub, liana, and tree). Similarities among the biomarker characteristics of plants with different growth forms were found but significant differences of wax biomarkers in plants from rain forest and savanna species occurred. Averaged distribution patterns of these biomes were provided and are assumed to be representative for the plants of these vegetation zones. Comparison with published data for tropical C_4 grasses dominating arid grasslands revealed trends to longer chain lengths and less negative stable carbon isotope ratios for *n*-alkanes from rain forest over savanna to grassland. For *n*-alkan-1-ols the same trend for stable carbon isotope composition is evident but chain length characteristics of these biomarkers did not reveal a clear trend: Averaged chain length distributions for rain forest species and tropical grasses are similar whereas the homologues synthesised by savanna plants are shorter.

The other two parts of this study elucidated how present-day continental conditions are mirrored by *n*-alkane characteristics of ocean-margin surface sediments constituting an isobathic transect from 1°N to 28°S off southwest Africa. Near the equator, chain length distribution as well as carbon isotope composition indicated a high contribution of C_3 plants from the rain forest on the adjacent continent. But especially at sampling locations not dominated by fluvial organic material a significant contribution of C_4 plant material, possibly transported by winds over large distances, was evident. The contribution of

savanna species and C₄ plants increased towards the south and is reflected by longer-chain *n*-alkanes with less negative stable carbon isotope compositions. Based on these analytical results calculations of C₄ plant contribution were performed and the values obtained correlated with the vegetation composition in postulated catchment areas. Furthermore, the C₄ plant contribution correlated with precipitation and aridity indices in these regions. Based on these potential catchment areas it was also evaluated how the hydrogen isotope composition of sedimentary *n*-alkanes reflects the δD ratios of precipitation. A good correlation was observed even though there are huge differences in environmental conditions and vegetation composition in the course of the transect. The apparent fractionation between the hydrogen isotope compositions of sedimentary *n*-alkanes and those of precipitation was fairly constant.

The results of this study substantiate the potential of long-chain plant wax *n*-alkanes and *n*-alkan-1-ols as proxies for the contribution of different terrestrial biomes to ocean margin sediments. Furthermore, the study presents correlations of *n*-alkanes characteristics with climatic conditions like precipitation and its hydrogen isotopic composition as well as aridity indices. The proxies, thus, may be a tool for forthcoming palaeo-environmental studies to unravel ancient climatic variations.

Kurzfassung

Die vorliegende Arbeit validiert die Aussagekraft von langkettigen *n*-Alkanen und *n*-Alkan-1-olen als Indikatoren für den Eintrag terrestrischen Pflanzenmaterials in geologische Archive. Schwerpunkt der Studie war die Analyse der Verteilungsmuster sowie der molekularen stabilen Kohlenstoff- und Wasserstoffisotopenzusammensetzungen dieser aus Pflanzenblattwachsen stammenden Biomarker. Ihr Potential zum Nachweis von Veränderungen der Vegetationszusammensetzung sowie klimatischer und hydrologischer Bedingungen wurde analysiert. Als Studiengebiet wurde Südwafrika gewählt, da dort ausgedehnte Breitengradparallele Vegetationszonen vorherrschen, deren Größe klimaabhängig ist und in denen Pflanzen vorkommen, die unterschiedliche Photosynthesemechanismen nutzen (C₃/C₄).

Im ersten Teil der Arbeit werden Analyseergebnisse für langkettige Blattwachsbestandteile von 69 C₃-Pflanzen aus Regenwald- und Savannen gebieten vorgestellt. Es zeigte sich kein Zusammenhang zwischen Biomarkercharakteristika und Wuchsform (Kraut, Busch, Liane oder Baum), während zwischen Regenwald- und Savannenspezies deutliche Unterschiede festgestellt wurden. Daher wurden gemittelte Verteilungsmuster für diese Vegetationszonen erstellt und mit bereits publizierten Daten von C₄-Gräsern verglichen, da diese Pflanzen die Graslandschaften arider Gebiete dominieren. Von Regenwald- über Savannenpflanzen bis hin zu den Gräsern wurden Trends zu längerkettigen *n*-Alkanen mit einer weniger negativen Kohlenstoffisotopenzusammensetzung gefunden. Die $\delta^{13}\text{C}$ -Werte der *n*-Alkanole zeigten den gleichen Trend, die Kettenlängenverteilung dieser Komponenten wich jedoch ab: Die gemittelte Kettenlängenverteilung der Regenwaldspezies und der Gräser war ähnlich, während die Savannenpflanzen kürzerkettige Homologe synthetisierten.

Die weiteren zwei Teile dieser Arbeit analysieren, wie die heutigen kontinentalen Bedingungen durch die Charakteristika der *n*-Alkane in Ozeanrandsedimenten widergespiegelt werden. Die Sedimente bilden einen isobathischen Transekt, der sich entlang Südwafrika von 1°N bis 28°S erstreckt. Auf Höhe des Äquators zeigten Kettenlängenverteilung und Kohlenstoffisotopenzusammensetzungen der *n*-Alkane einen hohen Eintrag von

C₃-Pflanzen des Regenwaldes an. Allerdings wiesen Lokationen, die nicht durch fluviatilen Eintrag dominiert wurden, einen stärkeren Eintrag von C₄-Material auf, was vermutlich auf äolischen Eintrag aus anderen Regionen zurückzuführen ist. Nach Süden hin steigt der Eintrag von C₄-Pflanzen an, was sich in längeren Ketten und einer weniger negativen Kohlenstoffisotopenzusammensetzung der Alkane widerspiegelt. Anhand der Kettenlängenparameter und $\delta^{13}\text{C}$ Werte wurden Berechnungen für den Eintrag von C₄-Pflanzen in die Sedimente durchgeführt, deren Ergebnisse mit der Vegetationszusammensetzung in postulierten Einzugsgebieten übereinstimmten. Zudem korrelierte der C₄-Pflanzeneintrag mit der Niederschlagsmenge und den Ariditätsindizes für diese Regionen. Die postulierten Einzugsgebiete waren weiterhin die Grundlage für die Untersuchung der Frage, in wieweit die Wasserstoffisotopenzusammensetzung des kontinentalen Niederschlages durch die δD Werte der sedimentierten *n*-Alkane widergespiegelt wird. Es zeigte sich eine gute Korrelation zwischen diesen Werten, obwohl die im Studiengebiet herrschenden klimatischen Bedingungen sowie die Vegetationszusammensetzung stark variieren. Dabei war die isotopische Fraktionierung zwischen der Wasserstoffisotopenzusammensetzung des kontinentalen Niederschlages und den δD -Werten der sedimentierten *n*-Alkane nahezu konstant.

Die Ergebnisse dieser Studie konkretisieren das Potential der langkettigen, aus Pflanzenwachsen stammenden *n*-Alkane und *n*-Alkan-1-ole als Indikatoren für den Eintrag verschiedener terrestrischer Pflanzengemeinschaften in Ozeansedimente. Darüber hinaus etabliert diese Studie Korrelationen der *n*-Alkancharakteristika mit der Niederschlagsmenge, der Aridität und der Wasserstoffisotopenzusammensetzung des Niederschlages. Diese Korrelationen könnten in zukünftigen Paläoumweltstudien genutzt werden, um von den *n*-Alkancharakteristika auf historische klimatische Variationen zu schließen.

Contents

Abstract	i
Kurzfassung (Abstract in German)	iii
Contents	v
Figure captions	viii
Table legends	x
Abbreviations	xii
1. Introduction	1
1.1 Scope and framework	1
1.2 General aspects of the African continent	2
1.3 Photosynthetic pathways	3
1.3.1 C ₃ photosynthetic pathway	4
1.3.2 Crassulacean Acid Metabolism	5
1.3.3 C ₄ photosynthetic pathway	6
1.4 Factors controlling the abundance of plants utilising C ₃ and C ₄ metabolisms	9
1.5 Stable isotope composition of biomarkers	11
1.5.1 Stable carbon isotope composition	12
1.5.2 Stable hydrogen isotope composition	17
1.6 Motivation and objectives of this project	21
1.7 Outline of the author's contribution	22
2. Distribution patterns and stable carbon isotopic composition of alkanes and alkan-1-ols from plant waxes of African rain forest and savanna C ₃ species	26
2.1 Abstract	26
2.2 Introduction	27
2.3 Sampling area, sampling and methods	29
2.3.1 Sampling area: Distribution of vegetation zones in Africa	29
2.3.2 Sample material	30
2.3.3 Analytical methods	34
2.4 Results	36
2.4.1 Content and carbon number distribution of long chain <i>n</i> -alkanes	36
2.4.2 Content and carbon number distribution of long chain <i>n</i> -alkan-1-ols	41
2.4.3 Stable carbon isotopic composition of plant material and individual lipids	45

2.5 Discussion	49
2.5.1 Contents and distribution patterns of <i>n</i> -alkanes and <i>n</i> -alkan-1-ols	49
2.5.2 Bulk and molecular isotopic composition	53
2.5.3 Leaf wax <i>n</i> -alkanes and <i>n</i> -alkan-1-ols as proxies for vegetation type	55
2.6 Conclusions	59
3. <i>n</i> -Alkane parameters derived from a deep-sea sediment transect off southwest Africa reflect continental vegetation and climate conditions	62
3.1 Abstract	62
3.2 Introduction	63
3.3 Material and methods	65
3.3.1 Sediment material	65
3.3.2 Analytical methods	67
3.4 Regional setting	69
3.4.1 Environmental conditions in southwest Africa	69
3.4.2 Vegetation in southwest Africa	69
3.4.3 Transport pathways for plant lipids	70
3.5 Results and Discussion	71
3.5.1 <i>n</i> -Alkane abundance	71
3.5.2 <i>n</i> -Alkane carbon stable isotope composition	76
3.6 Reconstructing C ₄ plant contribution	79
3.6.1 Calculations based on $\delta^{13}\text{C}$ values	79
3.6.2 Calculations based on ACL	80
3.6.3 Discussion of the calculated C ₄ plant contribution	81
3.6.4 Influence of environmental factors on C ₄ plant abundance	85
3.7 Conclusions	87
4. Stable hydrogen isotopic compositions of land plant-derived <i>n</i> -alkanes in marine sediments reflect δD values of continental precipitation	88
4.1 Abstract	88
4.2 Introduction	89
4.3 Material and Methods	90
4.3.1 Sediment material	90
4.3.2 Analytical methods	91
4.4 Regional setting	93
4.4.1 Hydrological conditions in southwest Africa	93
4.4.2 Vegetation of southwest Africa	94
4.4.3 Transport pathways and catchment areas for plant wax lipids	95

4.5 Results and discussion	96
4.5.1 Hydrogen isotope composition of <i>n</i> -alkanes	96
4.5.2 Correlation with the δD signal of precipitation	97
4.5.3 Apparent fractionation	101
4.5.4 Implications for palaeo-climatic studies	105
4.6 Conclusions	106
5. Summary and perspectives	107
6. References	111
7. Appendix	I
Danksagung (Acknowledgements in German)	
Lebenslauf (Curriculum vitae in German)	

Figure captions

(Abbreviated)

Fig. 1.1	Classification of African climate zones.	2
Fig. 1.2	Simplified scheme of the Calvin-Benson-Bassham Cycle (C ₃ photosynthesis) and the Crassulacean Acid Metabolism (CAM).	4
Fig. 1.3	Simplified pathways of the three variations of the Hatch-Slack Cycle (C ₄ photosynthesis).	7
Fig. 1.4	Diagrams for quantum yield of net CO ₂ uptake and photosynthesis rates of C ₃ and C ₄ plants.	9
Fig. 1.5	δ ¹³ C values of grasses and Bromelia species.	15
Fig. 1.6	Rainout effect on δD values.	19
Fig. 2.1	Simplified land cover map of Africa.	30
Fig. 2.2	Variation of Carbon Preference Index and lipid abundance for <i>n</i> -alkanes and <i>n</i> -alkan-1-ols.	37
Fig. 2.3	Averaged histogram representation of leaf wax <i>n</i> -alkanes of samples from rain forest lianas, shrubs, and trees as well as savanna herbs, shrubs, and trees.	40
Fig. 2.4	Averaged histogram representation of leaf wax <i>n</i> -alkan-1-ols of samples from rain forest lianas, shrubs, and trees as well as savanna herbs, shrubs, and trees.	44
Fig. 2.5	Stable carbon isotopic composition of plant material, <i>n</i> -alkanes, and <i>n</i> -alkanols.	45
Fig. 2.6	Averaged histogram representation of leaf wax <i>n</i> -alkanes and <i>n</i> -alkan-1-ols from samples from rain forest, savanna, and C ₄ grasses.	56
Fig. 2.7	Averaged values and standard deviation for chain length parameters of alkanes and <i>n</i> -alkan-1-ols for rain forest species, savanna plants, and C ₄ grasses.	58
Fig. 3.1	Map of southern Africa and presentations of continental environmental conditions.	65
Fig. 3.2	Simplified present-day land cover on map with sampling locations of the north to south transect and graphs of sediment analysis results.	73

Fig. 3.3	Results of sediment analysis for the north to south transect: Stable carbon isotope composition, calculated C ₄ plant abundance and comparison of stable carbon isotope composition results with literature data.	78
Fig. 3.4	Colour-coded map of proportion (%) of continental vegetation using C ₄ pathway.	82
Fig. 3.5	Correlation of contribution of C ₄ plant material with climatic parameters.	86
Fig. 4.1	Simplified present-day land cover map with sampling locations, clusters of wind trajectories, and graphs of environmental parameters.	91
Fig. 4.2	Stable hydrogen isotope composition of precipitation and <i>n</i> -alkanes as well as apparent fractionation and contribution by C ₄ plants to the sediments together with and map of southwest Africa showing sampling locations as well as hydrogen isotope composition of mean annual precipitation.	94
Fig. 4.3	Linear correlation of weighted mean averaged δD ratios of the sedimentary alkanes with hydrogen isotope composition of precipitation.	100

Table legends

(abbreviated)

Table 1.1	Factors influencing the carbon isotopic discrimination in C ₃ plants.	16
Table 2.1	C ₃ plant species studied.	32
Table 2.2	<i>n</i> -Alkane data of C ₃ plants studied.	38
Table 2.3	<i>n</i> -Alkan-1-ol data of C ₃ plants studied.	42
Table 2.4	Isotopic data of C ₃ plants studied.	47
Table 3.1	Sample information and analytical data for bulk material.	66
Table 3.2	Data for major terrestrial <i>n</i> -alkanes.	72
Table 3.3	Stable carbon isotope composition of major terrestrial <i>n</i> -alkanes.	77
Table 3.4	End member data and results for calculations of abundance of C ₄ plant derived material at the sample locations.	80
Table 3.5	Tentative scenarios for calculation of C ₄ plant contribution to sediments.	83
Table 3.6:	Pearson correlation coefficients of C ₄ material abundance in sediments and environmental parameters.	86
Table 4.1	Compilation of sample information.	92
Table 4.2	Stable hydrogen isotope composition of major terrestrial <i>n</i> -alkanes and weighted mean averaged stable hydrogen isotope composition.	97
Table 4.3	Hydrogen isotope composition of mean annual and growing-season precipitation for continental locations and Pearson correlation coefficients for linear correlation with <i>n</i> -alkane stable hydrogen isotope composition.	98
Table 4.4	Apparent hydrogen isotope fractionation between hydrogen isotope composition of <i>n</i> -alkanes and mean annual precipitation.	102
Table 4.5	Pearson correlation coefficients for apparent fractionation and environmental parameters.	103
Table 4.6	Contribution of C ₄ plants to the alkanes calculated from stable carbon isotope composition (chapter 3) and Pearson correlation coefficients for correlation with apparent hydrogen isotope fractionation.	105

Table 7.1	Data of averaged histogram representations of leaf wax <i>n</i> -alkanes of samples from rain forest and savanna plants with different growth forms (Fig. 2.3).	I
Table 7.2	Data of averaged histogram representations of leaf wax <i>n</i> -alkan-1-ols of samples from rain forest and savanna plants with different growth forms (Fig. 2.4).	II
Table 7.3	Data of averaged histogram representations of leaf wax <i>n</i> -alkanes and <i>n</i> -alkan-1-ols of samples from rain forest species, savanna plants and C ₄ grasses (Fig. 2.6).	III
Table 7.4	Data of averaged chain length parameters of <i>n</i> -alkanes and <i>n</i> -alkan-1-ols from C ₃ rain forest species, C ₃ savanna plants and C ₄ grasses (Fig. 2.7).	IV
Table 7.5	Mean annual precipitation and temperature as well as aridity index calculated for locations at ca. 350 km distance from the coast.	IV
Table 7.6	Data of the relative abundance of the dominant <i>n</i> -alkanes in the sediments of the north to south transect (Fig 3.2b).	V
Table 7.7	Data of locations employed as representatives of potential catchment areas.	VI
Table 7.8	Data of environmental conditions in southwest Africa calculated for locations with ca. 250 km distance to the coast.	VIII
Table 7.9	Monthly values of hydrologic parameters employed for the calculation of the hydrogen isotope composition of growing-season precipitation (Table 4.3).	IX

Abbreviations

Latin characters

A	Assimilation rate
a	Year
ACL	Average chain length
ACL _{x-y}	Average chain length for the chain length interval of x to y
ASE	Accelerated solvent extractor
b ₁ , b ₂ , b ₃ , b ₄	Discrimination against ¹³ CO ₂ by RuBisCO in C ₃ plants (b ₁), by PEPC in C ₄ and CAM plants (b ₂), by RuBisCO in C ₄ plants (b ₃) and during the light period in CAM plants (b ₄)
bsf	Below sea floor
°C	Degree Celsius
c _a	Ambient CO ₂ concentration in the air
CAM	Crassulacean Acid Metabolism
CBB Cycle	Calvin-Benson-Bassham Cycle
cm	Centimetre
c _i	CO ₂ concentration in the intercellular space of leaves
CPI	Carbon preference index
CPI _{x-y}	Carbon preference index for <i>n</i> -alkanes in the chain length interval x to y
d	Discrimination by the diffusion of CO ₂ into the leaf
DB5-HT	Non polar capillary column for high temperature gas chromatography
DM	Dry material
dm	Decimetre
°E	Degree east (longitude)
E	Element
EA	Elemental analyser
eV	Electron volt
Fig.	Figure
g	Gram
GC	Gas chromatography
GC-FID	Gas chromatography with a flame ionisation detector

GC-irm-MS	Gas chromatography coupled to an isotope ratio mass spectrometer
GeoB	Geosciences of the University of Bremen
i.d.	Inner diameter
irm-MS	Isotope ratio mass spectrometer
ICBM	Institute for Chemistry and Biology of the Marine Environment
ITCZ	Inter-Tropical Convergence Zone
kg	Kilogram
l	Litre
m	Metre
mg	Milligram
mhi	Mass number of the heavier isotope
min	Minute
mm	Millimetre
°N	Degree north (latitude)
n, n _c , n _δ	Number of samples (n) used for averaging content data (n _c) or isotopic data (n _δ)
n _{C4}	Proportion of the C ₄ plant wax signal to the total biomarker
NAD-ME	Nicotinamide adenine dinucleotide malate dehydrogenase enzyme
NADP-ME	Nicotinamide adenine dinucleotide phosphate malate dehydrogenase enzyme
NSO	Lipid fraction of polar heterocomponents
OA	Oxaloacetate
OIPC	Online Isotopes in Precipitation Calculator
p	Probability
p _{CO2}	Partial pressure of CO ₂
PCK	Phosphoenolpyruvate carboxykinase
PEP	Phosphoenolpyruvate
PEPC	Phosphoenolpyruvate carboxylase
PGA	Phosphoglycerate
PGAL	Phosphoglycerine aldehyde
R	Abundance ratio of a heavier to the lightest isotope
r	Pearson correlation coefficient

RuBisCO	Ribulose bisphosphate carboxykinase/oxygenase
RuBP	Ribulose bisphosphate
s	Second
°S	Degree south (latitude)
SD	Standard deviation
SLAP	Standard substance: Standard Light Arctic Precipitation
TCOC _{x-y}	Total content of odd carbon numbered <i>n</i> -alkanes in the chain length interval x to y
TCEC _{x-y}	Total content of even carbon numbered alkan-1-ols in the chain length interval x to y
TIC	Total inorganic carbon
TOC	Total organic carbon
v/v	Volumetric content
V-PDB	Standard substance: Vienna Pee Dee Belemnite Standard
V-SMOW	Standard substance: Vienna Standard Mean Ocean Water
WUE	Water use efficiency

Mathematical symbols and Greek characters

$\int^D dt$	Time integral during which CAM plants operate in the dark
$\int^L dt$	Time integral during which CAM plants operate the light
$\delta^{13}C$	Stable carbon isotope composition ($^{13}C/^{12}C$) relative to the V-PDB standard in per mil (‰)
$\delta^{13}C_{C3plant}, \delta^{13}C_{C4plant}, \delta^{13}C_{CAMplant}$	Isotope composition of the biosynthetic carbon of the C ₃ , C ₄ , and CAM plant
$\delta^{13}C_{CO2}$	Carbon isotope composition of the ambient CO ₂
$\delta^{13}C_{PM}$	Stable carbon isotope composition of bulk organic material
$\delta^{13}C_{PM}$	Stable carbon isotope composition of bulk plant material
$\delta^{13}C_{SWB}$	Stable carbon isotope composition of the leaf wax biomarker in the sediment
$\delta^{13}C_{SWB-C3plant}$	Stable carbon isotope composition of the wax biomarker in C ₃ plant leaf waxes
$\delta^{13}C_{SWB-C4plant}$	Stable carbon isotope composition of the wax biomarker in C ₄ plant leaf waxes
$\delta^{13}C_{WMA}$	Weighted mean averaged molecular stable carbon isotope composition

$\delta^{13}\text{C}_{\text{WMAx-y}}$	Weighted mean average of molecular carbon stable isotope composition of homologues in the chain length interval x to y
$\delta^{13}\text{C}_x$	Stable carbon isotope composition of the <i>n</i> -alkane with x carbon atoms
$\delta\text{D}, \delta^2\text{H}$	Stable hydrogen isotope composition ($^2\text{H}/^1\text{H}$) relative to the V-SMOW standard in per mil (‰)
δD	Stable hydrogen isotope composition of precipitation
δD_L	Stable hydrogen isotope composition of lipid
$\delta\text{D}_{\text{WMA}}$	Weighted mean averaged molecular stable hydrogen isotope composition
δD_x	Stable hydrogen isotope composition of a <i>n</i> -alkane with x carbon atoms
ϵ_a	Apparent hydrogen isotopic fractionation between continental precipitation and plant lipids
$\epsilon_{a\text{C}x}$	Apparent hydrogen isotopic fractionation between continental precipitation and a <i>n</i> -alkane with x carbon atoms
ϵ_{PM}	Stable carbon isotope fractionation between bulk plant material and individual lipids
$\epsilon_{a\text{WMA}29-33}$	Apparent hydrogen isotopic fractionation between continental precipitation and the weighted mean average of odd carbon numbered <i>n</i> -alkanes with 29 to 33 carbon atoms
μg	Microgram
μm	Micrometre
μmol	Micromol
μl	Microlitre
Φ	Extent of leakiness

1. Introduction

1.1 Scope and framework

Organic geochemistry, the scientific field in which this project was conducted, concerns the cycling of carbon, in all its various chemical appearances, in the Earth system. The major form of carbon, carbon dioxide, is strictly inorganic but it is converted by photosynthesis into a wide variety of organic compounds which directly, or after the modification by other organisms, can be preserved in soils and sediments where they may persist as chemical fossils. If these chemical fossils can unambiguously be linked to specific precursor molecules in living organisms, they can serve as markers for specific biological life forms and thus, are called biomarkers. For instance, long-chain *n*-alkanes and *n*-alkan-1-ols, which are in the focus of this study, are nearly exclusively synthesised by higher land plants as part of their epicuticular wax. Accordingly, they serve as biomarkers for the contribution of terrestrial plants to dusts, soils and sediments (e.g., Rommerskirchen et al., 2003; Schefuß et al., 2003a; Rao et al., 2009a). In addition, the chain length distribution and stable carbon and hydrogen isotope composition of these compounds are assumed to vary with respect to vegetation composition and hydrologic conditions (e.g., Chikaraishi and Naraoka, 2003; Bi et al., 2005; Smith and Freeman, 2006; Rao et al., 2009b; Tierney et al., 2010a,b). Vegetation zones and hydrologic conditions are in turn largely defined by climate. Therefore, the *n*-alkane and *n*-alkan-1-ol characteristics preserved in geological archives are used to elucidate past changes in vegetation composition and hydrologic conditions and to deduce their causal climatic variations (e.g., Schefuß et al., 2003b; Rommerskirchen et al., 2006a; Weijers et al., 2009).

Most valuable archives for geochemical studies are ocean margin sediments with long, undisturbed depositional sequences. But in order to achieve reliable correlations of biomarker characteristics preserved in sediments with continental vegetation, hydrology and climatic conditions it is essential to elucidate how recent conditions are mirrored in sedimentary archives. A suitable testing area for such investigations is the African continent, especially the western part with its nearly latitudinal vegetation regions which largely correspond to climatic zones.

1.2 General aspects of the African continent

The equator roughly represents the halfway mark for the latitudinal spread of the African continent. Consequently, Africa's climate is predominantly tropical and the climate zones vary in nearly mirror-image patterns to the north and south (Fig. 1.1). These patterns are not interrupted by the climatic influence of long mountain ranges. Instead, vast plains and plateaus are characteristic for Africa's geography while mountains only occur as widely scattered exceptions.

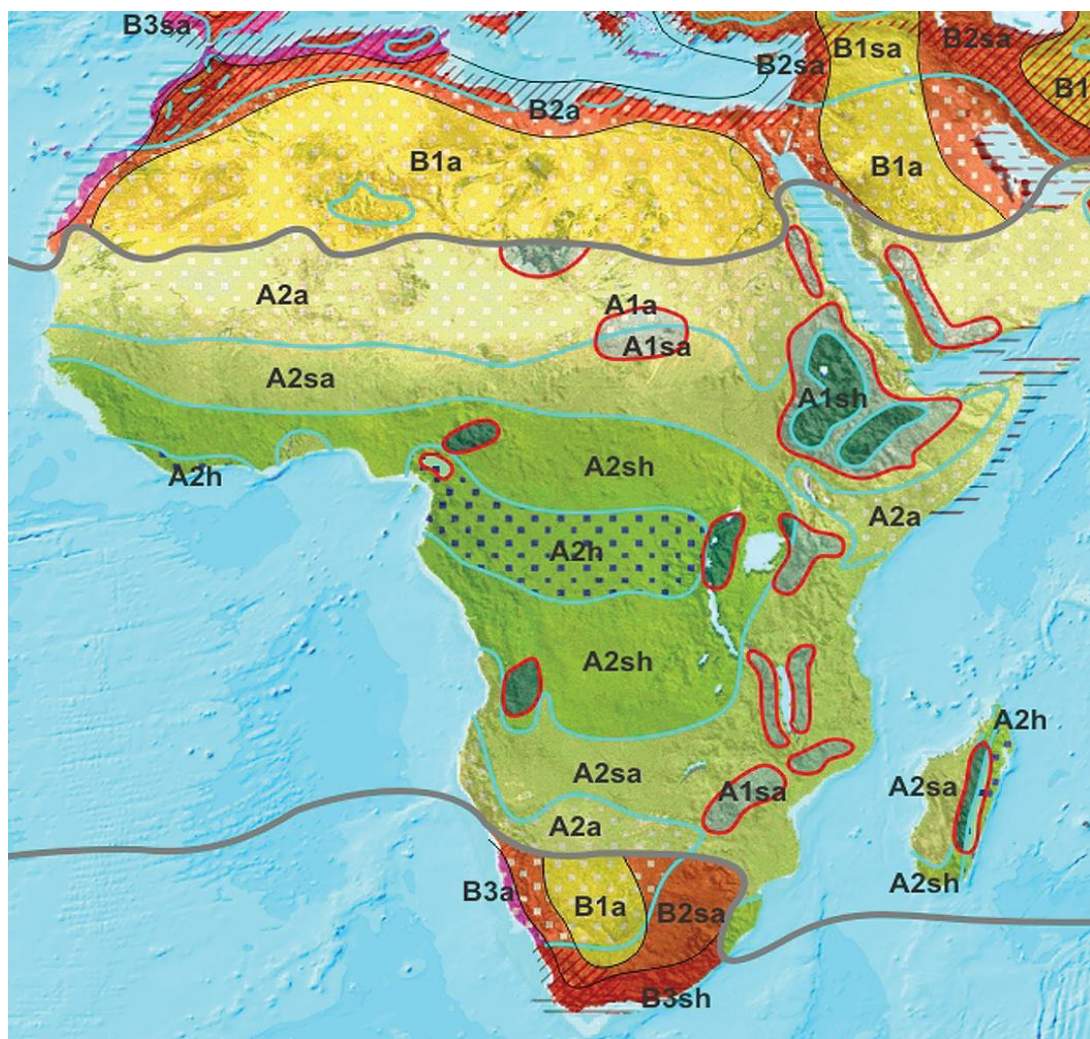


Fig. 1.1 Classification of African climate zones based on a model created by Lauer and Frankenberg (1985) with A and B representing tropical and sub-tropical climate, respectively. The tropical climates are further divided in cold (1) and warm (2). For the subtropical zone the subclassification represents high-continental (1), continental (2) and maritime (3) conditions. The uncapitalised letters represent humid (h), semi humid (sh), semi arid (sa) and arid (a) areas.

The primary determinant for the vegetation of Africa is precipitation, which in turn largely depends the air movement feeding the Inter-Tropical Convergence Zone (ITCZ). In simple terms, winds blow from two sub-tropical high-pressure belts towards the equator, where they meet and force air and moisture upwards. This upward movement cools the air and causes massive rainout feeding the tropical rain forest vegetation. The dry air cycles back towards the subtropics where it descends producing arid climates at latitudes of approximately 20°N and S. From the rain forest towards these arid desert regions the amount of precipitation decreases, and distinct rainy seasons occur because of the migration of the ITCZ due to changes in the latitudinal maximum of solar heating. Corresponding to the changes in mean annual rainfall from the equator towards the higher latitudes, there is a clear gradient from dense evergreen biomes dominated by woody species to dry open land cover with increasing grass abundance (Mayaux et al., 2004). Only at the high latitudes precipitation and accordingly the abundance of woody species increase again. Significant changes in these generalised vegetation zones result from local differences in elevation, edaphic characteristics, microclimate, wildlife, and human population. A detailed satellite-based map of Africa's land cover for the year 2000 was presented by Mayaux et al. (2004) and was the base for simplified maps presented in this study. More detailed information about vegetation, relevant wind systems, hydrologic and climatic conditions are presented in relation to thematic topics in Chapters 2 to 4.

1.3 Photosynthetic pathways

Photoautotrophic organisms convert carbon dioxide to organic compounds with the complex biochemical process of photosynthesis. The CO₂ fixation pathway implemented in the photosynthetic process has undergone evolutionary development. Thus, recent terrestrial plants employ different metabolic pathways (C₃, C₄, and CAM) which are described below to elucidate their influence on plant distribution and isotopic biomarker composition.

1.3.1 C_3 photosynthetic pathway

The majority of higher plant species (about 85 to 90%; according to Sage, 2001, 2004) use a photosynthetic pathway which fixes CO_2 during all-day open stomata into a three-carbon-atom molecular storage product, phosphoglycerate (PGA), by using the enzyme ribulose bisphosphate carboxykinase/oxygenase (RuBisCO; Leegood, 1999a; Fig 1.2a). Because of the three-carbon-atom storage product this photosynthetic pathway is named C_3 metabolism but it is also known as the Calvin-Benson-Bassham (CBB)

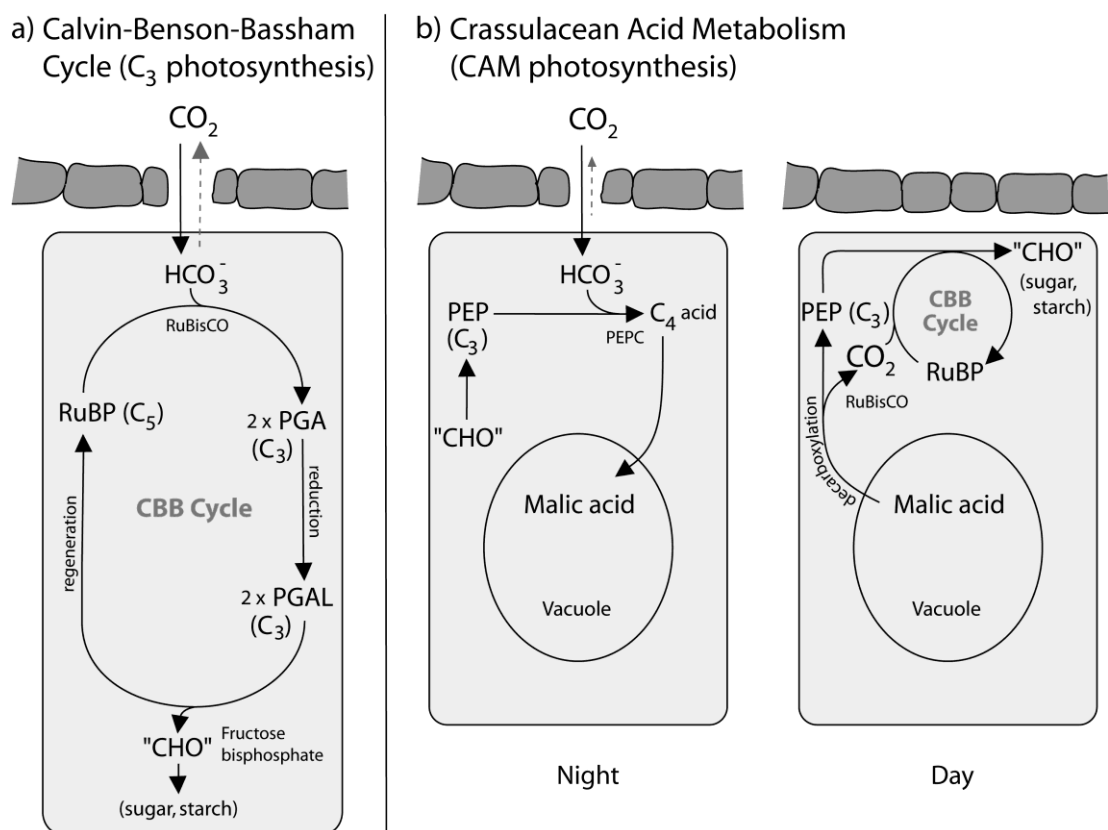


Fig. 1.2 Simplified scheme of a) the Calvin-Benson-Bassham (CBB) Cycle (C_3 photosynthesis) and b) the Crassulacean Acid Metabolism (CAM) photosynthesis according to Leegood (1999a; 1999b). The CBB Cycle can be divided into three phases: (1) carboxylation catalysed by RuBisCO, (2) reductive phase by which PGA is converted into phosphoglycerine aldehyde (PGAL), and (3) regeneration of the CO_2 acceptor ribulose bisphosphate (RuBP). The CAM photosynthesis shows the temporal separation of assimilation of CO_2 by phosphoenolpyruvate carboxylase (PEPC) prior to fixation in the CBB Cycle. Nocturnal CO_2 assimilation leads to malate storage in the vacuols. During the day, malate is decarboxylated to provide CO_2 for fixation in the CBB Cycle.

Cycle. Almost all trees and shrubs, most herbs as well as grasses preferring wet, cool growing seasons utilise this method of carbon fixation.

It is assumed that the C_3 pathway is the oldest way of photosynthesis among higher plants since their advent some 450 million years ago during a time of relatively high concentrations of atmospheric CO_2 (Sage, 2004). In the following Earth history there were periods when the environmental conditions for C_3 plants were less favourable. For example, relatively high O_2 concentrations like in the Carboniferous around 360 to 286 million years ago (Berner, 1993) or during the last 35 million years caused photorespiration in C_3 plants. Photorespiration is an energy-wasting process which originates in the bifunctional nature of RuBisCO. During photorespiration O_2 instead of CO_2 is assimilated and glycolate bisphosphate is generated which cannot be used in the CBB Cycle and needs to be recycled by a complex process which releases CO_2 . In this way up to 40% of newly fixed carbon can be released again as CO_2 especially under high-energy conditions in habitats of high light intensity and temperatures like, e.g., in tropical and subtropical regions. To counteract the photorespiration, C_3 plants operate with widely open stomata to maximise the CO_2 uptake. But this dramatically lowers their water use efficiency (WUE) by evaporative loss.

1.3.2 Crassulacean Acid Metabolism

A significant evolutionary step in the plant kingdom was the development of mechanisms for inhibiting photorespiration by concentrating CO_2 around RuBisCO. The oldest alternative photosynthetic pathway is the Crassulacean Acid Metabolism (CAM), which is named after the plant family in which this physiological system was first observed. The dual carboxylation pathway with initial CO_2 fixation by phosphoenolpyruvate carboxylase (PEPC) and, after intracellular release, secondly by RuBisCO, is separated temporally in the same tissue (Fig. 1.2b; Leegood, 1999b; Keeley and Rundel, 2003). Stomata are open at night to take in and fix CO_2 . The CO_2 is temporarily stored sub-cellularly in the vacuole, primarily as malic acid (Fig. 1.2b). During the day, closure of stomata in terrestrial plants reduces water loss to a minimum but also inhibits CO_2 uptake. But in CAM plants the internal carbon deficit is

overcome by decarboxylation of the stored malic acid. The process concentrates CO_2 around RuBisCO resulting in daytime internal inorganic carbon levels 2 to 60 times higher than ambient levels (Lüttge, 2002; Fig. 1.2b). Only if the stored malic acid is completely metabolised at daytime, the stomata open to assimilate fresh CO_2 in the normal C_3 pathway.

The CAM pathway is used by 20,000 to 30,000 species of the estimated 250,000 land plant species (Sage, 2001, 2004), mainly by highly specialised plants adapted to survive under extreme conditions. These plants often experience periods of drought with extreme water shortage. Therefore, CAM species often have particular morphological features such as large vacuoles for carbon and water storage, which give the tissues a succulent appearance. But this adaptation is an expensive process due to the energy need for the storage process. Thus, this metabolic pathway is generally a strategy for stress survival and not for high productivity. Furthermore, CAM plants grow slowly and can become very old. Therefore, the contribution of CAM-utilising plants to biomass production is low (Lüttge, 2004). Typical dry-subtropical vegetation consists of xerophytic (adapted to dry conditions) shrubs and CAM plants. The use of the CAM metabolism is best known from modern-day desert succulents but also from many epiphytes like bromeliads and orchids.

1.3.3 C_4 photosynthetic pathway

Another mechanism for inhibiting photorespiration by concentrating CO_2 around RuBisCO is the Hatch-Slack Cycle, in which CO_2 is initially fixed in a C_4 acid (Hatch and Slack, 1966). This mechanism is often referred to as C_4 photosynthetic pathway. The C_4 photosynthesis is fundamentally different from the more common C_3 pathway. First, CO_2 is actively fixed by PEPC instead of RuBisCO. Unlike in CAM plants, PEPC in C_4 species is active in the light. CO_2 is fixed in the mesophyll cells preliminarily as a dicarboxylic C_4 acid, oxaloacetate (OA), which can be converted into aspartate and/or malate depending on the metabolic subtype employed (Fig. 1.3). C_4 plants create an internal pool of C_4 acid which is transported to the bundle sheath tissue where CO_2 is released. Three C_4 sub-groups are known which possess different enzymes responsible for this decarboxylation: (1) Those using the

nicotinamide adenine dinucleotide phosphate malate dehydrogenase enzyme (NADP-ME; malate as CO_2 supplier), (2) those using the nicotinamide adenine dinucleotide malate dehydrogenase enzyme (NAD-ME; aspartate), and (3) those using the phosphoenolpyruvate carboxykinase enzyme (PCK; aspartate). In Fig. 1.3a-c these different mechanisms are shown in a simplified manner. The CO_2 thus released in the bundle sheath tissue is metabolised by RuBisCO which supplies the CO_2 to the subsequent CBB Cycle (Fig. 1.3).

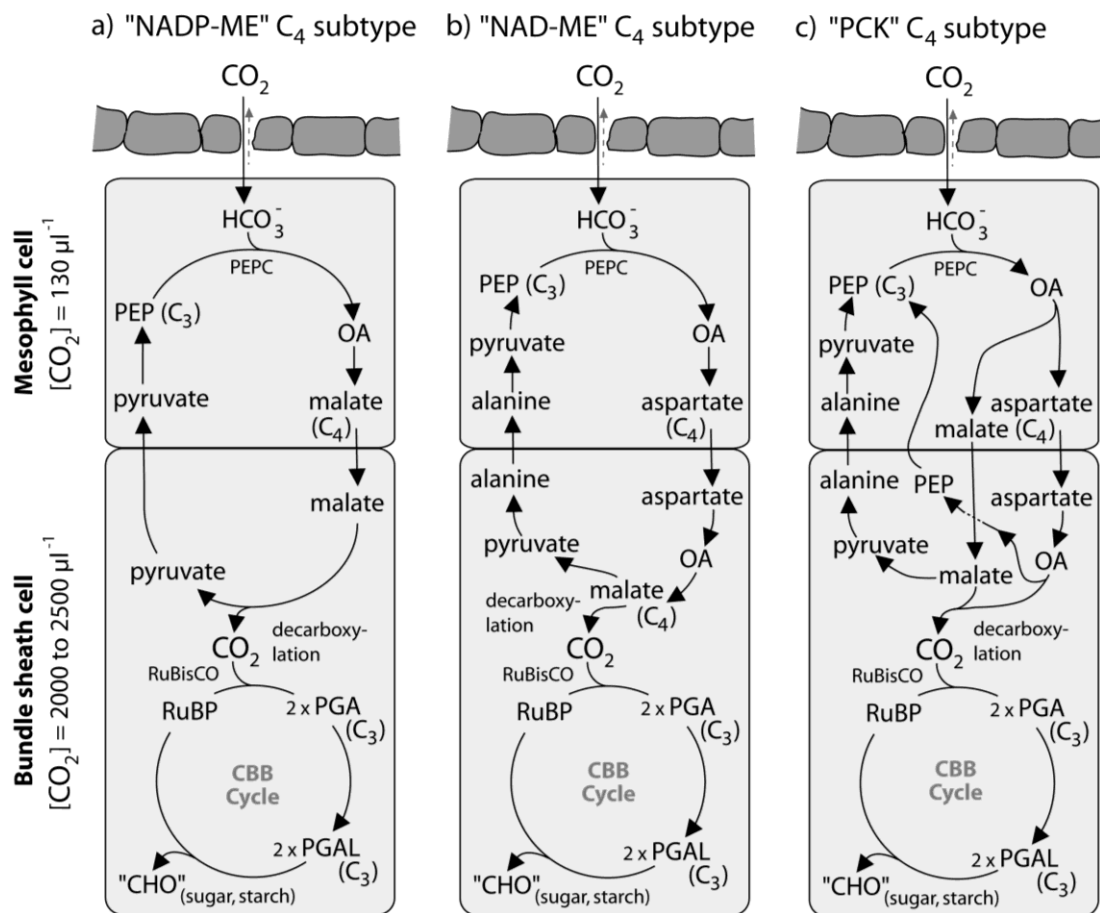


Fig. 1.3 Simplified pathways of the three carbon dioxide assimilation variations of the Hatch-Slack cycle (C₄ photosynthesis): a) "NADP-ME", b) "NAD-ME", and c) "PCK". Generally, atmospheric CO₂ is initially fixed inside leaf mesophyll cells in a reaction catalysed by PEPC. The resulting C₄ acids are decarboxylated inside the bundle sheath cells, providing a source of CO₂ for RuBisCO and the subsequent CBB Cycle. Values of the CO₂ concentration inside the bundle sheath and the mesophyll cells are from Ehleringer et al. (1997).

In contrast to CAM plants in which the two processes are separated in time, the C_4 pathway involves a separation in space. The leaf tissue is divided into two separated specialised compartments, the photosynthetic assimilation in the mesophyll cells and the adjacent photosynthetic reduction tissue of thick-walled bundle sheaths which surround the vascular bundles. This is called the “Kranz” anatomy (the German word “Kranz” means wreath) and can be found in almost all C_4 plants. The designation “Kranz” and non-“Kranz” is thus synonymous with C_4 and C_3 /CAM. Due to this space separation in photosynthesis, C_4 plants are able to control the supply of CO_2 to the RuBisCO enzyme without interference by the competing O_2 . Furthermore, the CO_2 concentrating mechanism leads to a 10 to 20 fold higher CO_2 concentration around RuBisCO than in the mesophyll cell (Fig. 1.3; Ehleringer et al., 1997). This minimises the opening of the stomata during the day which prevents evaporation and results in a high WUE especially in growth areas of high temperature, high irradiance, limited water supply and/or low atmospheric CO_2 concentration (Björkmann, 1976; Ehleringer et al., 1997; Collatz et al., 1998; Winslow et al., 2003; Sage, 2004).

It is believed that the physiological adaptation of the C_4 mechanism evolved independently many times within the last 7 to 30 million years in response to a decline in atmospheric CO_2 concentration. This led to its distribution among a wide range of phylogenetically unrelated plants (Sage, 2001). The C_4 mechanism is predominantly found in monocotyledons, most of them being grasses (about 60% of all C_4 species; Sage, 2001, 2004) followed by sedges and dicotyledons (Leegood, 1999b; Sage, 2001; Keeley and Rundel, 2003; Sage, 2004). C_4 plants are not represented in a high species number (only 7,500 to 10,000 species or about 3% of the approx. 250,000 land plant species; Sage, 2004). However, their environmental importance across the world is high because they provide the principal grass cover of the tropical and subtropical habitats due to their advantages over the more widespread C_3 pathway. The strategy of C_4 plants is not like that of CAM plants to merely survive in niches where C_3 plants cannot thrive. Instead, C_4 plants grow fast and outcompete C_3 plants in places where the climate is suitable to give them an advantage over the C_3 plants.

1.4 Factors controlling the abundance of plants utilising C₃ and C₄ metabolism

Primary factors controlling the C₃/C₄ plant abundance in a habitat are temperature and irradiation (Sage, 2001). In C₃ plants, the quantum yield of CO₂ uptake in normal air falls as the temperature rises due the onset of photorespiration. In contrast, the cost of fixing CO₂ in a C₄ plant remains constant in relation to changes in temperature (Fig. 1.4a). In the absence of possible photorespiration (at low O₂ concentration in the air) C₃ plants exhibit the

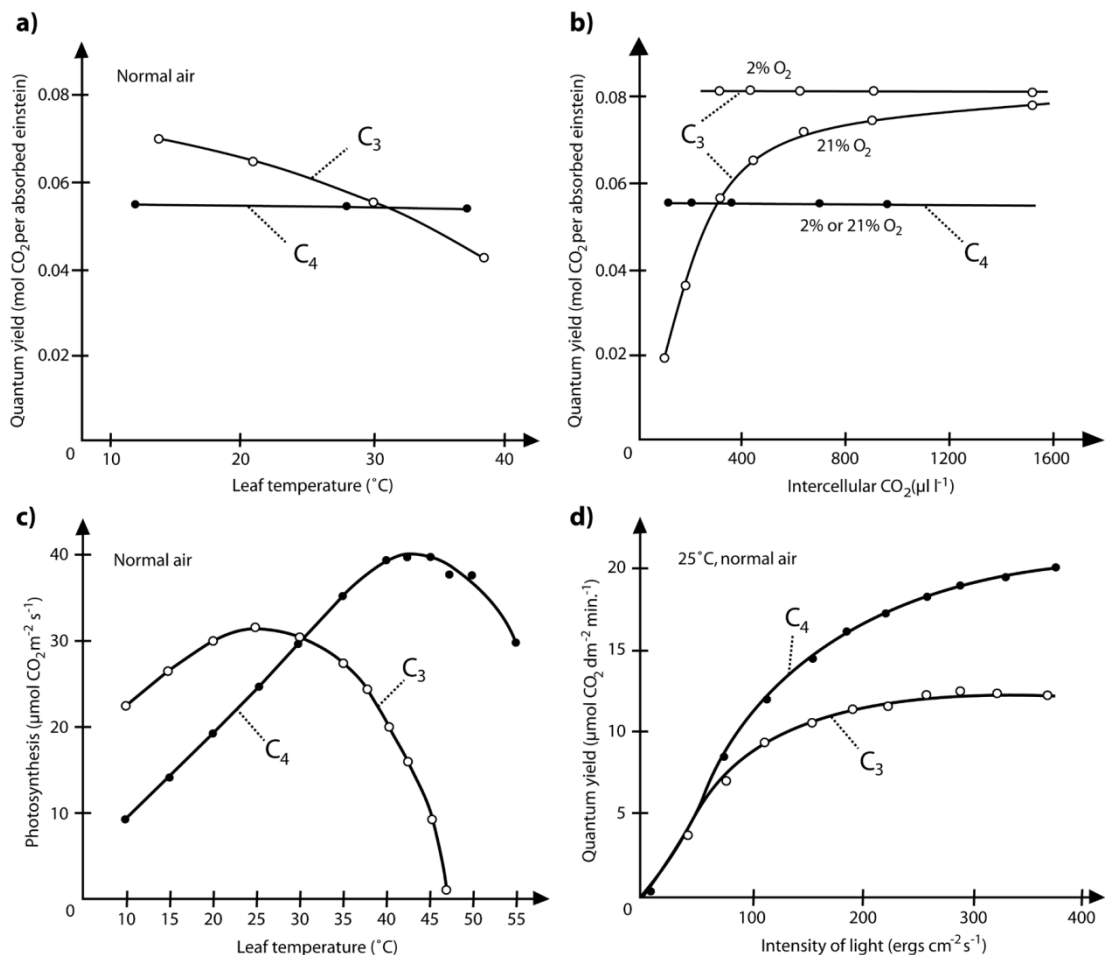


Fig. 1.4 Diagrams for quantum yield of net CO₂ uptake of *Encelia californica* (C₃) and *Atriplex rosea* (C₄) as a function of a) temperature in the air, b) CO₂ and O₂ concentration (after Osmond et al., 1980), c) the temperature dependence of photosynthesis in the prairie grasses *Agropyron smithii* (C₃) and *Bouteloua gracilis* (C₄; after Edwards et al., 1985), and d) the quantum yield of the closely related plants *Atriplex patula* (C₃) and *Atriplex rosea* (C₄) as a function of light intensity (Björkmann and Berry, 1973).

same constancy in the CO₂ uptake and are more efficient than C₄ plants (Fig. 1.4b). In normal air CO₂ assimilation has an optimum at 20 to 30°C in C₃ leaves and at 30 to 40°C in C₄ leaves (Fig. 1.4c). C₄ plants can only thrive in natural habitats if growing season temperature is above 12 to 14°C whereas lower night temperatures and colder seasons are tolerated (Sage, 2001).

With respect to light intensity C₃ and C₄ species perform photosynthesis at nearly the same rate at low illumination (Fig. 1.4d). At higher light intensities both photosynthetic types increase their photosynthesis rate, but rates for the C₄ species are above those of C₃ plants at full light intensity (Björkmann and Berry, 1973; Björkmann, 1976). Under these conditions energy is no limiting factor and C₄ species can take advantage of their CO₂ concentrating mechanism. In natural habitats C₄ plants require 30 to 50% of full sunlight intensity to be dominant in an area. Thus, the superiority of C₄ species becomes significant in sunny habitats where light is not dimmed by the shade of other plants or by clouds. Where light intensities average less than 20% of full sun on a clear day C₄ species rarely occur (Sage, 2001).

In areas, where temperature and light conditions are suitable for C₄ species, secondary factors gain importance for the C₄ plant abundance (Sage, 2001). Among these secondary factors aridity and the occurrence of distinct rainfall seasons support C₄ over C₃ biomass because C₄ plants have a higher WUE and grow faster. Prominent habitats with such conditions are tropical and subtropical environments where tree- and shrub-dominated vegetation mainly consists of C₃ species whereas grasses often use the C₄ metabolic pathway. In such areas aridity and the occurrence of distinct rainfall seasons also promote fires which harm woody species, while C₄ grass meristems are protected below ground or in fire-resistant tufts. In addition, C₃ plants grow slower under arid condition which elongates their establishment time and makes them even more vulnerable to fire.

Other secondary factors influencing the C₄ plant abundance are more local phenomena like edaphic characteristics or mechanical stress (Sage, 2001). Regarding edaphic characteristics, not only low nutrient availability obstructs woody species but also the soil moisture capacity is important. Only

deep soils enable water storage which supports perennial woody vegetation. Furthermore, salinity tends to favour C₄ species because the higher WUE reduces the salt load that the plants have to endure. Mechanical stress like logging, grazing, waves or flooding can also promote C₄ plants even in areas where the availability of water is not a limiting factor. In these cases not WUE but the faster growth of C₄ plants due to photorespiration prohibition is essential. An illustrative example for the fact that the occurrence of C₄ plants does not necessarily mean aridity are tropical sedges like the C₄ plant *Cyperus papyrus* (papyrus), which can be dominant in tropical African swamps (Jones, 1987).

The proportion of C₄ plants in a habitat is the result of a complex interplay of the cited factors which are climate dependent to a large extent. The C₄ plant abundance is inherently unstable, and small changes in climatic conditions can lead to rapid changes in vegetation composition. Thus, archives reporting the C₃/C₄ distribution on the continent can be used to deduce information about ancient continental vegetation and climate conditions.

1.5 Stable isotope composition of biomarkers

The isotope ratio of a component is expressed by δ values with units of permil (‰) relative to a standard substance, and its general form is represented by

$$\delta^{mhi} E = \left(\frac{R_{sample}}{R_{standard}} - 1 \right) \cdot 1000 \text{ (‰)} \quad \text{Equation 1.1}$$

where “mhi” is the mass number of the heavier isotope, “E” is the element and “R” is the abundance ratio of a heavier to the lightest, most abundant isotope.

Chemically isotopes are indistinguishable, but the physical difference in atomic radii causes reactions or processes to require slightly more energy if a heavier atom is involved. Thus, fractionation between the heavy and the light isotopes can occur in two ways. In biological systems, kinetic isotope effects during chemical transformation will lead to a higher reaction rate for the

lighter isotope and therefore enrich this isotope in the products. Secondly, thermodynamically controlled equilibrium effects play a role where concentration gradients or phase transitions occur. Furthermore, thermodynamic effects also have been claimed to be essential in inter- and intramolecular isotope exchange among different metabolites (Schidlowski, 1987). The advantage of stable isotope measurements on naturally occurring compounds is the fact that the isotopes comprise built-in tracers for physical processes and chemical reactions.

1.5.1 Stable carbon isotope composition

Geochemically the stable carbon isotopic ratio is the most widely accepted tool to determine if biogenic organic matter in sediments was synthesised of carbon fixated by the C₃ or C₄ pathway. The carbon component of most naturally occurring carbon-containing materials exhibit 98.9% of ¹²C, 1.1% of ¹³C and about 10⁻¹⁰% of the unstable radionuclide ¹⁴C. The stable carbon isotope composition is expressed according to Equation 1.1 as δ¹³C ratios relative to the Vienna-Pee Dee Belemnite (V-PDB) standard.

The production of biomass proceeds in two steps: The assimilation of carbon and the biosynthesis of cell components. As a consequence, the amount of ¹³C in biological molecules mainly depends on (1) the ¹³C content of the carbon source, (2) isotopic effects during the assimilation of carbon, and (3) isotopic effects during metabolism and biosynthesis (Hayes, 1993). The δ¹³C ratio of the atmospheric CO₂ is globally similar despite variations in very local conditions but the fixation of atmospheric carbon as well as the storage of carbon in the form of organic matter in plants passes through several equilibrium and kinetic reaction steps, which cause ¹³C/¹²C fractionation. In all the fixation processes the heavier ¹³C isotope will react slightly more slowly than the lighter isotope ¹²C and only a fraction of the source carbon will enter the process. This results in a relative enrichment of ¹²C and a depletion of ¹³C in the product at the end of the process and enrichment of ¹³C in the remaining fraction (which in the case of plants is the left-over CO₂). The route of fractionation in higher land plants starts with the diffusion of CO₂ from the atmosphere through the stomata. The CO₂ dissolves and is con-

verted into HCO_3^- in the lumen of the leaf. This causes a fractionation of about 4.4‰ in C_3 plants. The second fractionation step in the C_3 pathway is the enzymatic fixation of CO_2 . The carboxylation mediated by RuBisCO results in about 30‰ fractionation. The overall carbon isotopic composition is related to that of atmospheric CO_2 by the simplified model relationship for C_3 plants in Equation 1.2 (Farquar et al., 1982; Farquar et al., 1989).

In C_4 plants, discrimination against ^{13}C is more complex. The overall fractionation is described by the model in Equation 1.3. CO_2 diffuses through stomata, dissolves, is converted into HCO_3^- and fixed by PEPC into OA (Fig. 1.3). Then various transformations occur which are different for the various C_4 types (cf. Chapter 1.3.3). At equilibrium, the heavier isotope concentration in HCO_3^- is similar to that in C_3 plants. This discrimination depends on temperature, being 8.5‰ at 20°C, 7.9‰ at 25°C, and 7.4‰ at 30°C (Mook et al., 1974). PEPC discriminates against $\text{H}^{13}\text{CO}_3^-$ by about 2.2‰ (O'Leary, 1981).

$$\delta^{13}\text{C}_{\text{C}_3\text{plant}} = \delta^{13}\text{C}_{\text{CO}_2} - d - (b_1 - d) \frac{c_i}{c_a} \quad \text{Equation 1.2}$$

$$\delta^{13}\text{C}_{\text{C}_4\text{plant}} = \delta^{13}\text{C}_{\text{CO}_2} - d - (b_2 + b_3\Phi - d) \frac{c_i}{c_a} \quad \text{Equation 1.3}$$

$$\delta^{13}\text{C}_{\text{CAMplant}} = \delta^{13}\text{C}_{\text{CO}_2} - d - \frac{\int^{\text{D}} A(b_2 - d) \frac{c_i}{c_a} dt + \int^{\text{L}} A(b_4 - d) \frac{c_i}{c_a} dt}{\int^{\text{D}} A dt + \int^{\text{L}} A dt} \quad \text{Equation 1.4}$$

$\delta^{13}\text{C}_{\text{C}_3\text{plant}}$, $\delta^{13}\text{C}_{\text{C}_4\text{plant}}$, $\delta^{13}\text{C}_{\text{CAMplant}}$: Isotope composition of the biosynthetic carbon of the C_3 , C_4 , and CAM plant

$\delta^{13}\text{C}_{\text{CO}_2}$: Carbon isotope composition of the ambient CO_2

d : Discrimination by the diffusion of CO_2 into the leaf

b_1 , b_2 , b_3 , b_4 : Discrimination against $^{13}\text{CO}_2$ by RuBisCO in C_3 plants (b_1), by PEPC in C_4 and CAM plants (b_2), by RuBisCO in C_4 plants (b_3) and during the light period in CAM plants (b_4)

c_i : CO_2 concentration in the intercellular space of leaves

c_a : Ambient CO_2 concentration in the air

Φ : Extent of leakiness

$\int^{\text{D}} dt$ and $\int^{\text{L}} dt$: Denotes the time integral in the dark ($\int^{\text{D}} dt$) and that in the light ($\int^{\text{L}} dt$)

A : Assimilation rate

No further discrimination would occur if the bundle sheath cells were gas tight but some CO_2 and HCO_3^- is likely to leak into the mesophyll cells. The isotopic fractionation by RuBisCO cannot be fully expressed due to the internal carbon concentration mechanism and the dependence on the tightness of the bundle sheaths (in which RuBisCO is located). The extent of leakiness of the bundle sheath is given by Φ in the Equation 1.3 and determines to which extent fractionation occurs by RuBisCO (Farquar, 1983; Farquar et al., 1989).

Plants in the CAM mode take up CO_2 and synthesize OA using PEPC; the OA is then reduced and stored as malate (cf. Fig. 1.2). At dawn the plants close their stomata and decarboxylate the malate, refixing the released CO_2 using RuBisCO. The malate that is stored at night will show the same discrimination as for C_4 species without leakage. In the simplest case of C_4 fixation in the dark and possible C_3 fixation in the light, the average discrimination over a 24 h period is modelled by Equation 1.4 (Farquar et al., 1989).

Bender (1968) was the first to recognise that higher plants fall into distinct groups on the basis of the $\delta^{13}\text{C}$ ratio of their organic carbon and that this was related to the operation of C_3 and C_4 photosynthesis. Numerous studies confirmed that biomass of C_3 and C_4 plants exhibit distinctive $\delta^{13}\text{C}$ values (Fig. 1.5). The C_3 photosynthetic pathway produces organic matter with $\delta^{13}\text{C}$ values ranging from -22‰ to -38‰ , whereas the organic matter of C_4 plants is significantly enriched in ^{13}C and generally ranges from -9‰ to -20‰ (Tippie and Pagani, 2010). CAM plants are more difficult to distinguish because they use the C_3 pathway if water supply is sufficient. But under arid conditions the full CAM pathway is engaged and the isotopic signature is similar to that of C_4 plants. Therefore, CAM plants show $\delta^{13}\text{C}$ values in-between those of C_3 and C_4 plants (Fig. 1.5) depending on the climatic conditions of the habitat. They approximately range from -10‰ to -33‰ (Schidlowski, 1987).

Important controls on $\delta^{13}\text{C}$ values of plants causing the quoted ranges are the isotopic composition of the atmosphere and those environmental and physiological variables that influence the c_i/c_a ratios in Equations 1.2 to 1.4.

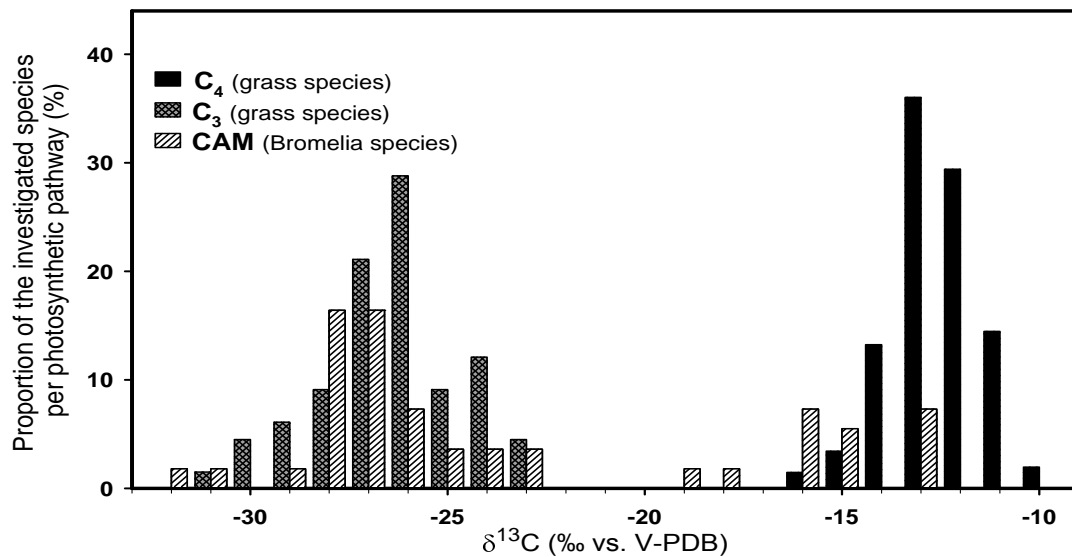


Fig. 1.5 $\delta^{13}\text{C}$ values of 474 grass species and of 55 Bromelia species, demonstrating the distinct difference in isotopic composition between C₃, C₄ and CAM plants. Values collected from Smith and Epstein (1971), de la Harpe et al. (1981), Hattersley, Koch et al. (1991), Lichtfouse et al. (1994), Schulze et al. (1996), Muzuka (1999), Pierce et al. (2002), and Boom (2004).

Especially the $\delta^{13}\text{C}$ values of C₃ plants are affected by several factors causing a wider range in $\delta^{13}\text{C}$ values compared to C₄ plants (cf. Fig. 1.5). Arens et al. (2000) collected factors from the literature that have been cited to influence carbon isotopic discrimination in C₃ plants (Table 1.1).

With the aid of stable carbon isotope measurements terrestrial organic material of C₃ and C₄ plants can be distinguished through their $\delta^{13}\text{C}$ values, which is of great use in the investigation of palaeo-vegetation. Possibly, CAM plants disturb the reliability of the assessments, but, looking at the present-day CAM plants, it seems unlikely that these species would have synthesised a large portion of plant biomass, since they usually occupy small ecological niches. C₃ and C₄ plants are in the focus of scientists working with stable isotopes to reconstruct palaeo-environments, especially palaeoclimatic conditions, by determining the climate-dependent proportion of representatives of the photosynthetic pathways in the vegetation. Leaves and their features such as Kranz anatomy are seldom preserved in fossil material. The only material omnipresent in geological archives is morphologically degraded organic material. But bulk marine sediments typically contain a mixture of ma-

rine and terrestrial organic matter and thus, bulk parameters cannot easily be used to deduce the contribution of plants employing different metabolic pathways from the adjacent continent. In contrast, specific biomarkers like

Table 1.1 Factors influencing the carbon isotopic discrimination in C_3 plants (adopted from Arens et al., 2000, for details see references therein). c_i : CO_2 concentration in the intercellular space of leaves; c_a : Ambient CO_2 concentration in the air.

Factor	Effect on c_i/c_a	Effect on $\delta^{13}C_{C3plant}$		
		Range	Direction	Ecological conditions
Recycled CO_2	Little	1-5‰	Negative	Within closed canopies or in ecosystems where soil outgasing is high
Low light	Increase	5-6‰	Negative	Forest understory
Water stress, low relative humidity	Decrease	3-6‰	Positive	Arid and semiarid climate
Osmotic stress	Decrease	3-10‰	Positive	High-salinity soils, extreme at high pCO_2
Low nutrients	Increase	4‰	Negative	Nutrient-poor soils
Low temperature	Increase	3‰	Negative	Polar regions during ice house times, high altitude
Reduced pCO_2 with altitude	Decrease	3-7‰	Positive	High mountains
Growth form and deciduousness	Increase/decrease	1-3‰	Negative/positive	Variation between trees, forbs, and grasses, and between evergreen and deciduous species
Age (juvenile versus adult)	Increase in juvenile	2‰	Negative in juvenile	Seedling or sapling versus reproductive individual
Sun versus shade leaves	Increase in sun	1-3‰	Negative in sun	Variation due to positive in the canopy relative to direction of sun
Seasonal variation	Increase/decrease	1-2‰	Negative/positive	Strongest effect in semiarid and arid climate

the *n*-alkanes and *n*-alkan-1-ols, mainly derive from higher land plants and, thus, are useful for such investigations (Pancost and Boot, 2004).

Long-chain *n*-alkanes (*n*-C₂₅ to *n*-C₃₅) with an odd-over-even carbon number predominance and long-chain *n*-alkan-1-ols (*n*-C₂₄ to *n*-C₃₄) with an even-over-odd carbon number predominance are part of all leaf waxes of higher terrestrial plants (Eglinton and Hamilton, 1967; Tulloch, 1976; Baker, 1982; Bianchi, 1995). During their biosynthesis, they become more depleted in ¹³C than the total biomass (by about 10‰ in the case of *n*-alkanes; Collister et al., 1994). Thus, their δ¹³C ratios vary between -32‰ and -39‰ in C₃ plants and between -18‰ and -25‰ in C₄ plants (Rieley et al., 1991, 1993; Collister et al., 1994). Neglecting the CAM plant contribution to the biomass and their contribution to preserved wax biomarkers in soils and sediments, a simple two-component mixing model, Equation 1.5, can be used to estimate the contribution of plants utilising C₃ or C₄ photosynthetic pathway by employing compound-specific stable carbon isotopic compositions.

$$\delta^{13}C_{SWB} = (1 - n_{C4}) \cdot \delta^{13}C_{WB-C3plant} + n_{C4} \cdot \delta^{13}C_{WB-C4plant} \quad \text{Equation 1.5}$$

δ¹³C_{SWB}: Measured δ¹³C value of sedimented leaf wax biomarker

δ¹³C_{WB-C3plant}: δ¹³C value of the wax biomarker in C₃ plant leaf waxes

δ¹³C_{WB-C4plant}: δ¹³C value of the wax biomarker in C₄ plant leaf waxes

n_{C4}: Proportion of the C₄ plant wax signal to the total biomarker

1.5.2 Stable hydrogen isotope composition

Hydrogen exhibits three naturally occurring isotopes, denoted as hydrogen-1 or protium (¹H or H; 99.98%), hydrogen-2 or deuterium (²H or D; 0.02%) and the unstable radionuclide hydrogen-3 or tritium (³H or T, trace amounts). The stable hydrogen isotope composition is expressed according to Equation 1.1 as δ²H or δD ratios relative to the Vienna-Standard Mean Ocean Water (V-SMOW) standard.

The only source for hydrogen in organic substances is meteoric water. This is liquid or solid water that falls or has fallen from the sky and includes

rain, fog, hail, sleet, and snow. Most precipitation on Earth occurs over the oceans whereas about 90% of oceanic water vapour condenses after minimal horizontal movement and falls back into the ocean. The remaining 10% are carried over the continents by winds. Over landmasses additional water vapour from freshwater sources can be picked up. If the air masses cool down, supersaturation occurs and much of the water vapour condenses and precipitates on land to reside in glaciers, groundwater systems, rivers and lakes. About one-third of continental precipitation is derived directly from oceanic water vapour. The remaining two thirds enter the atmosphere through evaporation from soils, lakes and rivers and, significantly, by evapotranspiration of plants (Sharp, 2007).

Evaporation and condensation of water are processes which both comprise stable isotope fractionation. Vapour pressures of lighter molecules are higher than those of heavier molecules of the same chemical compound. Accordingly lighter molecules of water preferentially escape from the surface of the liquid into the vapour phase upon evaporation. The opposite occurs upon condensation, with heavier molecules preferentially condensing out and leaving a vapour phase relatively enriched in isotopically lighter water. Most of these processes occur under Rayleigh conditions where one phase (e.g. condensate) is continuously removed from the system prohibiting back exchange between the two phases after separation.

Air masses experience a series of precipitation cycles during which both the vapour remaining and the precipitation become progressively lighter. A typical precipitation pattern is illustrated in Fig. 1.6. The water vapour over the ocean has a δD value of about -87‰ . Some vapour condenses and rains out a liquid phase with a δD value of -14‰ . The removal of this relatively heavy water leaves behind vapour with even lower δD values (-112‰), so that the next cycle of rainout has a δD of -31‰ . As the air mass moves farther inland and more and more precipitation cycles occur, the δD values of condensate become progressively more negative. This phenomenon is known as the continentality effect. If the moist atmospheric air masses are carried up high mountains rainout increases as temperature decreases. The

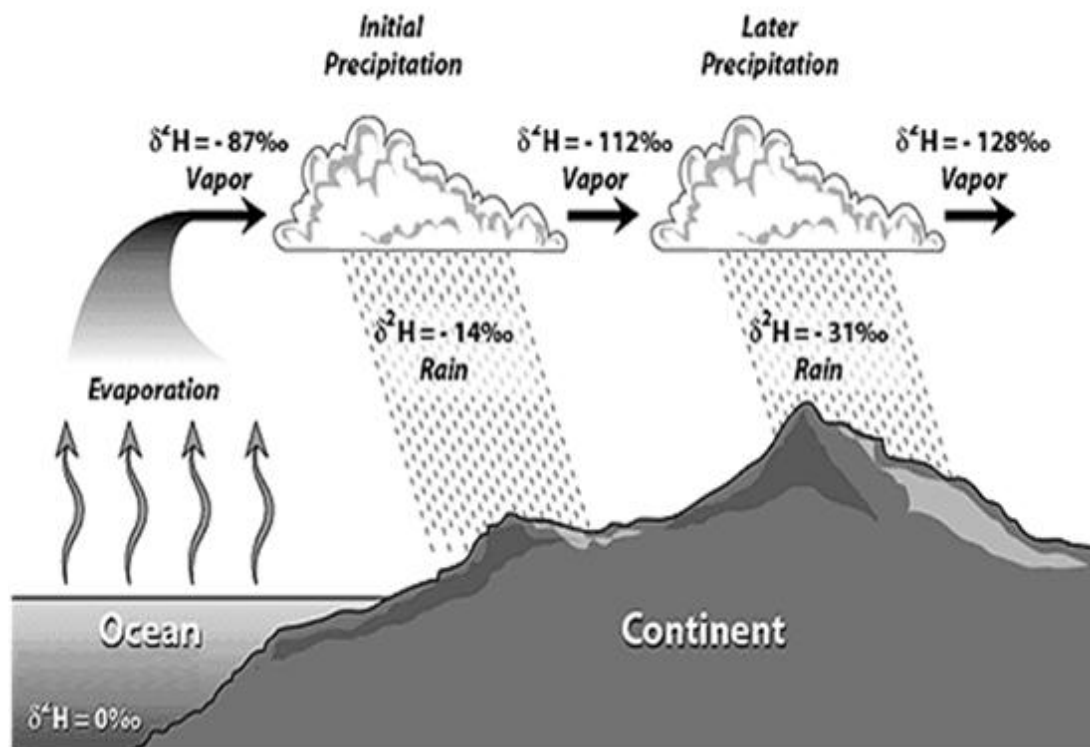


Fig. 1.6 Rainout effect on δD values (modified from SAHRA, 2010; based on Hoefs, 1997).

percentage of vapour remaining in the air mass decreases more rapidly resulting in stronger isotopic gradients along the mountain slope (altitude effect).

Another effect influencing the hydrogen isotope composition of precipitation, called amount effect, causes a negative correlation between mean δD values and amount of monthly precipitation in tropical regions. The hydrogen isotope composition of rain falling at a given tropical station is high in months with little rain and low during the rainy season. The effect is considered a tropical effect but it also occurs to a lesser extent at mid latitudes in the summer. Explanations for the amount effect are given only in qualitative terms because the behaviour of water in convecting air masses is very complicated. There are four associated processes (Sharp, 2007): (1) As air rises and cools to saturation, condensate falls through other droplets that formed below and can exchange with them, (2) the droplets can grow larger by taking on more vapour as they fall, (3) upon exiting the cloud the droplets can

evaporate into dry air, and (4) droplets can exchange with vapour present in non-saturated air below the cloud.

When droplets evaporate into very dry air, isotopically light molecules vaporize preferentially and with an isotope effect. Evaporation is most pronounced when the rainwater falls through dry, hot air. Additionally, when the amount of precipitation is low, the degree of cooling below the cloud mass is minimal. Under these conditions, the below-cloud air temperature is relatively high and significant evaporation can take place. During slightly more humid conditions, the probability of encounters between falling droplets and vapour molecules in the air increases and exchange can occur between them. As a result of such exchange reactions, the liquid becomes richer in the heavier isotopes because lighter isotopes preferentially remain in the vapour. The two processes of evaporation and exchange explain the enrichment of heavy isotopes in gentle tropical rain. At periods of intense tropical rainfall, rapidly ascending air masses result in deep cooling of the air mass, causing massive rainout with big rapidly falling droplets. Under these conditions fractionation, evaporation of droplets as well as exchange with vapour is low resulting in isotopically light precipitation.

The precipitation reaching the earth surface forms the soil water, which is the only source for hydrogen in most terrestrial plants. Thus, the hydrogen isotopic composition of plant wax *n*-alkanes depends on the δD ratios of precipitation, but it is also the result of fractionation during soil evaporation, plant transpiration and biosynthesis. For biosynthesis it was hypothesised that the fractionation of hydrogen is relatively constant (Sessions et al., 1999; Sachse et al., 2004; Feakins and Sessions, 2010). In contrast, different evaporation and evapotranspiration strengths can lead to changing extents of deuterium enrichment (Sternberg, 1988) whereas plant water enrichment is assumed to vary due to plant characteristics like ecological life form (tree, shrub, grass; Liu et al., 2006; Liu and Yang, 2008, Feakins and Sessions, 2010a) and metabolic pathway employed ($C_3/C_4/CAM$; Chikaraishi and Naraoka, 2003; Bi et al., 2005; Smith and Freeman, 2006; Feakins and Sessions, 2010b). The hydrogen isotope compositions of *n*-alkanes integrate these various factors. Despite these potentially obscuring influences, studies of lake sediments

comparing measured stable hydrogen isotope compositions of plant lipids with those of source waters have found a linear or nearly linear relationship. This suggests that lipid values can serve as direct proxies for the hydrogen isotope composition of precipitation (Sachse et al., 2004; Hou et al., 2008) and thus may report, e.g., past precipitation amount changes. For ocean margin sediments hitherto no transect study has elucidated this relationship.

1.6 Motivation and objectives of this project

A major goal of this study was the validation of relations between Africa's continental vegetation and plant lipid characteristics preserved in recent ocean margin sediments as well as elucidating potential correlations with climatic and hydrological conditions. Despite the many palaeo-environmental interpretations for sedimentary material in e.g., African lakes or ocean margin sediments (e.g., Schefuß et al., 2003b; Rommerskirchen et al., 2006a; Weijers et al., 2009; Tierney et al., 2010b) analytical data for C₃ plant material grown in its natural habitat was sparse and thus rain forest and savanna vegetation representatives were analysed. Furthermore, as previous studies of sediment transects revealed some inconsistencies, which were related to the use of sediment material from different water depths, an isobathic sediment transect recovered from the southwest African ocean margin was analysed. The key questions of the project are summarised as follows:

- What are the characteristics of distribution patterns and stable carbon isotope compositions of *n*-alkanes and *n*-alkan-1-ols derived from plant waxes of tropical African rain forest and savanna C₃ species?
- Are plant lipid characteristics influenced by the plant's life form (herb, liana, shrub, and tree)?
- Do the *n*-alkane distribution pattern and stable carbon isotopic composition of ocean margin surface sediments reflect the recent vegetation composition on the continent?
- Can sediment-derived *n*-alkane parameters be used to deduce vegetation composition in the catchment area?
- Which environmental conditions (precipitation, aridity) control vegetation composition?

- Does the *n*-alkane stable hydrogen isotope composition mirror the hydrogen isotope composition of continental precipitation?
- Does the apparent fractionation between the stable hydrogen isotope compositions of lipids and precipitation depend on climatic conditions or vegetation composition?

1.7 Outline of the author's contribution and the project parts

This thesis presents published material and material submitted or prepared for publication from two interdependent study areas within organic geochemistry. The first category deals with the carbon number distribution and molecular stable carbon isotope composition of long-chain *n*-alkanes and *n*-alkan-1-ols in leaf waxes of African rain forest and savanna C₃ plants. The results of the study on this topic are presented as Chapter 2. The second part of this thesis deals with the correspondence of the recent continental vegetation of southwest Africa with the lipid composition preserved in southeast Atlantic Ocean margin surface sediments. The recovery sites of the sediments constitute an isobathic (ca. 1300 m) transect from 2°N to 28°S. This part focuses on the *n*-alkane characteristics and was split into two publications. The first sediment transect publication (Chapter 3) deals with chain length distribution parameters and molecular stable carbon isotope characteristics. The second sediment transect manuscript (Chapter 4) analyses the correlation of the hydrogen isotope compositions of sediment-derived *n*-alkanes with those of the continental precipitation.

As all publications bear the names of several co-authors, it is clarified below which parts of the individual publications were contributed by the author herself. A short overview on the individual Chapters is also given.

Chapter 2: Distribution patterns and stable carbon isotopic composition of alkanes and alkan-1-ols from plant waxes of African rain forest and savanna C₃ species

For the first publication molecular stable carbon isotope compositions of long-chain wax *n*-alkanes and *n*-alkan-1-ols as well as their distribution patterns in waxes of 69 African C₃ plant species were analysed. The sample selection, the organisation of the cooperation as well as retrieval of rain forest plant leaf samples from the herbarium in Wageningen (The Netherlands) was handled by the author herself. She investigated 52 plants and Heiko Moossen analysed additional 17 rain forest plants for his diploma thesis, supervised by the author. The evaluation and interpretation of the results and the development of the concept, the writing and editorial handling of the publication was mainly done by the author herself, supported by suggestions from Florian Rommerskirchen (Marum, University of Bremen, Germany) and Jürgen Rullkötter (ICBM, University of Oldenburg, Germany).

This publication aims at the characterisation of the signatures of tropical and subtropical rain forest and savanna C₃ plants. Analytical results for 45 savanna species and 24 rain forest plants sampled in their natural habitats were presented. Contents and distribution patterns of long-chain *n*-alkanes and *n*-alkan-1-ols as well as bulk and molecular carbon isotopic data are presented. It arose that the variations of the analysed parameters among different growth forms (herb, shrub, liana, and tree) are small within the vegetation zones, but characteristic differences occur between the signatures of rain forest and savanna plants. Therefore, averaged histograms for rain forest and savanna C₃ plants were presented and compared with previously published data of tropical C₄ grasses (Rommerskirchen et al., 2006b). Trends to longer *n*-alkane chains and less negative carbon isotopic values are evident from rain forest over C₃ savanna to C₄ vegetation. For *n*-alkanols of rain forest plants the maximum of the averaged distribution pattern is between those of C₃ savanna plants and C₄ grasses. The characteristics of the averaged presentations for tropical and subtropical vegetation confirm these molecules to be useful biomarker proxies for studies analysing the expansion and contraction of African vegetation zones.

Chapter 3: *n*-Alkane parameters derived from a deep-sea sediment transect off southwest Africa reflect continental vegetation and climate conditions

For the second manuscript the stable carbon isotope compositions of long-chain wax *n*-alkanes as well as their distribution patterns in lipid fractions of ocean margin sediment samples constituting an isobathic transect off southwest Africa were evaluated. The samples were analysed by Tanja Badewien for her diploma thesis, supervised by the author. Additional analyses (bulk parameters) were done by technical assistants supervised by the author. The interpretation of the results, the development of the concept for the publication as well as the discussion of the results and the writing of the manuscript were handled by the author, supported by suggestions from Enno Schefuß (Marum, University of Bremen, Germany) and Jürgen Rullkötter (ICBM, University of Oldenburg, Germany).

The results for the sediment transect ranging from 2°N to 28°S reveal southward trends to longer chain lengths and less negative stable carbon isotope composition reflecting the changing contribution of plants employing different photosynthetic pathways (C₃ and C₄). Both the stable carbon isotope composition and the average chain-length distribution were found suitable to estimate the relative C₄ plant contribution to the sediments. The calculated C₄ plant proportion corresponded to the C₄ plant abundance in postulated continental catchment areas if non-latitudinal eolian transport was taken into account. Furthermore, the calculated C₄ contribution to the sediments correlates significantly with the mean annual precipitation and the aridity indices of the postulated catchment areas which may constitute a useful tool to deduce the aridity prevailing in ancient times. Thus, this part of the study corroborates and expands the potential of *n*-alkanes in continental margin sediments for the reconstruction of recent and ancient continental vegetation and climate conditions.

Chapter 4: Stable hydrogen isotopic compositions of land plant derived *n*-alkanes in marine sediments reflect δD values of continental precipitation

For the third manuscript the stable hydrogen isotope compositions of long-chain plant wax *n*-alkanes in lipid fractions of an isobathic deep-sea sediment transect were evaluated. The analytical work-up was done by Tanja Badewien for her diploma thesis, supervised by the author. The hydrogen isotope analyses of the aliphatic compounds were handled by the author. The interpretation of the results, the development of the concept for the publication as well as the discussion of the results and the writing of the manuscript were handled by the author, supported by suggestions from Enno Schefuß (Marum, University of Bremen, Germany) and Jürgen Rullkötter (ICBM, University of Oldenburg, Germany).

The hydrogen isotope ratios of the *n*-alkanes in the ocean margin sediments correlate with modelled hydrogen isotope compositions of mean annual, growing-season and end of growing-season precipitation of continental source areas along postulated transport pathways. Despite the huge gradient of climatic conditions and vegetation characteristics and neglecting potential inconsistencies in catchment area definitions, the apparent fractionations especially for the *n*-C₂₉ and *n*-C₃₁ alkane and mean annual precipitation are fairly constant ($-109 \pm 3\text{‰}$ and $-115 \pm 3\text{‰}$, respectively) and show no significant correlation with environmental conditions. This corroborates the potential of hydrogen isotope ratios of leaf wax *n*-alkanes preserved in continental margin sediments for palaeo-climatic studies. They may be directly converted into δD ratios of ancient precipitation by the presented fractionation factors to elucidate changes of the hydrogen isotope composition of precipitation on the adjacent continent and their potential climatic causes.

2. Distribution patterns and stable carbon isotopic composition of alkanes and alkan-1-ols from plant waxes of African rain forest and savanna C₃ species

Angela Vogts, Heiko Moossen, Florian Rommerskirchen, Jürgen Rullkötter

This chapter was published: Vogts, A., Moossen, H., Rommerskirchen, F., and Rullkötter, J., 2009. Distribution patterns and stable carbon isotopic composition of alkanes and alkan-1-ols from plant waxes of African rain forest and savanna C₃ species. *Organic Geochemistry* 40, 1037-1054, doi:10.1016/j.orggeochem.2009.07.011.

2.1 Abstract

Leaf wax components of terrestrial plants are an important source of biomass in the geological records of soils, lakes and marine sediments. Relevant to the emerging use of plant wax derived biomarkers as proxies for past vegetation composition this study provides key data for C₃ plants of tropical and subtropical Africa. We present analytical results for 45 savanna species and 24 rain forest plants sampled in their natural habitats. Contents and distribution patterns of long chain *n*-alkanes (*n*-C₂₅ to *n*-C₃₅) and *n*-alkan-1-ols (*n*-C₂₄ to *n*-C₃₄) as well as bulk and molecular carbon isotopic data are presented. The variations of the analysed parameters among different growth forms (herb, shrub, liana, and tree) are small within the vegetation zones, whereas characteristic differences occur between the signatures of rain forest and savanna plants. Therefore, we provide averaged histogram representations for rain forest and savanna C₃ plants. The findings were compared to previously published data of typical C₄ grass waxes of tropical and subtropical Africa. Generally, trends to longer *n*-alkane chains and less negative carbon isotopic values are evident from rain forest over C₃ savanna to C₄ vegetation. For *n*-alkanols of rain forest plants the maximum of the averaged distribution pattern is between those of C₃ savanna plants and C₄ grasses. The averaged presentations for tropical and subtropical vegetation and their characteristics may constitute useful biomarker proxies for studies analysing the expansion and contraction of African vegetation zones.

2.2 Introduction

Wax lipids cover all aerially exposed organs of higher land plants and can constitute of a wide range of chemical components. In virtually all plant waxes long chain *n*-alkanes and *n*-alkan-1-ols are abundant and can account for more than 60% of the epicuticular lipids (Tulloch, 1976). After the decay of plants both compound classes are relatively resistant against degradation, although the stability is assumed to decrease from *n*-alkanes to *n*-alkan-1-ols (Poynter and Eglinton, 1991). These components can persist in the area of production and lead to a signal of the plant wax composition of local species in the underlying soil or in the sediments of nearby water bodies (Jansen et al., 2008). On the other hand, depending on environmental conditions, wax lipids can be transported over substantial distances by rivers and wind (Bird et al., 1995; Conte and Weber, 2002). Thus, biomarkers of terrestrial plants can end up in soils as well as in lake or ocean sediments and give an integrated signal of the wax composition of the plant species within the catchment area. If deposition is continuous and there is no selective degradation of certain compounds, chronological geological records of the original wax components can develop.

Commonly analysed characteristics of *n*-alkanes and *n*-alkan-1-ols are their chain length distribution patterns. Long chain *n*-alkanes typically occur in the *n*-C₂₅ to *n*-C₃₅ range (Chibnall et al., 1934) with characteristic odd over even carbon number predominance (Eglinton and Hamilton, 1967) and *n*-alkanols in the *n*-C₂₂ to *n*-C₃₄ range with even over odd carbon number predominance (Baker, 1982). It has been suggested that plants of warmer tropical and subtropical climates biosynthesise longer chain wax components than plants in habitats of the temperate regions (Gagosian and Peltzer, 1986). This concept has been used as a proxy for climate dependent vegetation changes (e.g., Poynter et al., 1989; Rommerskirchen et al., 2006a).

Another valuable characteristic of plant wax constituents is their carbon isotopic composition. Carbon of plant constituents like leaf waxes can derive from different CO₂ fixation pathways. Nearly 90% of the estimated 250,000 land plant species use the C₃ photosynthetic pathway (CBB Cycle; Bassham et al., 1954), i.e. almost all woody species of temperate and wet tropical re-

2. Characteristics of C₃ rain forest and C₃ savanna plant wax lipids

gions (Sage, 2001). The C₄ metabolism (Hatch-Slack-Cycle; Hatch and Slack, 1966), another principal CO₂ fixation pathway, is an elaboration of the CBB Cycle and pre-concentrates CO₂ by a complex biochemical process (Hatch, 1987). This CO₂ concentrating mechanism prevents ineffective photorespiration and leads to an improved water use efficiency under conditions of high temperature, high light intensity, high salinity, limited water supply and/or low CO₂ concentrations (Downes, 1969; Björkmann, 1976). But extra energy is needed for the advantageous additional process. Hence, C₄ plants can outcompete C₃ plants successfully only in some regions like the sunny subtropical and tropical savanna and desert areas (Sage, 2004). The different CO₂ fixation pathways cause characteristic differences in the stable carbon isotope composition of plant material ($\delta^{13}\text{C}_{\text{PM}}$) from -21‰ to -35‰ and from -9‰ to -20‰ in C₃ and C₄ plants, respectively (O'Leary, 1988). Leaf wax lipids become more depleted in ¹³C during biosynthesis than the total biomass, so that their $\delta^{13}\text{C}$ values vary between -29‰ and -39‰ in C₃ and between -14‰ and -26‰ in C₄ plants, respectively (Bi et al., 2005 and references therein). Thus, the carbon isotopic composition of higher land plant lipids can be used to evaluate the contribution of C₃ and C₄ plants to geological archives.

One focus of studies combining stable carbon isotopic composition and chain length distribution patterns has been the African continent. Studies of geological records found a shift to longer chain homologues accompanied by heavier $\delta^{13}\text{C}$ values of these components from rain forest over savanna to open grassland regions. The authors of these investigations attributed their findings to an increase in abundance of C₄ vegetation, especially C₄ grasses growing in arid grasslands, accompanied by a decrease of woody C₃ species (Rommerskirchen et al., 2003; Schefuß et al., 2004; Rommerskirchen et al., 2006a; Weijers et al., 2009).

Relevant to the emerging use of the characteristics of long chain aliphatic biomarkers as proxies for continental vegetation changes in Africa, the present study provides comprehensive analytical data for the plant wax composition of tropical and subtropical species from Africa. We focused our investigation on C₃ plants with different growth forms (herb, shrub, liana, and

2. Characteristics of C₃ rain forest and C₃ savanna plant wax lipids

tree) sampled in their natural habitats and not under artificial conditions of greenhouses. Contents of wax *n*-alkanes and free *n*-alkan-1-ols as well as bulk and molecular stable carbon isotopic compositions are presented for 45 plant samples collected in savanna regions and 24 rain forest species. We combine our results with previously published analytical data from tropical and subtropical C₄ grasses from Rommerskirchen et al. (2006b). Thus, we expand the knowledge about the wax composition of tropical and subtropical African plants and provide key data for the increasing use of plant wax constituents for palaeoenvironmental studies.

2.3 Sampling area, samples and methods

2.3.1 Sampling area: *Distribution of vegetation zones in Africa*

In general, the vegetation types on the African continent grade south- and northwards from the equatorial evergreen rain forest over dry evergreen and deciduous forests, wood- and shrublands to grasslands and deserts (Fig. 2.1). At the high latitude coastlines southern subtropical and northern Mediterranean deciduous forests prevail. There is a clear gradient from the equator to the tropics from dense evergreen formations to dry open land cover plant classes, corresponding to the rainfall gradient (Mayaux et al., 2004).

Rain forest vegetation is characterised by a large diversity of species. Woody plants form the major part of the biome (Richards, 1996). Tall individual trees (emergents, up to 60 m) stand above a closed canopy of trees (10 to 40 m). Beneath the canopy are subdominant or younger trees and a layer of shrubs. Ground herbs are normally poorly represented in undisturbed rain forest. Epiphytic herbs are usually present, but they are only abundant in the wetter upland rain forest regions. Lianas are found in all layers of the rain forest and can constitute up to 30% of the rain forest flora (White, 1983). The evergreen African rain forest extends to about 9°S and N and is increasingly confined to river valleys towards its limits, whereas dry evergreen forests and further on also deciduous species gain importance. The closed forest (without grass layer) often abruptly passes into a wide zone of savanna wood- and shrublands (Richards, 1996). Deciduous woody species can cover up to

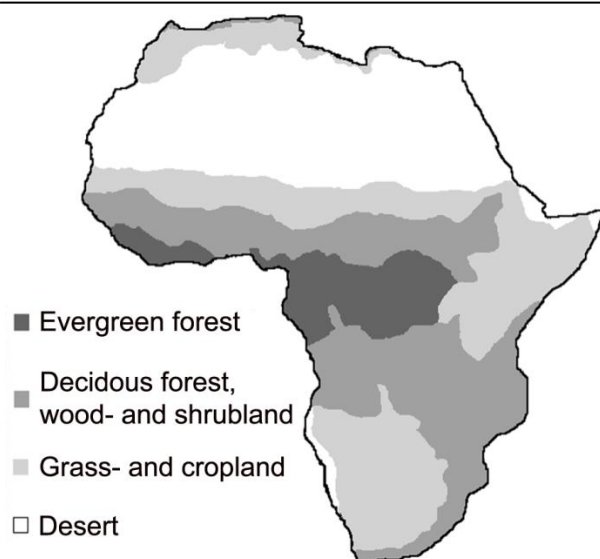


Figure 2.1 Simplified land cover map of Africa; based on Mayaux et al. (2004).

60% of the savanna (Cole, 1986) but the amount of woody C₃ vegetation decreases with increasing aridity, accompanied by increasing C₄ grass abundance.

2.3.2 Sample material

For this study we analysed 45 samples of C₃ plants collected in savanna regions and 24 rain forest species. Information about sampling localities and dates is compiled in Table 2.1. Of *Acacia mellifera* and *Colophospermum mopane* we analysed duplicate samples and of *Combretum indicum* we used three samples collected at different locations. The classification into trees or shrubs follows the description of the collectors. Some species can occur as tree or shrub depending on the growth conditions. Therefore, the two samples of *Acacia mellifera* are allocated to different growth form groups. The savanna species analysed comprise some of the dominant woody species of this vegetation zone (Scholes et al., 2002) like *Acacia* sp., *Colophospermum mopane*, *Burkea africana*, *Dichrostachys cinerea*, and *Grewia flavescens*. Among the herbaceous species are plants (*Ocimum basilicum*, *Ipomoea cordofana*), which were reported to be common, even sometimes dominant weeds in the Gezira Agricultural Scheme of Sudan (Karar et al.,

2. Characteristics of C₃ rain forest and C₃ savanna plant wax lipids

2005). Determination of abundant rain forest species is not that easy, because of the huge plant diversity in this vegetation zone. We therefore selected plants from sites near rivers, because we assume that these have a high contribution to the fluvial transport of terrestrial plant lipids to the lake and ocean sediments, which are the focus of palaeo-environmental studies.

Rain forest plant material was provided by Prof. Dr. Marc Sosef, Biosystematics Group, University of Wageningen, The Netherlands. The samples were collected during different field trips in the years 1992 to 2005 by J.J. Wieringa, F.J. Breteler, C.C.H. Jongkind, L.J.G. van der Maesen, N. Sokpon, and J.L.C.H. van Valkenburg at elevations up to 500 m. Plant material was dried between newspaper sheets at 70°C and stored at 20°C between such papers at the archive of the National Herbarium of the Netherlands (Wageningen branch). From the dried herbaria species we selected and sampled leaves with the support of F. Aleva and J. Wieringa. The plants were not poisoned or sprinkled with alcohol. We transported the samples in solvent rinsed vials and ground them for analysis. Newspaper sheets as a possible contamination source were analysed for *n*-alkanes and *n*-alkanols and revealed no significant amounts of these compounds in the chain length interval important for this study.

Savanna samples were made available by Dr. R.W. Mayes of the Macaulay Institute in Aberdeen (United Kingdom) and Dr. L. Dupont of the University of Bremen (Germany). Plants provided by Dr. R.W. Mayes were collected in Tanzania and Sudan in 1992 and 2003 for plant lipid analysis during animal diet studies. Collected material was considered to be representative of what animals would select to eat. Therefore, for some smaller plants either the whole plant or plant parts including stems and/or flowers were provided. Plant material from Tanzania was collected from small trees and shrubs (less than 3 m height) shaded by taller trees. The plants were used to provide forage to farm livestock and collected leaves were fully developed without signs of senescence. Scissors were used to harvest the samples into paper bags. Plant material was dried at 85 °C and stored in paper bags prior to grinding. Species from Sudan were collected from different rangeland areas and were sun dried prior to grinding. No detailed information was

Table 2.1 C₃ plant species studied: Analysed subspecies arranged according to growth form and habitat; used plant part, date, country, location, latitude and longitude of collection.

Habitat and growth form/Analysed Subspecies	Used plant parts	Collectet	Country, Location	Latitide	Longitude
Rainforest lianas					
<i>Combretum conchipetalum</i> Engl. & Diels	leaves	07/08/1992	Gabon, Maambi river	3°01'S	10°22'E
<i>Combretum racemosum</i> P.Beauv.	leaves	30/10/2000	Gabon, Ogooué-Ivindo	1°15.95'N	14°07.09'E
<i>Cuervea macrophylla</i> (Vahl) R.Wilczek ex N.Hallé	leaves	16/03/1994	Gabon, Nyanga river	2°56.2'S	10°21.8'E
<i>Landolphia mannii</i> Dyer	leaves	16/03/1994	Gabon, Nyanga river	2°57.2'S	10°21.6'E
<i>Paullinia pinnata</i> L.	leaves	25/12/2000	Gabon, Zadié river	1°00.75'N	13°58.96'E
<i>Psychotria ealensis</i> De Wild.	leaves	25/12/2000	Gabon, Zadié river	1°00.75'N	13°58.96'E
Rainforest shrubs					
<i>Coffea</i> sp. L.	leaves	05/05/1992	Gabon, Ogooué River	0°48'S	12°5'E
<i>Combretum erosum</i> Jongkind	leaves	21/01/1999	Gabon, Ogooué-Lolo	0°41'S	11°55'E
<i>Combretum indicum</i> (L.) DeFilipps	leaves	26/11/2003	Gabon, Nyanga River	2°58.53'S	10°28.77'E
<i>Combretum indicum</i> (L.) DeFilipps	leaves	12/12/1998	Benin, Zou, Covè	7°2'N	2°28'E
<i>Combretum indicum</i> (L.) DeFilipps	leaves	08/11/1999	Benin, Mono River	6°5'N	1°36'E
<i>Combretum molle</i> R.Br. ex G.Don	leaves	18/11/1999	Benin, Atakora, Kouandé	10°04.5'N	1°33.9'E
<i>Englerina gabonensis</i> (Engl.) S.Balle	leaves	07/08/1992	Gabon, Maambi river	3°01'S	10°22'E
<i>Ficus natalensis</i> subsp. <i>leprieurii</i> (Miq.) C.C.Berg	leaves	06/01/2001	Congo, Djoua river	1°22.6'N	14°05.3'E
<i>Ficus thonningii</i> Blume	leaves	17/11/1999	Benin, Perma river	10°08.1'N	1°26.9'E
<i>Oxyanthus unilocularis</i> Hiern	leaves	16/03/1994	Gabon, Nyanga river	2°56.5'S	10°19.7'E
<i>Stipularia africana</i> P.Beauv.	leaves	25/12/2000	Gabon, Zadié river	1°00.75'N	13°58.96'E
Rainforest trees					
<i>Berlinia confusa</i> Hoyle	leaves	05/05/1992	Gabon, Ogooué-Lolo	0°40'S	13°E
<i>Cynometra mannii</i> Oliv.	leaves	14/04/2005	Gabon, Ogooué-Maritime	1°59.71'S	10°25.83'
<i>Ficus ottoniifolia</i> (Miq.) Miq.	leaves	03/03/1990	Gabon, Ogooué-Ivindo	0°51'N	13°27'E
<i>Oncoba spinosa</i> Forssk.	leaves	10/08/2005	Burkina Faso, Bougouriba	n.d.	n.d.
<i>Psychotria djumaensis</i> De Wild.	leaves	25/12/2000	Gabon, Zadié river	1°00.75'N	13°58.96'E
<i>Treulia africana</i> Decne.	leaves	05/05/1992	Gabon, Ogooué River	0°48'S	12°5'E
<i>Uapaca guineensis</i> Müll. Arg.	leaves	03/11/2003	Gabon, Ngounié	1°37.6'S	10°42.3'
Savanna herbs					
<i>Abutilon graveolens</i> Roxb. ex Hornem.	whole plant with fruits	2003, season unknown	Sudan	n.d	n.d
<i>Achyranthes aspera</i> L.	whole plant	2003, season unknown	Sudan	n.d	n.d
<i>Digeria muricata</i> L.	whole plant with flower	2003, season unknown	Sudan	n.d	n.d
<i>Heliotropium</i> L. sp.	whole plant	2003, season unknown	Sudan	n.d	n.d
<i>Ipomoea cordofana</i> Choisy	whole plant with fruits	2003, season unknown	Sudan	n.d	n.d
<i>Ocimum basilicum</i> L.	whole plant	2003, season unknown	Sudan	n.d	n.d
<i>Vigna</i> L. sp.	whole plant	2003, season unknown	Sudan	n.d	n.d
<i>Xanthium brasiliicum</i> Vell.	whole plant with fruits	2003, season unknown	Sudan	n.d	n.d

Table 2.1 (continued)

Habitat and growth form/Analysed Subspecies	Used plant parts	Collectet	Country, Location	Latitude	Longitude
<i>Acacia nebrownii</i> Burtt Davy	leaves	12/04/2005	Namibia, Namatomi	18°45'S	16°56'E
<i>Catophractes alexandri</i> D.Don	leaves	13/04/2005	Namibia, Baobab Corner	18°29'S	13°46'E
<i>Crassocephalum mannii</i> (Hook.f.) Milne-Redh.	whole plant	1992 (wet season)	Tanzania, Morogoro	n.d.	n.d.
<i>Dichrostachis cinera</i> L.	leaves	13/04/2005	Namibia, Baobab Corner	18°29'S	13°46'E
<i>Grewia flavescens</i> Juss.	leaves	09/04/2005	Namibia, Omatjenni	20°25'S	16°29'E
<i>Grewia flavescens</i> Juss.	leaves	13/04/2005	Namibia, Baobab Corner	18°29'S	13°46'E
<i>Gymnosporia buxifolia</i> (L.) Szyszyl	leaves	09/04/2005	Namibia, Omatjenni	20°25'S	16°29'E
<i>Salvadora persica</i> Wall.	leaves	15/04/2005	Namibia, Welwitschia Plain	22°42'S	14°57'E
Savanna trees					
<i>Acacia erioloba</i> E.Mey.	leaves	15/04/2005	Namibia, Welwitschia Plain	22°42'S	14°57'E
<i>Acacia karroo</i> Hayne	leaves	09/04/2005	Namibia, Omatjenni	20°25'S	16°29'E
<i>Acacia kirkii</i> Oliv.	leaves	13/04/2005	Namibia, Baobab Corner	18°29'S	13°46'E
<i>Acacia luederitzii</i> Engl.	leaves	09/04/2005	Namibia, Omatjenni	20°25'S	16°29'E
<i>Acacia mellifera</i> (Vahl) Benth.	leaves	20/01/2003	Sudan	n.d.	n.d.
<i>Acacia senegal</i> (L.) Willd.	leaves	20/01/2003	Sudan, Hashab	n.d.	n.d.
<i>Adansonia digitata</i> L. ³	leaves	13/04/2005	Namibia, Baobab Corner	18°29'S	13°46'E
<i>Albizia anthelmintica</i> (A. Rich.) Brongn.	leaves	09/04/2005	Namibia, Omatjenni	20°25'S	16°29'E
<i>Balanites aegyptiaca</i> (L.) Del.	leaves	20/05/2003	Sudan, Higlig	n.d.	n.d.
<i>Boscia albitrunca</i> (Burch.) Gilg & Ben.	leaves	09/04/2005	Namibia, Omatjenni	20°25'S	16°29'E
<i>Boscia foetida</i> Schinz	leaves	09/04/2005	Namibia, Omatjenni	20°25'S	16°29'E
<i>Burkea africana</i> Hook	leaves	13/04/2005	Namibia, Baobab Corner	18°29'S	13°46'E
<i>Colophospermum mopane</i> (Kirk ex Benth.) Kirk ex J.Léon.	leaves	12/04/2005	Namibia, Namatomi	18°45'S	16°56'E
<i>Colophospermum mopane</i> (Kirk ex Benth.) Kirk ex J.Léon.	leaves	13/04/2005	Namibia, Baobab Corner	18°29'S	13°46'E
<i>Combretum apiculatum</i> Sond.	leaves	13/04/2005	Namibia, Baobab Corner	18°29'S	13°46'E
<i>Combretum imberbe</i> Wawra	leaves	12/04/2005	Namibia, Namatomi	18°45'S	16°56'E
<i>Commiphora glaucescens</i> Engl.	leaves	13/04/2005	Namibia, Baobab Corner	18°29'S	13°46'E
<i>Commiphora merkeri</i> Engl.	leaves	13/04/2005	Namibia, Baobab Corner	18°29'S	13°46'E
<i>Euclea pseudebenus</i> E.Mey.	leaves	15/04/2005	Namibia, Welwitschia Plain	22°42'S	14°57'E
<i>Faidherbia albida</i> (Delile) A.Chev.	leaves	15/04/2005	Namibia, Welwitschia Plain	22°42'S	14°57'E
<i>Leucaena leucocephala</i> (Lam.) de Wit	leaves	1992 (wet season)	Tanzania, Morogoro	n.d.	n.d.
<i>Morus alba</i> L.	leaves	1992 (wet season)	Tanzania, Morogoro	n.d.	n.d.
<i>Sclerocarya birrea</i> (A. Rich.) subsp. <i>caffra</i> (Sond.) Kokwaro	leaves	13/04/2005	Namibia, Baobab Corner	18°29'S	13°46'E
<i>Sesbania sesban</i> (L.) Merr.	leaves	1992 (wet season)	Tanzania, Morogoro	n.d.	n.d.
<i>Tamarix usneoides</i> E.Mey. ex Bunge	leaves	15/04/2005	Namibia, Welwitschia Plain	22°42'S	14°57'E
<i>Terminalia prunioides</i> M.A.Lawson	leaves	13/04/2005	Namibia, Baobab Corner	18°29'S	13°46'E
<i>Ziziphus mucronata</i> Willd.	leaves	13/04/2005	Namibia, Baobab Corner	18°29'S	13°46'E
<i>Ziziphus spina-christi</i> (L.) Willd.	leaves	20/01/2003	Sudan	n.d.	n.d.

2. Characteristics of C₃ rain forest and C₃ savanna plant wax lipids

available about sampling location and the amount of light the plants from Sudan received. Ground samples of Tanzanian and Sudanese plants were stored in annealed glassware.

Savanna plant material provided by Dr. L. Dupont was collected together with E. Marais during a field trip in Namibia in 2005. All samples originate from open areas and were taken at reaching height. During sampling care was taken to prevent contamination by skin contact. Samples were transported to Germany in paper bags. They were freeze dried and ground.

2.3.3 Analytical methods

In order to ascertain comparability with previous data obtained from geological samples, we used workup methods established for the analysis of long chain land plant wax components in marine sediments (Rommerskirchen et al., 2003; Rommerskirchen et al., 2006a). To avoid lipid contamination, skin contact with the samples was carefully avoided during the analytical procedure. All glassware and laboratory equipment was cleaned with dichloromethane and *n*-hexane. All chemicals were appropriately pure for gas chromatographic residue analysis.

Plant material (0.1 to 0.7 g) was extracted in an Accelerated Solvent Extractor (ASE) using dichloromethane and methanol (99/1, v/v; three times 5 min, 70 bar, 100°C). ASE extraction is faster and less solvent consuming compared to ultrasonication or Soxhlet extraction while yielding comparable results. Completeness of extraction was confirmed by repeated extractions of randomly selected samples. Squalane and 5 α -androstane-3 β -ol were added to the extracts as internal standards for compound class separation and analysis because their behaviour during liquid and gas chromatography is similar to the lipids of interest and they do not occur in plant waxes.

The total extracts were dissolved in *n*-hexane and insoluble components were removed by filtration over NaSO₄. The *n*-hexane soluble plant constituents were separated by medium pressure liquid chromatography (Radke et al., 1980) into fractions of aliphatic/alicyclic hydrocarbons, aromatic hydrocarbons and polar heterocomponents (NSO). From the NSO fraction carboxylic acids were separated by column chromatography with potassium

2. Characteristics of C₃ rain forest and C₃ savanna plant wax lipids

hydroxide impregnated silica gel as stationary phase. The *n*-alkanols were isolated from the neutral heterocomponents by the urea adduction procedure described by Rommerskirchen et al. (2006b). Blank samples of purified sand underwent the same workup procedure as the plant samples and showed no contamination.

The wax lipids were analysed by gas chromatography with flame ionisation detection (GC-FID) using a high temperature capillary column (J&W, DB-5HT, 30 m length, 0.25 mm inner diameter, 0.1 µm film thickness) with helium as carrier gas. The GC oven was programmed from 60°C (2 min) to 350°C at a rate of 3°C min⁻¹, followed by an isothermal phase of 15 min. The injector temperature was programmed from 60°C (5 s) to 350°C (60 s) at 10°C s⁻¹. Compound identification was performed using an identical GC system coupled to a Finnigan SSQ 710 B mass spectrometer operated in electron impact mode (70 eV) at a scan rate of 1 scan s⁻¹ over the mass/charge ratios range from 50 to 650.

Plant wax biomarkers were identified by comparison of retention times with those in standard mixtures and their contents calculated as µg g⁻¹ dry plant material (DM) based on signal intensities of biomarkers and internal standards in the GC-FID traces. The differences in response between homologues of different chain lengths and internal standards were found to be negligibly small (coefficients of variation below 6%) and no trends of the response factors with chain length was observed. Squalane was used as internal standard for the *n*-alkanes whereas 5α-androstan-3β-ol was used for *n*-alkan-1-ol quantification. For an assessment of systematic variations in the distribution patterns of biomarkers, contents of individual homologues were converted into percentages of biomarkers within the homologous series to allow comparison of samples after averaging.

Bulk isotopic composition of ground, dried plant material ($\delta^{13}\text{C}_{\text{PM}}$) was determined using a Carlo Erba Elemental Analyser (EA) 1108 coupled to a MAT 252 isotope ratio mass spectrometer (irm-MS). Molecular isotopic compositions were analysed by a GC system coupled to a MAT 252 or MAT 253 isotope ratio mass spectrometer (GC-irm-MS). Calibration of isotope analysis was performed by injecting several pulses of CO₂ at the beginning and at the

2. Characteristics of C₃ rain forest and C₃ savanna plant wax lipids

end of each GC run, by using squalane as an internal standard and by measurement of certified standards between sample runs. For analysis, *n*-alkanols were converted to their trimethylsilyl ether derivatives. Carbon isotopic values of *n*-alkanols are corrected for the contribution of the trimethylsilyl group from derivatisation. GC-irm-MS and EA-irm-MS analyses were run in duplicate or triplicate with standard deviations better than 0.5‰. Isotopic ratios are expressed as $\delta^{13}\text{C}$ values in per mil relative to the V-PDB standard. The $\delta^{13}\text{C}$ ratios are expressed as single weighted mean averages for the odd carbon numbered *n*-C₂₅ to *n*-C₃₅ alkanes ($\delta^{13}\text{C}_{\text{WMA25-35}}$) as well as for the even carbon numbered *n*-C₂₂ to *n*-C₃₄ alkanols ($\delta^{13}\text{C}_{\text{WMA24-34}}$) in order to encompass the variability of data for individual homologues. Biosynthetic stable carbon isotope fractionation between bulk plant material and individual lipids (ϵ_{PM}) was calculated using following equation (Chikaraishi et al., 2004):

$$\epsilon_{\text{PM}} = 1000[(\delta^{13}\text{C}_{\text{WMA}}+1000)/(\delta^{13}\text{C}_{\text{PM}}+1000)-1]$$

2.4 Results

2.4.1 Content and carbon number distribution of long chain *n*-alkanes

The total content of odd carbon numbered *n*-C₂₅ to *n*-C₃₅ alkanes (TCOC₂₅₋₃₅) of all samples varies significantly between 7.4 $\mu\text{g g}^{-1}$ DM and 2770 $\mu\text{g g}^{-1}$ DM (Fig. 2.2). Lipids in the aliphatic/alicyclic hydrocarbon fractions are dominated by homologous series of *n*-alkanes mainly in the carbon number range of 25 to 35. Shorter and longer chain *n*-alkanes were detected only in small quantities. A distinct odd/even predominance leads to high CPI₂₅₋₃₅ values (carbon preference index for *n*-C₂₅ to *n*-C₃₅ alkanes; modified after Bray and Evans, 1961) ranging from 3.3 to 30 (Fig. 2.2). The overall chain length distribution, best expressed by the average chain length parameter in the odd carbon number range from 25 to 35 (ACL₂₅₋₃₅; Poynter et al., 1989), ranges from 27.08 to 31.91. In our data set the distribution of *n*-alkanes of most plants maximises either at the *n*-C₂₉ or the *n*-C₃₁ homologue. Other maxima were observed for six samples of savanna trees (*n*-C₂₇ alkane), whereas three savanna herbs exhibit a maximum at the *n*-C₃₃ alkane (cf. Table 2.2).

2. Characteristics of C₃ rain forest and C₃ savanna plant wax lipids

Averaged *n*-alkane distribution patterns of all plants are shown in Fig. 2.3. Histograms are separately presented for several growth forms within the different vegetation zones. Averaged histogram representations for samples of trees, shrubs and lianas from the rain forest show similarly narrow patterns with abundant *n*-C₂₉ and *n*-C₃₁ alkanes. Other individual alkanes contribute less than 10% to the compound class. The histograms maximise at the *n*-C₂₉ alkane and in the shrubs the *n*-C₃₁ alkane is slightly more abundant than in the other two plant types (Fig. 2.3a-c).

Averaged leaf wax *n*-alkane distribution patterns of savanna plants (Fig. 2.3d-f) exhibit a wider carbon number range and a more bell shaped distribution of odd carbon number *n*-alkanes compared to the rain forest species. The main *n*-alkanes of savanna plant leaf waxes have carbon numbers from 27 to 33, and the maximum always occurs at the C₃₁ homologue. The abundance of *n*-C₂₅ to *n*-C₂₉ alkanes decreases from trees over shrubs to herbs, whereas the abundance of the *n*-C₃₁ (for shrubs) and *n*-C₃₃ alkanes (for herbs) increases. This is numerically expressed by ACL₂₅₋₂₅ values increasing from 29.54 to 30.47.

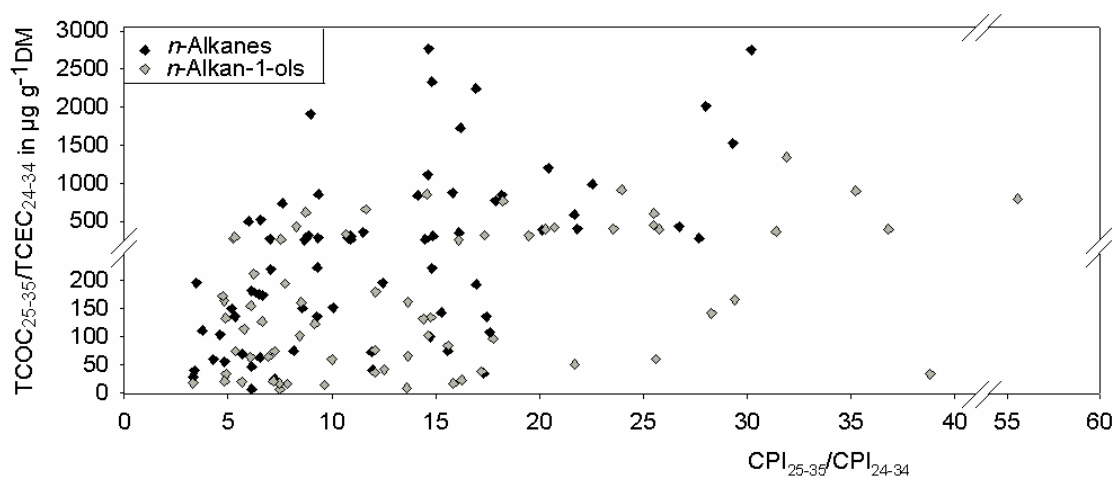


Fig. 2.2 Variation of Carbon Preference Index (CPI) and lipid abundance for *n*-alkanes (black) and *n*-alkan-1-ols (grey).

Table 2.2 *n*-Alkane data of C₃ plants studied: Analysed subspecies arranged according to growth form and habitat; individual *n*-alkane content in µg g⁻¹ dry matter (DM), TCOC₂₅₋₃₅, CPI₂₅₋₃₅ and ACL₂₅₋₃₅ values. Boldface values: Distribution pattern maxima.

Habitat and growth form	<i>n</i> -Alkane content (µg g ⁻¹ DM)													TCOC ₂₅₋₃₅	CPI ₂₅₋₃₅	ACL ₂₅₋₃₅
	24	25	26	27	28	29	30	31	32	33	34	35	36			
Analysed subspecies																
Rainforest lianas																
<i>Combretum conchipetalum</i>	8.2	8.8	5.0	25.4	13.1	810	23.1	135	2.3	5.6	n.d.	1.1	n.d.	986	22.6	29.22
<i>Combretum racemosum</i>	4.3	3.3	n.d.	4.1	n.d.	156	7.6	106	2.4	8.5	n.d.	n.d.	n.d.	278	27.7	29.81
<i>Cuervea macrophylla</i>	2.1	2.6	1.5	2.8	1.2	88.6	6.4	93.1	2.3	6.0	n.d.	n.d.	n.d.	193	17.0	30.00
<i>Landolphia mannii</i>	3.7	6.8	3.3	31.2	6.2	237	6.3	97.5	2.0	12.9	1.2	3.4	1.6	389	20.1	29.46
<i>Paullinia pinnata</i>	3.8	5.8	3.8	17.2	7.7	427	23.7	380	11.1	13.7	n.d.	n.d.	n.d.	844	18.2	29.90
<i>Psychotria ealensis</i>	4.4	4.7	2.0	15.2	7.4	453	15.4	103	1.9	4.3	n.d.	n.d.	n.d.	581	21.7	29.30
Rainforest shrubs																
<i>Coffea</i> sp.	10.1	15.7	13.0	12.5	8.1	484	25.9	317	6.0	33.8	1.5	13.3	1.3	876	15.8	29.87
<i>Combretum erosum</i>	2.5	3.6	1.9	21.6	3.5	100	1.6	18.5	2.3	n.d.	n.d.	n.d.	n.d.	143	15.3	28.86
<i>Combretum indicum</i>	7.4	5.5	5.3	36.7	14.9	1091	31.6	779	18.7	96.0	1.2	2.3	n.d.	2010	28.0	29.93
<i>Combretum indicum</i>	9.9	5.5	2.8	4.2	2.3	373	24.5	1019	21.7	122	0.6	2.6	n.d.	1526	29.3	30.65
<i>Combretum indicum</i>	30.1	28.6	25.6	22.0	15.3	202	26.5	538	20.9	61.9	1.3	1.2	0.3	854	9.4	30.37
<i>Combretum molle</i>	6.6	6.1	3.6	19.3	3.7	41.4	3.4	23.5	9.9	12.9	1.2	1.0	n.d.	104	4.6	29.40
<i>Englerina gabonensis</i>	6.9	7.3	4.2	79.4	94.9	1933	57.9	308	n.d.	n.d.	n.d.	n.d.	n.d.	2328	14.8	29.18
<i>Ficus natalensis</i> subsp. <i>Leprieurii</i>	3.9	5.5	1.6	25.6	12.1	611	26.7	125	2.5	2.4	n.d.	n.d.	n.d.	769	17.9	29.24
<i>Ficus thonningii</i>	6.3	8.2	8.7	11.4	6.8	84.4	6.9	63.3	4.0	7.9	n.d.	n.d.	n.d.	175	6.5	29.59
<i>Oxyanthus unilocularis</i>	1.6	2.6	1.4	9.6	10.6	363	27.8	415	15.7	42.3	3.3	1.4	n.d.	834	14.1	30.17
<i>Stipularia africana</i>	1.2	5.7	0.7	9.2	0.9	19.5	1.3	31.2	1.7	9.0	n.d.	n.d.	n.d.	74.6	15.6	29.77
Rainforest trees																
<i>Berlinia confusa</i>	7.5	7.9	3.6	114.3	67.6	1907	53.5	201	6.1	10.9	1.4	1.4	1.0	2242	16.9	29.09
<i>Cynometra mannii</i>	27.7	12.9	4.8	13.4	5.7	343	7.5	29.2	n.d.	1.9	n.d.	n.d.	n.d.	401	21.8	28.97
<i>Ficus ottoniifolia</i>	4.3	4.3	2.4	11.0	3.8	124	5.4	76.2	3.2	6.5	0.2	0.1	n.d.	222	14.8	29.63
<i>Oncoba spinosa</i>	n.d.	n.d.	n.d.	n.d.	n.d.	97.6	9.0	223	12.6	27.5	n.d.	n.d.	n.d.	348	16.1	30.60
<i>Psychotria djumaensis</i>	2.3	2.7	1.1	16.3	6.8	359	7.4	53.2	0.8	1.7	n.d.	n.d.	n.d.	432	26.7	29.16
<i>Treulia africana</i>	3.7	6.7	4.4	18.7	7.6	173	14.7	99.7	7.8	11.2	n.d.	n.d.	n.d.	309	8.9	29.58
<i>Uapaca guineensis</i>	2.8	3.1	1.6	2.3	1.9	75.9	14.6	141	9.4	32.6	1.6	2.0	n.d.	256	8.7	30.58
Savanna herbs																
<i>Abutilon graveolens</i>	4.8	11.9	3.2	20.4	8.5	46.4	7.1	42.2	4.4	13.8	0.9	1.4	0.5	136	5.3	29.44
<i>Achyranthes aspera</i>	6.6	8.8	5.6	10.1	9.5	24.9	12.4	47.4	20.7	100.0	6.3	5.2	0.6	196	3.5	31.40
<i>Digeria muricata</i>	4.8	16.2	3.5	26.0	4.6	45.1	9.3	116.0	5.3	19.6	0.4	0.4	0.2	223	9.3	29.88
<i>Heliotropium</i> sp.	3.6	13.4	2.4	15.1	4.9	51.9	5.5	36.6	3.1	32.3	0.8	2.1	0.8	151	8.6	29.87
<i>Ipomoea cordofana</i>	2.6	9.7	1.7	13.9	2.5	21.1	3.9	90.4	12.2	130.0	4.8	19.2	0.6	284	10.8	31.64
<i>Ocimum basilicum</i>	4.5	16.4	5.5	44.3	7.7	79.3	16.8	135.1	31.6	191.6	17.1	26.2	1.4	493	6.0	31.11
<i>Vigna</i> sp.	3.4	4.0	1.9	14.3	2.9	30.3	2.4	83.9	7.7	62.7	0.7	1.1	n.d.	196	12.4	30.94
<i>Xanthium brasiliicum</i>	2.4	4.3	2.3	33.6	8.9	70.5	9.2	51.6	4.4	13.5	0.9	1.5	0.7	175	6.7	29.47

Table 2.2 (continued)

Habitat and growth form	n-Alkane content (µg g ⁻¹ DM)													TCOC ₂₅₋₃₅	CPI ₂₅₋₃₅	ACL ₂₅₋₃₅
	Analysed subspecies	24	25	26	27	28	29	30	31	32	33	34	35			
Savanna shrubs																
<i>Acacia mellifera</i>	0.9	5.0	3.6	49.2	9.7	50.0	5.7	160	11.2	20.3	n.d.	n.d.	n.d.	285	9.3	29.99
<i>Acacia nebrownii</i>	0.4	1.6	0.6	6.5	1.3	7.9	0.6	6.3	0.6	2.6	0.1	0.2	n.d.	25.0	7.2	29.19
<i>Catophractes alexandri</i>	3.8	17.7	5.7	142.8	18.9	671	75.3	1505	82.9	428	5.4	5.0	n.d.	2770	14.7	30.59
<i>Crassocephalum mannii</i>	0.9	5.3	1.7	21.2	2.9	33.8	9.6	167	8.6	32.5	0.9	3.4	0.7	263	10.9	30.60
<i>Dichrostachis cinera</i>	n.d.	6.5	0.8	11.1	1.4	28.8	1.9	68.9	3.6	20.4	n.d.	1.0	n.d.	137	17.4	30.30
<i>Grewia flavescens</i>	n.d.	10.2	1.2	51.0	21.2	1494	50.3	1145	18.4	55.5	n.d.	n.d.	n.d.	2755	30.2	29.86
<i>Grewia flavescens</i>	1.9	1.9	9.7	22.3	7.4	435	32.7	598	24.3	47.0	1.5	4.1	0.8	1108	14.6	30.22
<i>Gymnosporia buxifolia</i>	1.8	3.4	3.0	22.1	6.0	46.5	9.2	112	10.6	34.9	2.2	2.0	n.d.	221	7.0	30.44
<i>Salvadora persica</i>	0.2	0.6	1.2	4.4	1.9	7.4	3.9	14.3	1.6	1.9	0.2	0.3	0.2	29.1	3.3	29.92
Savanna trees																
<i>Acacia erioloba</i>	1.4	8.3	9.8	39.2	13.9	47.4	3.3	12.1	1.5	4.3	n.d.	n.d.	n.d.	111	3.8	28.37
<i>Acacia karroo</i>	0.6	30.2	2.3	15.8	2.1	42.0	1.2	11.9	0.2	0.6	n.d.	0.1	n.d.	101	14.7	27.75
<i>Acacia kirkii</i>	n.d.	4.7	3.3	13.7	9.1	47.5	4.7	176	10.3	59.8	n.d.	n.d.	n.d.	301	10.9	30.81
<i>Acacia luederitzii</i>	1.1	7.6	4.7	16.5	6.0	80.1	2.8	28.9	0.8	3.4	n.d.	n.d.	n.d.	137	9.3	29.06
<i>Acacia mellifera</i>	3.0	10.9	6.2	62.8	11.5	40.0	5.8	53.1	5.3	15.8	n.d.	n.d.	n.d.	183	6.1	29.00
<i>Acacia senegal</i>	2.1	5.8	3.8	21.4	13.8	70.8	6.9	42.3	3.7	10.1	0.3	0.5	0.6	151	5.2	29.41
<i>Adansonia digitata</i>	2.2	8.8	7.5	83.9	34.8	154	39.5	325	6.7	153	6.2	8.0	1.0	732	7.6	30.51
<i>Albizia anthelmintica</i>	0.9	4.4	3.3	12.0	8.3	129	3.2	7.0	0.2	n.d.	n.d.	n.d.	n.d.	153	10.1	28.82
<i>Balanites aegyptiaca</i>	2.2	4.0	3.4	15.0	4.1	12.7	2.5	6.5	1.0	1.6	0.2	0.2	0.7	39.9	3.4	28.36
<i>Boscia albitrunca</i>	n.d.	4.4	n.d.	24.9	1.9	5.8	n.d.	n.d.	n.d.	n.d.	n.d.	n.d.	n.d.	35.1	17.3	27.08
<i>Boscia foetida</i>	1.1	1.6	1.5	23.3	14.7	132	15.8	97.5	5.6	12.8	0.5	1.9	n.d.	269	7.0	29.76
<i>Burkea africana</i>	n.d.	3.6	n.d.	38.1	4.4	72.1	12.3	765	71.1	742	15.3	100.2	3.6	1721	16.2	31.91
<i>Colophospermum mopane</i>	6.1	19.4	10.2	34.2	12.9	32.7	16.6	242	35.2	193	2.9	2.0	n.d.	523	6.6	31.14
<i>Colophospermum mopane</i>	0.7	3.8	1.0	6.6	1.0	5.5	1.4	28.0	7.6	23.9	0.8	1.7	n.d.	69.4	5.7	30.92
<i>Combretum apiculatum</i>	0.6	2.2	0.5	6.9	0.8	9.5	1.2	39.2	3.2	15.0	0.2	0.2	n.d.	72.9	11.9	30.61
<i>Combretum imberbe</i>	1.1	7.6	2.9	14.8	3.8	25.1	2.8	7.5	1.0	1.3	0.3	0.2	n.d.	56.4	4.8	28.31
<i>Commiphora glaucescens</i>	2.3	10.9	5.0	33.2	6.2	50.9	8.2	182	9.0	70.3	1.6	8.4	0.9	355	11.5	30.65
<i>Commiphora merkeri</i>	n.d.	3.0	0.5	5.8	1.7	11.9	2.5	20.4	2.8	5.9	n.d.	0.5	n.d.	47.5	6.1	29.92
<i>Euclea pseudebenus</i>	1.2	4.6	2.2	10.2	2.2	41.0	27.0	1052	167	798	14.0	3.5	0.1	1909	9.0	31.76
<i>Faidherbia albida</i>	0.3	0.8	0.6	4.2	0.4	1.8	0.1	0.5	n.d.	0.2	n.d.	n.d.	n.d.	7.4	6.1	27.71
<i>Leucaena leucocephala</i>	0.9	8.6	1.9	13.6	3.3	33.9	2.1	17.2	1.0	2.1	0.4	n.d.	n.d.	75.4	8.2	28.75
<i>Morus alba</i>	0.6	4.8	1.5	22.5	2.9	46.0	6.3	166	9.1	65.9	0.5	0.4	0.2	305	14.9	30.75
<i>Sclerocarya birrea</i> subsp. <i>Caffra</i>	4.0	13.6	7.6	217.1	24.8	484	15.9	377	8.2	94.4	1.5	8.8	0.8	1196	20.4	29.58
<i>Sesbania sesban</i>	1.4	16.3	1.7	18.2	2.9	16.8	2.3	7.7	1.2	3.6	0.2	0.3	0.1	62.8	6.5	27.88
<i>Tamarix usneoides</i>	0.4	1.7	0.6	7.4	1.1	26.0	2.7	69.4	1.6	3.5	0.1	n.d.	n.d.	108	17.6	30.22
<i>Terminalia prunioides</i>	0.7	6.7	2.2	34.5	5.1	143	7.2	67.5	2.8	5.5	0.2	0.4	n.d.	258	14.5	29.25
<i>Ziziphus mucronata</i>	0.9	2.4	0.9	17.3	1.2	8.7	0.5	8.5	0.7	2.9	n.d.	1.7	n.d.	41.5	12.0	28.87
<i>Ziziphus spina-christi</i>	1.4	6.6	2.6	13.1	3.4	12.9	2.7	13.6	3.3	11.7	1.0	2.3	0.2	60.2	4.3	29.58

2. Characteristics of C₃ rain forest and C₃ savanna plant wax lipids

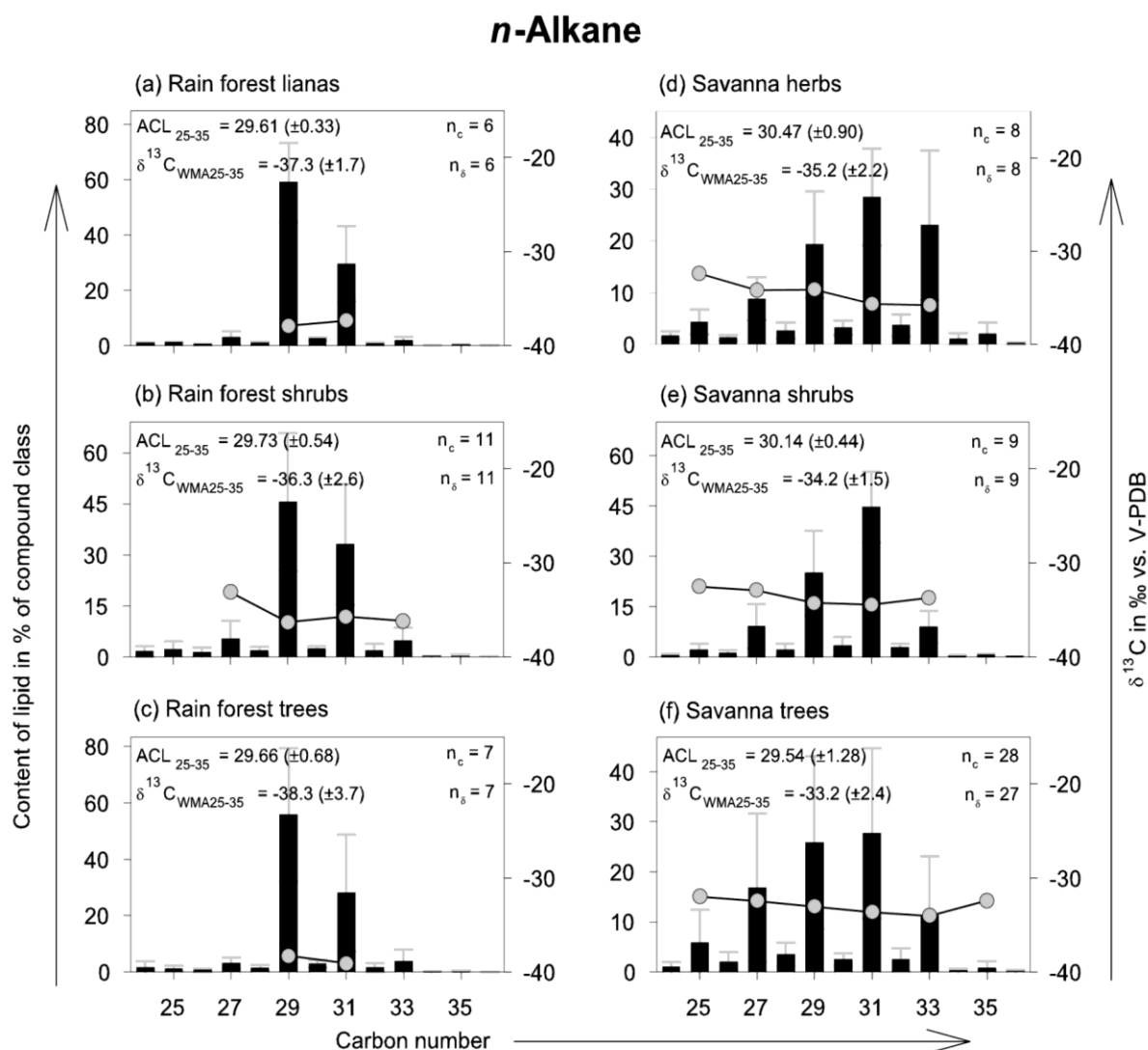


Fig. 2.3 Averaged histogram representation of leaf wax *n*-alkanes of samples from a) rain forest lianas, b) rain forest shrubs, c) rain forest trees, d) savanna herbs, e) savanna shrubs, and f) savanna trees. Displayed are *n*-C₂₄ to *n*-C₃₆ alkanes (in % of compound class, left Y-axis; black bars), overlain by averaged molecular stable carbon isotope data (○; $\delta^{13}\text{C}$ in ‰ versus V-PDB, right Y-axis). The diagrams are individually normalised to the most abundant homologue. ACL: Mean average chain length *n*-alkanes (*n*-C₂₅ to *n*-C₃₅; ACL₂₅₋₃₅) including the standard deviation (in brackets). $\delta^{13}\text{C}_{\text{WMA}}$: Mean weighted mean average of carbon isotopic values of odd-carbon-numbered *n*-C₂₅ to *n*-C₃₅ alkanes ($\delta^{13}\text{C}_{\text{WMA25-35}}$) including the standard deviation (in brackets); n_c : Number of species used for averaging of content data; n_δ : Number of species used for averaging of isotopic data. Data of graphical presentations is compiled in Table 7.1.

2.4.2 Content and carbon number distribution of long chain

***n*-alkan-1-ols**

Free wax *n*-alkan-1-ols exhibit a pronounced even/odd carbon number predominance of long chain components, which mainly comprise the *n*-C₂₄ to *n*-C₃₄ homologues. Shorter and longer chain *n*-alkanols are present in small quantities. The predominance of even carbon number homologues leads to high CPI₂₄₋₃₄ values in the range of 3.3 to 56 (carbon preference index for *n*-C₂₄ to *n*-C₃₄ alkanols; Fig. 2.2, Table 2.3). The total content of even carbon numbered *n*-alkanols (TCEC₂₄₋₃₄) varies significantly from 6.4 to 1340 µg g⁻¹ DM (Fig. 2.2) plants of this study are dominated by the *n*-C₃₀ or *n*-C₂₈ alkanol. Other maxima were only observed for three rain forest species (*n*-C₃₂ alkanol) as well as five savanna plants and one rain forest tree, which exhibit the *n*-C₂₆ homologue as most abundant alkan-1-ol.

Averaged *n*-alkanol distribution patterns for rain forest and savanna plants are shown in Fig. 2.4. For plants of both vegetation zones bell shaped distributions of even carbon numbered homologues were observed. The distribution patterns of rain forest plant *n*-alkanols centre at the *n*-C₃₀ homologue for lianas, shrubs and trees. The amount of *n*-C₂₈ alkanol decreases from trees over lianas to shrubs whereas the abundance of the *n*-C₃₂ alkanol increases. This is numerically expressed by ACL₂₄₋₃₄ values increasing from 29.48 to 29.72 (Fig. 2.4a-c).

Distribution patterns of savanna plants maximise at the *n*-C₂₈ alkanol. Savanna herbs exhibit the *n*-C₂₆ alkanol as the second most abundant homologue, whereas the *n*-C₃₀ alkanol is more common in shrubs and almost as abundant as the major homologue in trees (Fig. 2.4d-f).

Table 2.3 *n*-Alkan-1-ol data of C₃ plants studied: Analysed subspecies arranged according to growth form and habitat; individual *n*-alkanol content in µg g⁻¹ dry matter (DM), TCEC₂₄₋₃₄, CPI₂₄₋₃₄ and ACL₂₄₋₂₄ values. Boldface values: Distribution pattern maxima.

Habitat and growth form Analysed subspecies	<i>n</i> -Alkanol content (µg g ⁻¹ DM)													TCEC ₂₄₋₃₄	CPI ₂₄₋₃₄	ACL ₂₄₋₂₄
	23	24	25	26	27	28	29	30	31	32	33	34	35			
Rainforest lianas																
<i>Combretum conchipetalum</i>	0.2	0.9	0.1	1.8	0.1	7.1	1.3	38.9	0.8	9.9	n.d.	1.9	n.d.	60.5	25.6	30.01
<i>Combretum racemosum</i>	n.d.	0.4	n.d.	1.7	0.1	6.1	0.5	5.7	0.3	2.6	0.1	0.6	n.d.	17.1	15.8	29.18
<i>Cuervea macrophylla</i>	0.1	0.4	n.d.	0.6	0.0	0.7	0.1	1.0	0.2	2.0	0.3	1.6	0.1	6.4	7.5	30.59
<i>Landolphia mannii</i>	0.1	0.3	0.1	2.7	0.1	3.0	0.3	1.9	0.1	1.0	0.1	0.5	n.d.	9.4	13.6	28.44
<i>Paullinia pinnata</i>	2.2	17.5	0.4	4.3	0.6	11.7	6.2	40.4	7.0	48.9	3.4	4.5	n.d.	127	6.6	29.77
<i>Psychotria ealensis</i>	0.1	0.3	0.1	0.4	0.2	2.9	1.2	9.9	0.5	2.4	0.1	0.6	n.d.	16.4	7.8	29.87
Rainforest shrubs																
<i>Coffea</i> sp.	0.5	16.9	1.1	3.0	0.6	39.7	15.5	792	7.1	38.3	0.8	9.4	0.1	899	35.2	29.91
<i>Combretum erosum</i>	0.3	22.9	1.6	81.0	5.0	135	6.4	109	2.3	66.2	1.2	32.2	0.1	447	25.5	28.95
<i>Combretum indicum</i>	n.d.	0.2	n.d.	1.4	0.1	3.6	0.7	3.5	0.3	3.8	0.2	2.1	n.d.	14.6	9.6	30.16
<i>Combretum indicum</i>	0.1	1.5	0.2	2.8	0.5	8.9	1.0	23.2	0.6	12.7	n.d.	2.5	n.d.	51.5	21.7	29.95
<i>Combretum indicum</i>	0.2	1.4	0.3	3.4	0.6	7.9	1.9	13.4	n.d.	7.4	n.d.	2.9	n.d.	36.4	12.1	29.68
<i>Combretum molle</i>	0.4	6.4	2.4	47.2	6.5	50.4	6.1	35.5	1.9	15.9	1.4	6.0	0.1	161	8.5	28.31
<i>Englerina gabonensis</i>	0.2	5.9	0.9	35.1	1.5	17.7	2.3	15.4	0.5	10.4	n.d.	n.d.	n.d.	84.6	15.6	27.75
<i>Ficus natalensis</i> subsp. <i>Leprieurii</i>	0.9	22.2	1.4	28.9	2.4	4.9	21.6	274	30.6	252	11.3	35.7	n.d.	618	8.7	30.63
<i>Ficus thonningii</i>	0.1	1.2	0.2	3.2	1.4	32.2	3.7	85.1	4.6	83.5	4.3	46.4	0.5	251	16.1	31.07
<i>Oxyanthus unilocularis</i>	0.1	1.2	0.1	1.1	0.3	7.9	3.2	65.1	3.4	40.9	1.5	18.6	0.2	135	14.8	30.96
<i>Stipularia africana</i>	0.1	2.0	0.2	1.3	0.1	4.8	0.5	7.9	0.3	5.7	0.1	1.5	n.d.	23.1	16.2	29.60
Rainforest trees																
<i>Berlinia confusa</i>	0.1	0.8	0.2	3.1	0.7	6.7	2.0	6.4	0.3	1.8	0.2	1.2	0.1	20.1	5.7	28.90
<i>Cynometra mannii</i>	0.1	2.6	0.5	13.8	0.2	2.2	1.0	15.7	0.4	3.5	n.d.	0.3	n.d.	38.2	17.2	28.25
<i>Ficus ottoniifolia</i>	0.1	0.9	0.2	2.0	0.3	6.0	2.6	31.0	0.2	1.9	n.d.	n.d.	n.d.	41.7	12.5	29.49
<i>Oncoba spinosa</i>	n.d.	n.d.	n.d.	1.0	n.d.	7.0	0.1	7.7	0.2	12.5	0.5	5.7	n.d.	34.0	38.8	30.88
<i>Psychotria djumaensis</i>	n.d.	0.3	n.d.	0.4	0.2	2.9	1.2	9.5	0.5	3.1	0.1	0.7	n.d.	16.9	7.5	29.97
<i>Treulia africana</i>	0.1	1.4	0.1	3.8	0.3	4.7	1.0	4.3	0.8	4.6	0.5	2.2	n.d.	20.9	7.2	29.28
<i>Uapaca guineensis</i>	0.1	1.6	0.8	7.1	0.5	7.5	1.4	4.6	1.8	7.1	1.6	6.2	0.2	34.0	4.9	29.58
Savanna herbs																
<i>Abutilon graveolens</i>	0.2	4.4	1.5	33.3	2.4	33.3	1.8	24.6	1.3	7.3	n.d.	n.d.	n.d.	103	14.6	27.94
<i>Achyranthes aspera</i>	2.9	11.3	2.0	28.9	9.5	107	n.d.	15.2	n.d.	n.d.	n.d.	n.d.	n.d.	162	13.7	27.55
<i>Digeria muricata</i>	0.3	11.2	1.2	28.0	1.7	34.3	2.2	20.4	n.d.	2.7	n.d.	n.d.	n.d.	96.6	17.8	27.49
<i>Heliotropium</i> sp.	n.d.	19.1	6.8	163	18.6	124	3.5	18.0	1.0	5.1	n.d.	n.d.	n.d.	330	10.7	26.95
<i>Ipomoea cordofana</i>	0.1	1.8	0.4	6.3	0.6	16.2	2.0	21.3	2.3	10.5	0.5	3.9	0.2	59.9	10.0	29.47
<i>Ocimum basilicum</i>	0.2	0.4	0.2	1.7	1.4	9.4	1.7	3.6	1.9	2.3	0.1	0.7	n.d.	18.1	3.3	28.86
<i>Vigna</i> sp.	0.9	0.9	0.2	5.6	2.0	76.6	5.9	25.8	n.d.	18.0	0.8	5.6	0.4	133	14.4	29.07
<i>Xanthium brasiliicum</i>	7.2	4.5	2.3	17.6	3.2	22.8	4.5	25.6	n.d.	4.0	n.d.	n.d.	n.d.	74.5	7.2	28.19

Table 2.3 (continued)

Habitat and growth form	<i>n</i> -Alkanol content (µg g ⁻¹ DM)													TCEC ₂₄₋₃₄	CPI ₂₄₋₃₄	ACL ₂₄₋₂₄
	Analysed subspecies	23	24	25	26	27	28	29	30	31	32	33	34			
Savanna shrubs																
<i>Acacia mellifera</i>	n.d.	9.5	1.3	72.0	10.0	394	19.0	239	8.8	45.0	2.4	3.7	n.d.	763.2	18.2	28.65
<i>Acacia nebrownii</i>	n.d.	n.d.	3.8	20.8	6.0	72.8	13.6	52.1	6.0	8.5	n.d.	n.d.	n.d.	269.5	5.2	28.63
<i>Catophractes alexandri</i>	0.1	5.2	1.7	4.6	2.1	9.6	n.d.	1.4	n.d.	n.d.	n.d.	n.d.	n.d.	20.8	4.8	26.69
<i>Crassocephalum mannii</i>	0.3	1.3	0.2	23.9	3.0	98.9	1.8	14.8	n.d.	n.d.	n.d.	n.d.	n.d.	142.5	28.3	27.94
<i>Dichrostachis cinera</i>	11.6	23.3	n.d.	117	7.3	332	6.7	291	n.d.	30.6	n.d.	n.d.	n.d.	794.0	55.6	28.47
<i>Grewia flavescens</i>	0.4	2.4	0.6	17.1	2.8	52.4	7.3	49.5	10.2	26.1	3.8	8.0	n.d.	155.3	6.1	29.34
<i>Grewia flavescens</i>	0.7	4.4	1.0	30.0	5.0	71.0	5.5	44.0	8.9	36.0	3.9	10.0	0.5	195.4	7.7	29.10
<i>Gymnosporia buxifolia</i>	0.7	1.4	0.5	4.7	4.4	51.2	7.2	29.9	n.d.	15.4	n.d.	n.d.	n.d.	102.5	8.5	29.04
<i>Salvadora persica</i>	0.5	2.4	1.4	17.1	7.5	78.7	8.8	14.0	6.8	15.9	2.1	5.2	0.9	133.3	4.9	28.59
Savanna trees																
<i>Acacia erioloba</i>	0.3	1.1	0.6	5.1	3.6	50.1	4.7	58.4	3.4	5.9	0.9	2.8	n.d.	123	9.2	29.16
<i>Acacia karroo</i>	n.d.	1.8	0.6	37.0	11.0	461	28.0	832	2.4	8.8	n.d.	n.d.	n.d.	1341	31.9	29.21
<i>Acacia kirkii</i>	n.d.	3.3	0.9	20.8	7.0	153	6.3	116	3.8	20.6	n.d.	n.d.	n.d.	314	17.3	28.83
<i>Acacia luederitzii</i>	0.7	1.0	n.d.	9.7	4.0	167	13.0	210	2.5	8.2	n.d.	n.d.	n.d.	396	20.3	29.08
<i>Acacia mellifera</i>	2.3	1.4	0.3	10.6	5.8	264	6.6	113	2.6	6.1	n.d.	n.d.	n.d.	395	25.8	28.56
<i>Acacia senegal</i>	0.2	1.2	0.3	6.5	1.2	54.2	4.1	103	n.d.	1.7	n.d.	n.d.	n.d.	166	29.4	29.17
<i>Adansonia digitata</i>	2.1	9.5	9.0	35.6	17.0	264.3	7.0	564	4.9	39.7	n.d.	n.d.	n.d.	913	23.9	29.29
<i>Albizia anthelmintica</i>	1.5	12.8	8.4	15.5	n.d.	24.0	n.d.	12.1	n.d.	n.d.	n.d.	n.d.	n.d.	64.5	6.9	27.10
<i>Balanites aegyptiaca</i>	0.4	0.8	0.3	5.0	2.7	106	7.3	55.9	4.2	10.6	0.3	2.0	n.d.	180	12.1	28.85
<i>Boscia albitrunca</i>	0.8	4.4	1.2	40.0	11.0	426	31.0	149	11.0	33.0	1.8	1.7	n.d.	654	11.6	28.52
<i>Boscia foetida</i>	0.4	1.0	0.3	3.5	3.5	85.0	22.0	100	5.8	18.0	1.9	4.6	n.d.	212	6.2	29.36
<i>Burkea africana</i>	n.d.	6.3	1.1	10.7	2.1	29.3	6.8	17.9	n.d.	n.d.	n.d.	n.d.	n.d.	64.1	6.1	27.83
<i>Colophospermum mopane</i>	0.7	32.4	4.8	46.9	5.0	17.6	1.3	5.3	2.8	7.2	2.7	4.4	0.4	114	5.8	26.61
<i>Colophospermum mopane</i>	2.2	38.2	15.3	99.3	7.3	23.6	7.5	3.1	n.d.	n.d.	n.d.	n.d.	n.d.	164	4.8	25.90
<i>Combretum apiculatum</i>	0.2	13.6	3.1	53.0	5.8	77.5	7.1	43.1	4.3	43.8	11.5	30.4	n.d.	261	7.5	29.08
<i>Combretum imberbe</i>	0.2	1.4	0.4	10.3	2.1	22.7	3.8	36.6	n.d.	5.8	n.d.	n.d.	n.d.	76.9	12.1	28.91
<i>Commiphora glaucescens</i>	1.9	92.5	22.3	124	20.5	62.6	3.1	11.6	n.d.	n.d.	n.d.	n.d.	n.d.	290	5.3	25.95
<i>Commiphora merkeri</i>	n.d.	51.6	3.3	119	6.3	158	0.2	66.7	0.3	0.9	n.d.	n.d.	n.d.	396	36.8	27.22
<i>Euclea pseudebenus</i>	0.8	40.8	11.2	38.8	5.5	60.0	8.1	20.9	7.5	12.3	n.d.	n.d.	n.d.	173	4.7	27.13
<i>Faidherbia albida</i>	13.7	n.d.	22.6	18.8	31.9	649	4.1	185	n.d.	n.d.	n.d.	n.d.	n.d.	853	14.6	28.39
<i>Leucaena leucocephala</i>	0.3	1.0	0.2	4.9	1.5	69.0	7.9	183	0.5	91.0	1.3	18.4	0.2	367	31.4	30.25
<i>Morus alba</i>	n.d.	3.3	0.8	19.0	2.4	28.5	1.5	14.7	n.d.	n.d.	n.d.	n.d.	n.d.	65.6	13.7	27.67
<i>Sclerocarya birrea</i> subsp. <i>Caffra</i>	0.2	1.2	0.4	3.6	1.3	21.4	5.2	29.3	4.7	14.0	1.8	5.2	0.6	74.7	5.4	29.79
<i>Sesbania sesban</i>	0.5	1.1	0.3	8.9	4.1	122	10.5	163	0.4	84.6	1.2	19.7	n.d.	399	23.6	29.91
<i>Tamarix usneoides</i>	n.d.	17.9	2.1	68.2	3.9	348	13.8	139	3.5	28.0	n.d.	n.d.	n.d.	601	25.5	28.30
<i>Terminalia prunioides</i>	0.7	1.8	0.4	4.4	0.8	40.7	8.0	228	4.8	28.2	1.7	5.2	n.d.	309	19.5	29.89
<i>Ziziphus mucronata</i>	0.8	8.7	0.8	35.0	7.5	295	7.8	55.0	2.4	18.6	1.3	4.6	n.d.	417	20.7	28.26
<i>Ziziphus spina-christi</i>	n.d.	4.2	1.9	110	19.0	212	16.0	57.0	9.5	32.0	4.1	11.0	0.7	426	8.3	28.17

2. Characteristics of C₃ rain forest and C₃ savanna plant wax lipids

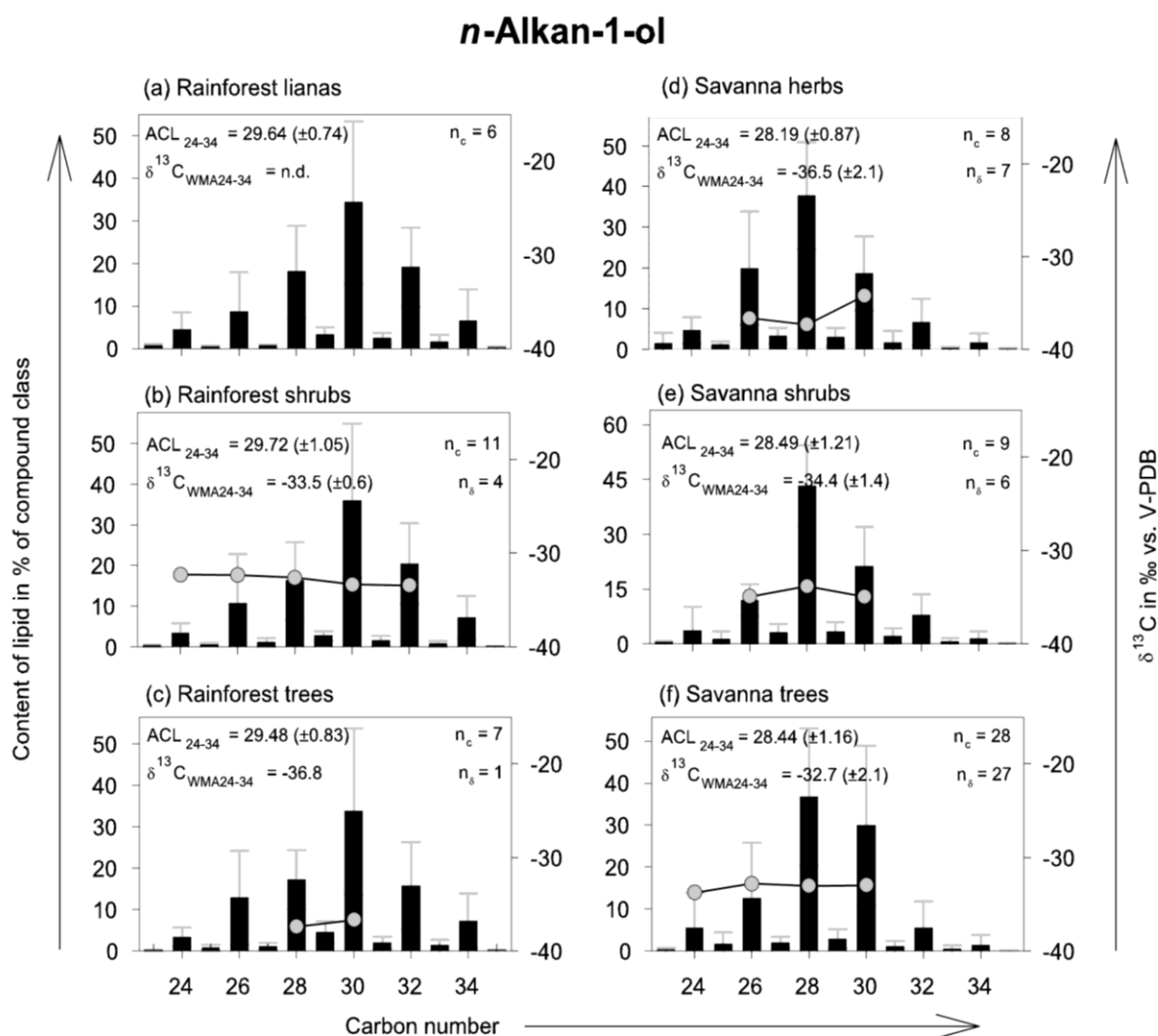


Fig. 2.4 Averaged histogram representation of leaf wax *n*-alkan-1-ols of samples from a) rain forest lianas, b) rain forest shrubs, c) rain forest trees, d) savanna herbs, e) savanna shrubs, and f) savanna trees. Displayed are *n*-C₂₃ to *n*-C₃₅ alkan-1-ols (in % of compound class, left Y-axis; black bars), overlain by averaged molecular stable carbon isotope data (○; $\delta^{13}\text{C}$ in ‰ versus V-PDB, right Y-axis). The diagrams are individually normalised to the most abundant homologue. ACL: Mean average chain length of *n*-alkanols (*n*-C₂₄ to *n*-C₃₄; ACL₂₄₋₃₄) including the standard deviation (in brackets). $\delta^{13}\text{C}_{\text{WMA}}$: Mean weighted mean average of carbon isotopic values of even-carbon-numbered *n*-C₂₄ to *n*-C₃₄ alkanols ($\delta^{13}\text{C}_{\text{WMA24-34}}$) including the standard deviation (in brackets); n_c : Number of species used for averaging of content data; n_δ : Number of species used for averaging of isotopic data; n.d.: Not determined. Data of graphical presentations is compiled in Table 7.2.

2. Characteristics of C₃ rain forest and C₃ savanna plant wax lipids

2.4.3 Stable carbon isotopic composition of plant material and individual lipids

Stable carbon isotopic compositions of whole plant material ($\delta^{13}\text{C}_{\text{PM}}$) vary from -24‰ to -36‰ (Table 2.4). Rain forest species exhibit the most negative values, and for plants of this vegetation zone a trend of averaged $\delta^{13}\text{C}_{\text{PM}}$ values from lianas (-29.1‰) and shrubs (-29.3‰) to trees (-30.5‰) is evident. But apart from one exceptionally negative value (-36.0‰ for *Ficus ottoniifolia*) all $\delta^{13}\text{C}_{\text{PM}}$ ratios for rain forest species roughly span the same range (Fig. 2.5a, triangles). For savanna species averaged $\delta^{13}\text{C}_{\text{PM}}$ ratios for trees (-26.9‰) and shrubs (-27.1‰) are virtually congruent, whereas herbs (average -27.6‰) have slightly more negative values (Fig. 2.5a, circles). The highest $\delta^{13}\text{C}_{\text{PM}}$ value of -24.0‰ was observed for the savanna tree *Tamarix usneoides*. Even though the ranges of $\delta^{13}\text{C}_{\text{PM}}$ values overlap, a trend to more negative values from savanna to rain forest species is obvious.

The weighted mean average of $\delta^{13}\text{C}$ values for the $n\text{-C}_{25}$ to $n\text{-C}_{35}$ alkanes ($\delta^{13}\text{C}_{\text{WMA25-35}}$) range from -28‰ to -45‰, whereas individual homologues from the same plant in some cases vary up to 4.7‰ (Table 2.4). The fractionation between bulk plant material and $\delta^{13}\text{C}_{\text{WMA25-35}}$ values (ϵ_{PM}) is

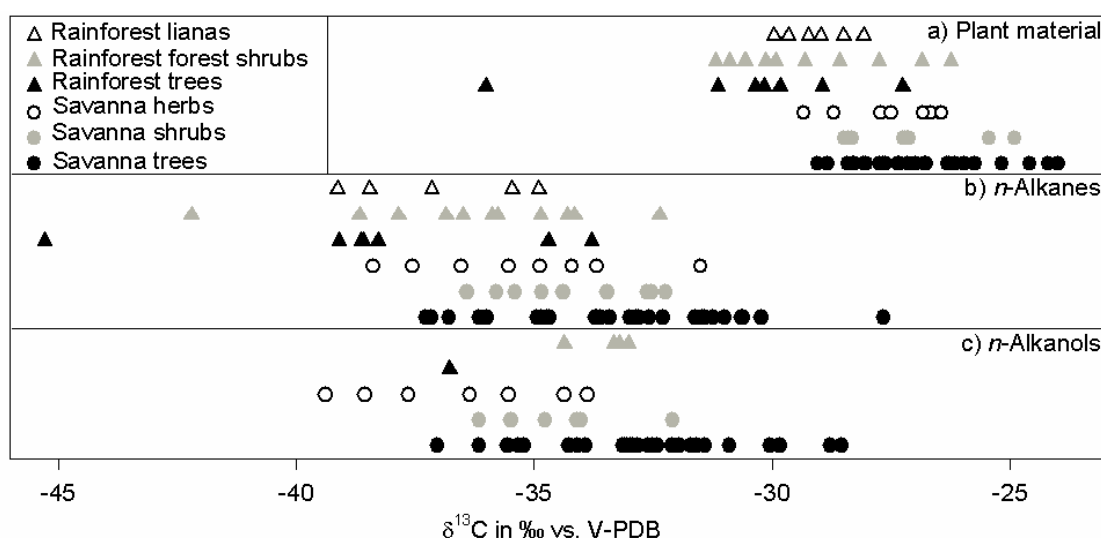


Fig. 2.5 Stable carbon isotopic composition of a) plant material, b) weighted mean average of $n\text{-C}_{25}$ to $n\text{-C}_{35}$ alkanes, and c) weighted mean average of $n\text{-C}_{24}$ to $n\text{-C}_{34}$ alkanols in ‰ versus V-PDB. Triangles: C₃ rain forest plants. Circles: C₃ savanna plants.

2. Characteristics of C₃ rain forest and C₃ savanna plant wax lipids

7.2 ± 2.2‰ on average (Table 2.4). Rain forest plants show $\delta^{13}\text{C}_{\text{WMA25-35}}$ ratios from -32‰ to -45‰ which centre at $-37.1 \pm 2.8\text{‰}$. The trend to more negative values of $\delta^{13}\text{C}_{\text{PM}}$ observed for rain forest trees has a correspondence in the $\delta^{13}\text{C}_{\text{WMA25-35}}$ ratios (Fig. 2.3a-c), but most rain forest plant $\delta^{13}\text{C}_{\text{WMA25-35}}$ values span the same range (Fig. 2.5b, triangles). Only two rain forest species (*Ficus ottoniifolia*, *Englerina gabonensis*) exhibit values lower than -40‰.

For savanna plants molecular $\delta^{13}\text{C}_{\text{WMA25-35}}$ values vary between -27‰ and -38‰ and centre at $-33.8 \pm 2.3\text{‰}$. The presentation of individual values (Fig. 2.5b, circles) shows similar ranges for savanna trees and shrubs with a narrower range for shrubs. Only one savanna tree (*Tamarix usneoides*) exhibits a $\delta^{13}\text{C}_{\text{WMA25-35}}$ ratio higher than -30‰. Like the $\delta^{13}\text{C}_{\text{PM}}$ values for savanna plants also individual values and averaged ratios for *n*-alkanes presented in Fig. 2.3d-f exhibit more negative values for herbs. The observed trend to more negative values of $\delta^{13}\text{C}_{\text{PM}}$ from savanna to rain forest species is also evident for the carbon isotopic composition of *n*-alkanes.

Due to small abundances and coelution molecular carbon isotopic data for *n*-alkanols cannot be provided for all plants. The weighted mean average of $\delta^{13}\text{C}$ values for the *n*-C₂₄ to *n*-C₃₄ alkanols ($\delta^{13}\text{C}_{\text{WMA24-34}}$) range from -28‰ to -40‰, whereas values of individual homologues from the same plant wax vary by up to 5.2‰ (Table 2.4). The fractionation between bulk plant material and $\delta^{13}\text{C}_{\text{WMA24-34}}$ values (ϵ_{PM}) is $6.3 \pm 2.6\text{‰}$ on average (Table 2.4).

Rain forest plants exhibit $\delta^{13}\text{C}_{\text{WMA24-34}}$ ratios from -30‰ to -37‰ which centre at $-34.1 \pm 1.6\text{‰}$ whereas molecular $\delta^{13}\text{C}_{\text{WMA24-34}}$ values of savanna plants range from -28‰ to -40‰ centring at $-33.7 \pm 2.1\text{‰}$. Like for $\delta^{13}\text{C}_{\text{PM}}$ and $\delta^{13}\text{C}_{\text{WMA25-35}}$ values the individual (Fig. 2.5c, circles) and averaged *n*-alkanol carbon isotopic ratios (Fig. 2.4d-e) of savanna plants exhibit a trend to more negative values from savanna trees and shrubs to herbs. Possibly, due to the small data set for rain forest species the observed general tendency for $\delta^{13}\text{C}_{\text{PM}}$ and $\delta^{13}\text{C}_{\text{WMA25-35}}$ to more negative values in rain forest species is not visible in the carbon isotopic composition of the corresponding *n*-alkanols.

Table 2.4 Isotopic data of C₃ plants studied: Analysed subspecies arranged according to growth form and habitat; stable carbon isotopic composition of analysed plant material and molecular stable carbon isotopic composition of *n*-alkanes and *n*-alkanols.

Habitat and growth form	$\delta^{13}\text{C}_{\text{PM}}$ (‰ vs. V-PDB)	$\delta^{13}\text{C}$ of <i>n</i> -alkanes (‰ vs. V-PDB)						$\delta^{13}\text{C}$ of <i>n</i> -alkanols (‰ vs. V-PDB)									
		25	27	29	31	33	35	$\delta^{13}\text{C}_{\text{WMA25-35}}$	ϵ_{PM}	24	26	28	30	32	34	$\delta^{13}\text{C}_{\text{WMA24-34}}$	ϵ_{PM}
Analysed subspecies																	
Rainforest lianas																	
<i>Combretum conchipetalum</i>	-29.2	n.d.	n.d.	-37.3	-36.2	n.d.	n.d.	-37.2	8.2	n.d.	n.d.	n.d.	n.d.	n.d.	n.d.	n.d.	n.d.
<i>Combretum racemosum</i>	-29.7	n.d.	n.d.	-38.7	-38.1	n.d.	n.d.	-38.5	9.1	n.d.	n.d.	n.d.	n.d.	n.d.	n.d.	n.d.	n.d.
<i>Cuerveva macrophylla</i>	-28.5	n.d.	n.d.	-38.2	-38.7	n.d.	n.d.	-38.5	10.3	n.d.	n.d.	n.d.	n.d.	n.d.	n.d.	n.d.	n.d.
<i>Landolphia mannii</i>	-28.1	n.d.	n.d.	n.d.	n.d.	-34.9	n.d.	-34.9	7.1	n.d.	n.d.	n.d.	n.d.	n.d.	n.d.	n.d.	n.d.
<i>Paullinia pinnata</i>	-30.0	n.d.	n.d.	-39.7	-38.5	n.d.	n.d.	-39.1	9.5	n.d.	n.d.	n.d.	n.d.	n.d.	n.d.	n.d.	n.d.
<i>Psychotria ealensis</i>	-29.0	n.d.	n.d.	-35.5	-35.3	n.d.	n.d.	-35.5	6.7	n.d.	n.d.	n.d.	n.d.	n.d.	n.d.	n.d.	n.d.
Rainforest shrubs																	
<i>Coffea</i> sp.	-29.9	n.d.	n.d.	-35.1	-34.6	n.d.	n.d.	-34.9	5.1	n.d.	n.d.	n.d.	-34.4	n.d.	n.d.	-34.4	4.6
<i>Combretum erosum</i>	-30.6	n.d.	-33.0	-32.3	-32.0	n.d.	n.d.	-32.4	1.9	n.d.	n.d.	-33.5	-32.5	-32.9	n.d.	-33.0	2.5
<i>Combretum indicum</i>	-26.3	n.d.	n.d.	-35.6	-36.1	-37.0	n.d.	-35.9	10.0	n.d.	n.d.	n.d.	n.d.	n.d.	n.d.	n.d.	n.d.
<i>Combretum indicum</i>	-26.9	n.d.	n.d.	-35.6	-36.1	-34.0	n.d.	-35.8	9.2	n.d.	n.d.	n.d.	n.d.	n.d.	n.d.	n.d.	n.d.
<i>Combretum indicum</i>	-27.8	n.d.	-34.5	-36.7	-36.5	n.d.	n.d.	-36.5	9.1	n.d.	n.d.	n.d.	n.d.	n.d.	n.d.	n.d.	n.d.
<i>Combretum molle</i>	-28.6	n.d.	-31.9	-34.3	-35.7	n.d.	n.d.	-34.2	5.8	n.d.	-33.5	-33.1	n.d.	n.d.	n.d.	-33.3	4.9
<i>Englerina gabonensis</i>	-31.2	n.d.	n.d.	-42.2	n.d.	n.d.	n.d.	-42.2	11.5	n.d.	n.d.	n.d.	n.d.	n.d.	n.d.	n.d.	n.d.
<i>Ficus natalensis</i> subsp. <i>Leprieurii</i>	-30.1	n.d.	n.d.	-38.8	n.d.	n.d.	n.d.	-38.7	8.9	n.d.	n.d.	n.d.	n.d.	n.d.	n.d.	n.d.	n.d.
<i>Ficus thonningii</i>	-30.9	n.d.	n.d.	-37.8	-37.9	-37.9	n.d.	-37.8	7.2	-32.3	-32.4	-32.6	-33.4	-33.5	n.d.	-33.5	2.7
<i>Oxyanthus unilocularis</i>	-29.3	n.d.	n.d.	-36.8	-37.0	-35.8	n.d.	-36.8	7.8	n.d.	n.d.	n.d.	n.d.	n.d.	n.d.	n.d.	n.d.
<i>Stipularia africana</i>	-30.6	n.d.	n.d.	-34.3	n.d.	n.d.	n.d.	-34.3	3.9	n.d.	n.d.	n.d.	n.d.	n.d.	n.d.	n.d.	n.d.
Rainforest trees																	
<i>Berlinia confusa</i>	-27.3	n.d.	n.d.	-34.7	n.d.	n.d.	n.d.	-34.7	7.7	n.d.	n.d.	n.d.	n.d.	n.d.	n.d.	n.d.	n.d.
<i>Cynometra mannii</i>	-30.2	n.d.	n.d.	-39.1	n.d.	n.d.	n.d.	-39.1	9.3	n.d.	n.d.	n.d.	n.d.	n.d.	n.d.	n.d.	n.d.
<i>Ficus ottoniifolia</i>	-36.0	n.d.	n.d.	-44.9	-45.9	n.d.	n.d.	-45.3	9.7	n.d.	n.d.	-37.4	-36.7	n.d.	n.d.	-36.8	0.8
<i>Oncoba spinosa</i>	-29.8	n.d.	n.d.	-38.0	-38.4	n.d.	n.d.	-38.3	8.8	n.d.	n.d.	n.d.	n.d.	n.d.	n.d.	n.d.	n.d.
<i>Psychotria djumaensis</i>	-29.0	n.d.	n.d.	-33.9	-33.1	n.d.	n.d.	-33.8	5.0	n.d.	n.d.	n.d.	n.d.	n.d.	n.d.	n.d.	n.d.
<i>Treulia africana</i>	-30.4	n.d.	n.d.	-38.1	-39.4	n.d.	n.d.	-38.6	8.6	n.d.	n.d.	n.d.	n.d.	n.d.	n.d.	n.d.	n.d.
<i>Uapaca guineensis</i>	-31.1	n.d.	n.d.	-39.3	-38.6	-37.2	n.d.	-38.6	7.8	n.d.	n.d.	n.d.	n.d.	n.d.	n.d.	n.d.	n.d.
Savanna herbs																	
<i>Abutilon graveolens</i>	-26.5	-32.2	-33.4	-33.6	-34.4	-33.5	n.d.	-33.7	7.5	n.d.	-36.4	-34.2	-31.8	n.d.	n.d.	-34.4	8.2
<i>Achyranthes aspera</i>	-26.7	n.d.	n.d.	-32.2	-34.2	-35.9	n.d.	-34.9	8.5	n.d.	n.d.	n.d.	n.d.	n.d.	n.d.	n.d.	n.d.
<i>Digeria muricata</i>	-27.7	n.d.	-37.9	-36.9	-37.7	-37.6	n.d.	-37.6	10.2	n.d.	-37.8	-37.5	n.d.	n.d.	n.d.	-37.6	10.3
<i>Heliotropium</i> sp.	-27.5	-32.6	-33.5	-36.0	-36.2	-36.2	n.d.	-35.5	8.3	n.d.	-37.6	-39.9	n.d.	n.d.	n.d.	-38.6	11.5
<i>Ipomoea cordofana</i>	-26.8	n.d.	-33.7	-34.6	-36.7	-37.1	n.d.	-36.5	10.1	n.d.	n.d.	n.d.	-35.5	n.d.	n.d.	-35.5	9.0
<i>Ocimum basilicum</i>	-29.3	n.d.	-30.3	-29.1	-31.8	-33.1	-28.2	-31.5	2.2	n.d.	-37.0	-37.7	-32.5	n.d.	n.d.	-36.3	7.3
<i>Vigna</i> sp.	-28.7	n.d.	-36.2	-36.6	-39.4	-38.4	n.d.	-38.4	10.1	n.d.	-38.0	-40.3	-37.1	n.d.	n.d.	-39.4	11.1
<i>Xanthium brasiliicum</i>	-26.4	n.d.	n.d.	-33.7	-34.8	-34.7	n.d.	-34.2	8.0	n.d.	-33.1	-34.4	n.d.	n.d.	n.d.	-33.9	7.7

Table 2.4 (continued)

Habitat and growth form	$\delta^{13}\text{C}_{\text{PM}}$ (‰ vs. V-PDB)	$\delta^{13}\text{C}$ of <i>n</i> -alkanes (‰ vs. V-PDB)						$\delta^{13}\text{C}$ of <i>n</i> -alkanols (‰ vs. V-PDB)									
		25	27	29	31	33	35	$\delta^{13}\text{C}_{\text{WMA25-35}}$	ϵ_{PM}	24	26	28	30	32	34	$\delta^{13}\text{C}_{\text{WMA24-34}}$	ϵ_{PM}
Analysed subspecies																	
Savanna shrubs																	
<i>Acacia mellifera</i>	-27.2	n.d.	-31.6	-32.6	-32.8	n.d.	n.d.	-32.5	5.5	n.d.	n.d.	-31.3	-33.4	n.d.	n.d.	-32.1	5.0
<i>Acacia nebrownii</i>	-24.9	n.d.	-30.6	-32.3	-33.9	n.d.	n.d.	-32.2	7.6	n.d.	n.d.	n.d.	n.d.	n.d.	n.d.	n.d.	n.d.
<i>Catophractes alexandri</i>	-27.1	n.d.	n.d.	-34.0	-34.6	n.d.	n.d.	-34.4	7.5	n.d.	n.d.	n.d.	n.d.	n.d.	n.d.	n.d.	n.d.
<i>Crassocephalum mannii</i>	-28.3	n.d.	n.d.	-33.8	-35.1	-34.6	n.d.	-34.8	6.8	n.d.	n.d.	n.d.	-35.7	-34.5	n.d.	-35.5	7.4
<i>Dichrostachis cinera</i>	-28.5	-31.6	-32.9	-33.8	-32.5	-31.6	n.d.	-32.6	4.3	n.d.	n.d.	n.d.	n.d.	n.d.	n.d.	n.d.	n.d.
<i>Grewia flavescens</i>	-27.2	n.d.	n.d.	-36.1	-35.4	n.d.	n.d.	-35.8	8.9	n.d.	-34.5	-33.8	-35.1	-36.2	n.d.	-34.8	7.8
<i>Grewia flavescens</i>	-28.4	n.d.	n.d.	-35.7	-37.0	-35.5	n.d.	-36.4	8.3	n.d.	-35.8	-35.9	-36.8	n.d.	n.d.	-36.2	8.0
<i>Gymnosporia buxifolia</i>	-25.4	n.d.	-35.3	-33.9	-33.1	-32.8	n.d.	-33.5	8.3	n.d.	n.d.	-34.0	n.d.	n.d.	n.d.	-34.0	8.9
<i>Salvadora persica</i>	-27.2	-33.5	-34.3	-36.3	-35.5	-34.1	n.d.	-35.4	8.5	n.d.	-34.5	-34.0	-33.8	-34.4	n.d.	-34.1	7.2
Savanna trees																	
<i>Acacia erioloba</i>	-29.1	-33.7	-34.4	-34.6	-36.3	-34.8	n.d.	-34.7	5.8	n.d.	n.d.	-34.3	-32.1	n.d.	n.d.	-33.1	4.2
<i>Acacia karroo</i>	-27.7	-31.9	-32.3	-32.2	-33.7	n.d.	n.d.	-32.3	4.7	n.d.	n.d.	-33.6	-31.9	n.d.	n.d.	-32.5	4.9
<i>Acacia kirkii</i>	-28.0	n.d.	n.d.	-35.5	-37.1	-37.1	n.d.	-36.8	9.1	n.d.	n.d.	n.d.	-31.4	n.d.	n.d.	-31.4	3.5
<i>Acacia luederitzii</i>	-27.4	-30.2	-31.4	-31.3	-30.1	-31.4	n.d.	-31.0	3.8	n.d.	n.d.	-32.3	-31.2	-32.6	n.d.	-31.7	4.5
<i>Acacia mellifera</i>	-26.2	-33.1	-32.6	-33.6	-33.0	n.d.	n.d.	-33.0	7.0	n.d.	n.d.	-33.2	-32.0	n.d.	n.d.	-32.8	6.9
<i>Acacia senegal</i>	-27.1	n.d.	-34.5	-32.3	-34.9	-35.2	n.d.	-33.6	6.7	n.d.	n.d.	-33.8	-32.5	n.d.	n.d.	-32.9	6.0
<i>Adansonia digitata</i>	-27.0	n.d.	-35.3	-36.0	-36.0	-37.0	n.d.	-36.2	9.5	n.d.	n.d.	-32.2	-28.7	n.d.	n.d.	-29.8	2.9
<i>Albizia anthelmintica</i>	-27.3	-31.4	-33.0	-33.5	n.d.	n.d.	n.d.	-33.4	6.3	n.d.	n.d.	n.d.	-28.8	n.d.	n.d.	-28.8	1.5
<i>Balanites aegyptiaca</i>	-26.3	n.d.	-30.8	-31.5	-31.8	n.d.	n.d.	-31.2	5.1	n.d.	-33.1	-34.4	-34.2	n.d.	n.d.	-34.3	8.3
<i>Boscia albitrunca</i>	-26.8	n.d.	n.d.	n.d.	n.d.	n.d.	n.d.	n.d.	n.d.	n.d.	n.d.	-27.9	-29.9	-30.6	n.d.	-28.5	1.8
<i>Boscia foetida</i>	-26.3	n.d.	n.d.	-34.3	-30.9	-32.8	n.d.	-32.9	6.8	n.d.	n.d.	-32.6	-32.6	n.d.	n.d.	-32.6	6.5
<i>Burkea africana</i>	-28.3	n.d.	n.d.	n.d.	-36.0	-36.0	n.d.	-36.0	8.0	n.d.	n.d.	-31.6	n.d.	n.d.	n.d.	-31.6	3.4
<i>Colophospermum mopane</i>	-24.2	n.d.	-29.3	-30.1	-30.6	-30.9	n.d.	-30.6	6.6	n.d.	-30.0	n.d.	n.d.	n.d.	n.d.	-30.0	6.0
<i>Colophospermum mopane</i>	-28.3	n.d.	n.d.	-31.9	-32.3	-30.4	n.d.	-31.5	3.3	-33.8	-32.4	-33.6	n.d.	n.d.	n.d.	-33.1	4.9
<i>Combretum apiculatum</i>	-25.2	n.d.	n.d.	n.d.	-34.7	-34.8	n.d.	-34.7	9.9	-33.8	-33.2	-33.7	-33.5	-35.0	-36.2	-34.1	9.2
<i>Combretum imberbe</i>	-26.0	-32.4	-28.9	-32.1	-33.1	n.d.	n.d.	-31.4	5.6	n.d.	-32.9	-31.2	-32.4	-30.5	n.d.	-31.9	6.2
<i>Commiphora glaucescens</i>	-26.8	-30.6	-30.4	-30.9	-30.1	-30.1	-29.4	-30.2	3.6	n.d.	n.d.	-31.9	-35.1	n.d.	n.d.	-32.4	5.8
<i>Commiphora merkeri</i>	-28.4	n.d.	-36.0	-37.7	-37.7	-36.3	n.d.	-37.3	9.2	-33.5	-33.2	-32.7	-33.3	n.d.	n.d.	-33.1	4.8
<i>Euclea pseudebenus</i>	-24.6	n.d.	n.d.	n.d.	-31.0	-30.2	n.d.	-30.6	6.2	-33.9	n.d.	n.d.	n.d.	n.d.	n.d.	-33.9	9.6
<i>Faidherbia albida</i>	-27.7	n.d.	-33.2	-31.9	n.d.	n.d.	n.d.	-32.8	5.3	n.d.	n.d.	-35.6	n.d.	n.d.	n.d.	-35.6	8.2
<i>Leucaena leucocephala</i>	-27.6	-33.3	-32.4	-36.9	-33.6	n.d.	n.d.	-34.9	7.5	n.d.	n.d.	-36.3	-36.6	-35.2	n.d.	-36.2	8.8
<i>Morus alba</i>	-28.0	n.d.	-35.5	-35.5	-37.4	-38.1	n.d.	-37.2	9.5	n.d.	n.d.	-30.0	-32.7	n.d.	n.d.	-30.9	3.0
<i>Sclerocarya birrea</i> subsp. <i>Caffra</i>	-28.1	n.d.	-31.4	-31.7	-31.7	n.d.	n.d.	-31.6	3.7	n.d.	n.d.	-35.4	-38.2	n.d.	n.d.	-37.0	9.3
<i>Sesbania sesban</i>	-28.8	-32.9	-34.9	-36.3	-37.1	-33.5	n.d.	-34.9	6.3	n.d.	n.d.	n.d.	-36.7	-33.2	-33.3	-35.3	6.7
<i>Tamarix usneoides</i>	-24.0	n.d.	-28.9	-28.1	-27.4	n.d.	n.d.	-27.7	3.8	n.d.	n.d.	n.d.	n.d.	n.d.	n.d.	n.d.	n.d.
<i>Terminalia prunioides</i>	-25.7	n.d.	-31.8	-33.0	-36.2	n.d.	n.d.	-33.7	8.2	n.d.	n.d.	-33.3	-31.7	-33.6	n.d.	-32.1	6.6
<i>Ziziphus mucronata</i>	-25.7	-29.7	-32.6	-29.9	-33.8	-34.4	n.d.	-32.6	7.1	n.d.	n.d.	-32.9	-33.3	n.d.	n.d.	-33.0	7.5
<i>Ziziphus spina-christi</i>	-26.8	-32.6	-32.3	-32.3	-35.0	-35.4	-35.5	-33.7	7.2	n.d.	-34.9	-35.0	-36.6	n.d.	n.d.	-35.2	8.8

2.5 Discussion

2.5.1 Contents and distribution patterns of *n*-alkanes and *n*-alkan-1-ols

The total contents and carbon preference indices of wax *n*-alkanes and *n*-alkan-1-ols from individual plant species do not reveal any systematic trend related to growth form (herb, shrub, liana or tree) or habitat (rain forest, savanna; Fig. 2.2). Contents, carbon preference indices as well as distribution pattern ranges and maxima are within the range of other studies (e.g., Dove and Mayes, 1991; Maffei, 1996; Schwark et al., 2002; Ali et al., 2005; Jansen et al., 2006; Rommerskirchen et al., 2006b). The absence of significant amounts of shorter chain alkanes as well as the generally high CPI values (above three) indicate that no significant contamination occurred during sampling or storage. Contact with human skin lipids, animal fur or petrochemical products would have contributed shorter chain homologues with low or no predominance of the odd carbon numbers (Bortz et al., 1989).

Although in our data set there is no correlation between abundance of *n*-alkanes and *n*-alkan-1-ols in plant waxes and their corresponding CPI ratios (Fig. 2.2), low CPI values (<5) were only observed for plants containing less 250 µg g⁻¹ DM of a given compound class. This corroborates a statement of Tulloch (1976) that even carbon number *n*-alkanes are sometimes more common in waxes that contain only small amounts of hydrocarbons. The abundance of minor amounts of even carbon number *n*-alkanes as well as odd carbon number *n*-alkanols in plant waxes originates from variations in the beginning of the biosynthesis. Instead of utilising a building block with two carbon atoms a molecule with three carbon atoms is used for the synthesis of fatty acids, which are the precursor molecules of *n*-alkanes and *n*-alkan-1-ols (Shepherd, 2003). It is unknown why different building blocks are being used at the beginning of the synthesis reactions (or why the extent differs in plants) and thus lead to differences in CPI values.

In the rain forest plants the *n*-C₂₄ to *n*-C₃₄ alkanols are in most cases less abundant than the *n*-C₂₅ to *n*-C₃₅ alkanes in the same species whereas in most savanna plant waxes a similar abundance of the two compound classes or a higher abundance of *n*-alkanols was observed (Tables 2.2 and 2.3). This may be related to the age of the leaves, because a decrease of the

2. Characteristics of C₃ rain forest and C₃ savanna plant wax lipids

amount of free *n*-alkanols during maturation of the plant was reported (Avato et al., 1990; Bianchi and Bianchi, 1990). Therefore, lower *n*-alkanol than *n*-alkane contents in rain forest plant waxes in this study may partly be explained by the degree of senescence of the plant at the time of sample collection.

The total wax content of an entire plant can depend on the changing contributions of different plant parts. For grasses a decrease of *n*-alkane and *n*-alkanol contents from flowers over leaves to stems was observed (Dove et al., 1996; Smith et al., 2001; Rommerskirchen et al., 2006b). In this study, whole plants including stems and partly flowers or fruits were only analysed of savanna herbs and one savanna shrub (*Crassocephalum mannii*). For these samples no significant difference in TCOC₂₅₋₃₅ or TCEC₂₄₋₃₄ values due to the contribution of different plant parts was observed. Dove et al. (1996) noted that the increase in *n*-alkane content in floral parts was less marked in legumes compared to grasses. Also plants of this study do not show any indication of large variance in the amount of *n*-alkanes and *n*-alkanols covering the different plant parts.

Maxima of *n*-alkane und *n*-alkanol distribution patterns of analysed species in some cases vary in chain length by up to five carbon atoms (e.g. *Colophosoermum mopane*; Tables 2.2 and 2.3). This chain length variation between compound classes points to a degree of separation in the synthetic pathways for precursor pools that feed into the synthesis of *n*-alkanes and *n*-alkanols (Shepherd, 2003). During biosynthesis both compound classes are formed from the same precursor molecules (intermediate even carbon number aldehydes). By defunctionalisation of these aldehydes odd carbon number *n*-alkanes are being synthesised whereas even carbon number primary alcohols are produced by reduction of the corresponding aldehydes. If both compound classes are synthesised from the same precursor pool, alkanes and alkanols should differ only by one carbon atom. But products of the reductive and decarbonylative pathways often differ greatly in length – as also observed in this study – and indicate separation in the elongation systems producing the intermediate aldehydes for the two compound classes (Shepherd, 2003).

2. Characteristics of C₃ rain forest and C₃ savanna plant wax lipids

Our limited survey does not reveal any systematics on the taxonomic levels of order, family or subfamily. The inconsistent distribution patterns of the same species sampled from different locations during various field trips points to the limitation of chemotaxonomic surveys using *n*-alkanes and *n*-alkanols. Triplicate samples of the rain forest shrub *Combretum indicum* show distribution patterns with different maxima for *n*-alkanes and *n*-alkanols. Duplicate samples of *Acacia mellifera* produced different distribution patterns of *n*-alkanes and similar distribution pattern maxima of *n*-alkanols. Distribution patterns of both compound classes of duplicate samples of *Colophospermum mopane* resemble each other. Stránský and Streibl (1969) also noted that similar species of deciduous trees sometimes have widely differing lipid patterns and concluded that the distribution of *n*-alkanes is of limited value as a taxonomic criterion. Despite this, for grasses specific patterns of lipid constituents were reported to remain constant under different environmental conditions (Tribe et al., 1968). Chemotaxonomic surveys of C₃ grasses (Maffei, 1996) and C₄ grasses (Rommerskirchen et al., 2006b) revealed characteristic lipid distributions on a subfamily level.

Whereas *n*-alkane distribution patterns of rain forest plants do not reveal significant differences related to growth form, a trend to longer *n*-alkanes from savanna trees over shrubs to herbs is evident. One possible explanation may be the adaptation to different temperature gradients within the habitats. The difference of temperature between bottom and top of the rain forest canopy are only a few degrees Celsius. In open areas with high irradiation, like in savannas and deserts, the temperatures are very high at the ground (up to 50 °C) but at a few decimetres above the ground the air temperature decreases significantly (Geiger, 1950). Because of this temperature gradient, savanna herbs covering the ground may synthesise longer chain *n*-alkanes with higher melting points compared to nearby taller plants. This behaviour also applies to the duplicate samples of *Acacia mellifera*: the plant sample which originated from a shrub exhibits longer chain homologues than the leaves collected from the tree. However, the observed differences may also be influenced by local environmental conditions or sampling season. Furthermore, desert plants endure even higher temperatures but synthesise

2. Characteristics of C₃ rain forest and C₃ savanna plant wax lipids

n-alkanes occurring in nearly the same range of chain length as found in plants analysed in this study (Proksch et al., 1981). This may render temperature of the habitat as the sole cause for differences in chain length of plant lipids unreliable.

Distribution patterns of *n*-alkanols from plants of this study show bell shaped curves. Furthermore, triacontanol (*n*-C₃₀) is abundant in all plants of this study and sometime the dominant homologue. In contrast, *n*-alkanol distribution patterns of grasses are dominated by only one particular homologue (*n*-C₂₆, *n*-C₂₈ or *n*-C₃₂) whereas triacontanol is absent in most cases (Tulloch, 1976; Rommerskirchen et al., 2006b). This absence of triacontanol in most grass wax lipids was related to the reported role of this substance as plant growth stimulator with high biological activity (Ries et al., 1977; Shakhidoyatov et al., 1997). In contrast, plants of our study showed bell shaped distribution patterns including the *n*-C₃₀ alkanol and thus, did not provide any indication of additional functions of this compound.

It is unknown whether the chemical adaptation of plant waxes to environmental conditions is caused by genetic or ecogenic processes. Dodd et al. (1998) showed that populations adapted to warmer and more arid conditions had higher proportions of alkanes with longer chains in their waxes than those of the same population adapted to cooler and more humid conditions. They concluded that the plants primarily have an ecogenic adaptation of their waxes to their habitat to impede the cuticular water loss. The adaptation to environmental factors is thought to be stimulated by light intensities on enzyme genes involved in wax biosynthesis during the fatty acid elongation or in earlier chain elongations (Shepherd and Griffiths, 2006). In contrast, Dodd and Afzal-Rafii (2000) proposed a strong genetic influence on adaptation of hydrocarbons to environmental conditions within the plant species of the family Cupressaceae. Of the many genes involved in wax biosynthesis, relatively few have known identities or functions. The mutation of certain genes responsible for enzymes, which are involved in the elongation process during wax production, leads to reduced levels of long chain alkanes (Shepherd and Griffiths, 2006). But these genetic defects affect the whole long chain carbon number range due to the blockage of fatty acid elongation from *n*-C₁₆ and

2. Characteristics of C₃ rain forest and C₃ savanna plant wax lipids

n-C₁₈ primers to longer chain homologues and do not only cause a slight change in the distribution pattern maximum of one or two carbon atoms as found in our samples. As yet, the processes controlling the carbon number distributions have not been conclusively described and further analyses are required.

2.5.2 Bulk and molecular carbon isotopic composition

Most $\delta^{13}\text{C}$ values of ground leaf material as well as *n*-alkanes and *n*-alkanols of the C₃ species of this study are in the characteristic range for C₃ plants of -21‰ to -35‰ for bulk material (O'Leary, 1988) and -29‰ and -39‰ for plant lipids (Bi et al., 2005 and references therein). In general, our results indicate a trend to more negative values from savanna to rain forest C₃ plants for bulk and *n*-alkane carbon isotope ratios. For *n*-alkanols a corresponding trend was not observed, possibly due to sparse isotopic data.

A large number of factors including light intensity, humidity, use of recycled CO₂, CO₂ concentration, osmotic stress, temperature, altitude and plant age influence the carbon isotopic composition of plants (Arens et al., 2000 and references therein). The observed carbon isotopic variations of plants in our sample set may be the result of a complex interaction of all or several of these factors. However, some environmental parameters like osmotic stress, temperature and altitude only lead to significant carbon isotope variation when plants from extreme habitats like high salinity environments, polar regions or high mountains, respectively, are included in the sample set. Another parameter, plant age, is not well known for all analysed samples and most likely varies within the sample set. But variation of carbon isotope composition with plant age was reported to be lower than 2‰ or even not significant (Donovan and Ehleringer, 1991). Thus, osmotic stress, temperature, altitude and plant age are assumed to be factors of minor or even negligible influence regarding the carbon isotopic difference between rain forest and savanna C₃ plants.

Other environmental factors like light intensity, humidity, use of recycled CO₂ and CO₂ concentration differ significantly between rain forest and savanna habitats and thus are assumed to be the main factors leading to differ-

2. Characteristics of C₃ rain forest and C₃ savanna plant wax lipids

ences in carbon isotopic composition of C₃ plants from the two habitats. One major parameter explaining the observed trend may be the deficit of light in closed canopies. Ehleringer et al. (1986) reported that decreasing photon flux leads to increasing intracellular CO₂ concentration in laboratory experiments. High intracellular CO₂ concentration causes stronger discrimination against ¹³C during photosynthesis. Several studies have shown that the carbon isotopic composition of plant material can vary within canopies due to position of the plant (Vogel, 1978; Medina and Minchin, 1980; Schleser and Jayasekera, 1985; Ehleringer et al., 1986). In all these studies leaf carbon isotope ratios became more negative in going from exposed, exterior positions to interior, more shaded positions of the plants.

Furthermore, water supply and air humidity are much higher in the rain forest than in the savanna. Therefore, rain forest plants do not have to close their stomata completely to prevent transpiration and can operate with more widely open stomata compared to savanna species. This leads to high intracellular CO₂ concentration in rain forest plants. In contrast, savanna plants close their stomata partly or completely to reduce water loss especially during the mid-day temperature maximum (Farquar et al., 1982). With reduced stomatal conductance nearly all CO₂ within the leaf is assimilated and there is little fractionation of carbon isotopes. High effects of stomatal closure may have caused the relatively high isotopic values for the *n*-alkanes of *Tamarix usneoides* ($\delta^{13}\text{C}_{\text{WMA25-35}}$ of -27.7‰) exceeding the range typical for C₃ plants. At places of high irradiation also the uptake of intracellular CO₂ released from the process of photorespiration is possible. Such CO₂ will be more negative than CO₂ in the atmosphere because it has already undergone fractionation.

An additional explanation for more negative values of rain forest plant material may be a different isotopic composition of the source CO₂ and higher CO₂ concentrations caused by recycling effects and soil respiration. Less wind penetration into the lower part of the rain forest due to the closed canopy structure causes slower air exchange and an accumulation of CO₂ depleted in ¹³C. Buchmann et al. (1997) reported the CO₂ concentration to be 200 ppm higher and $\delta^{13}\text{C}$ values for CO₂ to be 2.0 to 6.3‰ more negative at the forest floor than in the troposphere at an Amazonian rain forest sampling

2. Characteristics of C₃ rain forest and C₃ savanna plant wax lipids

site. The uptake of CO₂ depleted in ¹³C may be a partial explanation of more negative carbon isotopic ratios of rain forest plants but the aerial accumulation of CO₂ depleted in ¹³C decreases with height and CO₂ concentration is not constant in the course of the day. Buchmann et al. (1997) calculated source air effects to account only for about 20% of the difference in carbon isotope ratios within the tropical canopy forest they studied in the Amazonian rain forest. Nevertheless, very negative $\delta^{13}\text{C}_{\text{PM}}$ values among the rain forest plants like -36.0‰ for *Ficus ottonifolia* and $\delta^{13}\text{C}_{\text{WMA25-35}}$ ratios of less than -40‰ for *Ficus ottonifolia* and *Englerina gabonensis* may be explained by source CO₂ effects. Such negative values have previously been observed for leaf samples of the undergrowth (<1 m) in the Amazonian rain forest (Medina and Minchin, 1980).

2.5.3 Leaf wax n-alkanes and n-alkan-1-ols as proxies for vegetation type

In studies reconstructing the vegetational composition in a continental setting, chain length distributions and stable carbon isotopic measurements of aliphatic biomarkers have been and are still being used to deduce the C₃ and C₄ plant contribution to geological archives. Our study attempts to enlarge the available information on end member distribution patterns and carbon isotopic compositions of land plant wax constituents for the application as proxies for vegetation type. But one should bear in mind that the plants we analysed grew in the wild at different sampling locations and under different conditions and that they are not well described in every case. Therefore, local settings like edaphic characteristics, sampling seasons, daily sun exposure as well as the age of the plant material (young sprout or aged leaves) are largely unknown and can influence the results. This may limit the use of the presented data and averaged presentations.

Despite the uncertainties mentioned and the limited database significant similarities were observed for the different growth forms within one habitat. Therefore, we calculated averaged histogram representations (Fig. 2.6) as well as averaged presentations of common chain length parameters (Fig. 2.7) for C₃ rain forest plants and C₃ savanna plants, and we compare

2. Characteristics of C₃ rain forest and C₃ savanna plant wax lipids

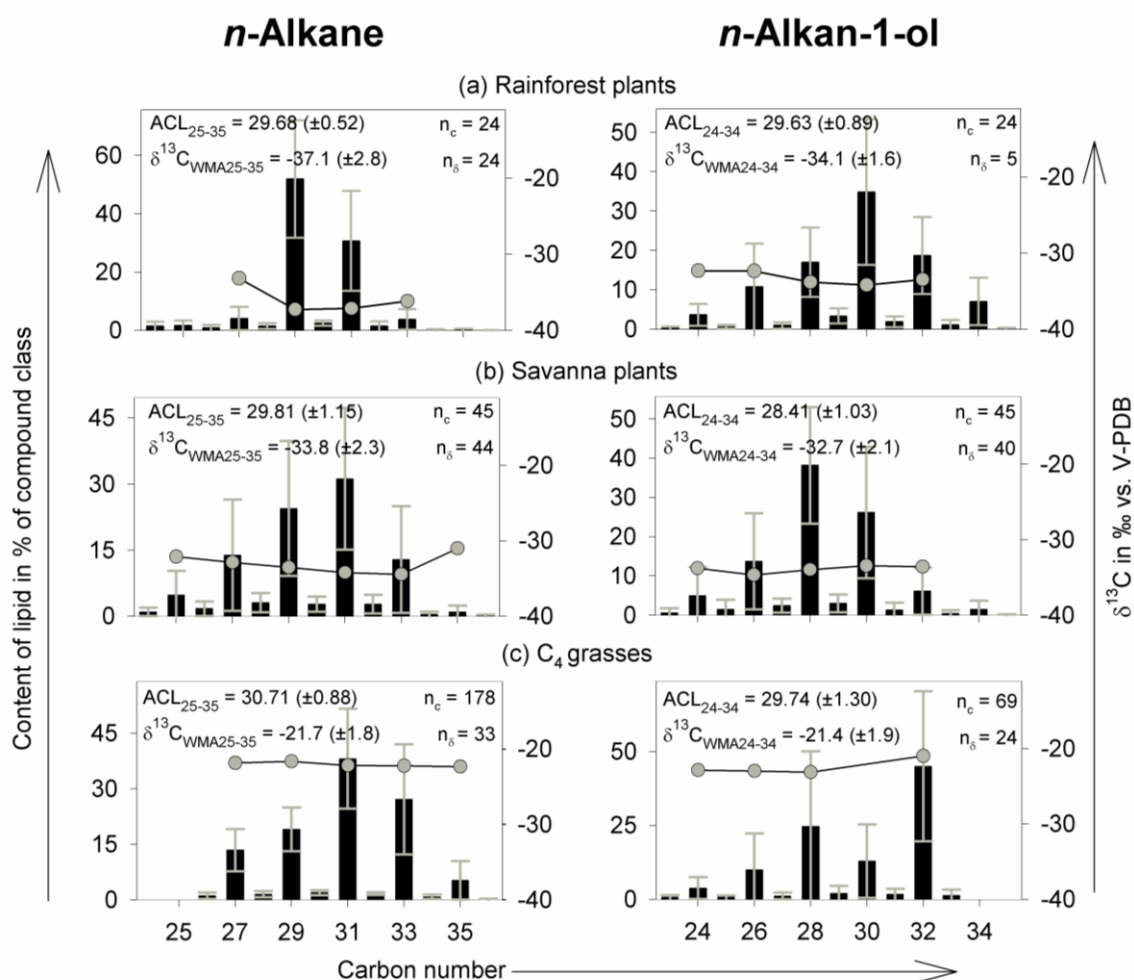


Figure 2.6 Averaged histogram representation of leaf wax *n*-alkane and *n*-alkan-1-ol of samples from a) rain forest, b) savanna and c) C₄ grasses (adopted from Rommerskirchen et al., 2006b). Displayed are *n*-C₂₄ to *n*-C₃₆ alkanes and *n*-C₂₃ to *n*-C₃₅ alkan-1-ols (in % of compound class, left Y-axis; black bars), overlain by averaged molecular stable carbon isotope data (○; $\delta^{13}\text{C}$ in ‰ versus V-PDB, right Y-axis). The diagrams are individually normalised to the most abundant homologue. ACL: Mean average chain length of *n*-alkanes (*n*-C₂₅ to *n*-C₃₅; ACL_{25-35}) or *n*-alkanols (*n*-C₂₄ to *n*-C₃₄; ACL_{24-34}) including the standard deviation (in brackets). $\delta^{13}\text{C}_{\text{WMA}}$: Mean weighted mean average of molecular carbon isotopic values including the standard deviation (in parentheses); n_c : Number of species used for averaging of content data; n_δ : Number of species used for averaging of isotopic data. Data of graphical presentations is compiled in Table 7.3.

them to data of C₄ grasses compiled by Rommerskirchen et al. (2006b). These graphs may roughly be representative for C₃ rain forest, C₃ savanna and C₄ grassland vegetation. This averaging is justified by the fact that storage of terrestrial plant waxes in continental or marine sedimentary archives

2. Characteristics of C₃ rain forest and C₃ savanna plant wax lipids

in nearly all cases involves an averaging effect by mixing plant debris from different growth settings and with different biological life histories.

From rain forest over savanna to grassland a shift to *n*-alkanes with longer chain lengths was observed. Whereas the *n*-C₂₉ alkane is the main component in the averaged histogram representation for rain forest plants, the *n*-C₃₁ alkane dominates the distribution patterns of savanna plants and C₄ grasses. In savanna plant waxes the *n*-C₂₉ alkane is the second most abundant homologue, whereas in C₄ grasses the *n*-C₃₃ alkane is more common. This is numerically expressed by increasing ACL₂₅₋₃₅ values (Fig. 2.7a) and an increasing relative abundance of the *n*-C₃₃ alkane (Fig. 2.7e) as well as in a decreasing *n*-C₂₉/*n*-C₃₁ ratio (Fig. 2.7c). The shift from a dominance of the *n*-C₂₉ alkane in forest species to the *n*-C₃₁ alkane as most abundant homologue for non-forest species is not a characteristic only obtained for tropical regions. It has also been reported for plants and geological archives of other vegetation zones as well (e.g., van Bergen et al., 1997; Jansen et al., 2006), whereas the *n*-C₂₇ alkane is more abundant and sometimes dominates in temperate forest species (Schwark et al., 2002).

For *n*-alkanols a similar tendency to longer chain lengths from C₃ savanna plants to C₄ grasses was observed (Fig. 2.4, right side). However, *n*-alkanols of rain forest plants do not corroborate this trend. The maximum of the averaged distribution pattern for *n*-alkanols (*n*-C₃₀ alkanol) of rain forest plants puts them between C₃ savanna plants (*n*-C₂₈ alkanol) and C₄ grasses (*n*-C₃₂ alkanol). This is also displayed by the ACL₂₄₋₃₄ values (Fig. 2.7b). For the *n*-C₂₈/*n*-C₃₀ ratio of the *n*-alkanols (Fig. 2.7c) an increase was observed from rain forest over savanna to C₄ grasses. The high value of this parameter for the C₄ grasses is caused by the low abundance of the C₃₀ alkanol in some leaf wax distribution patterns (Rommerskirchen et al., 2006b). The relative abundance of the *n*-C₃₂ alkanols displayed in Fig. 2.7f shows high values for C₄ plants. Hence, in conjunction with $\delta^{13}\text{C}_{32}$ values it may constitute a useful marker for C₄ grass rich vegetation as found by Rommerskirchen et al. (2006a).

The observation of rain forest species synthesising alkanols with longer chains than savanna plants is contrary to the results of a former studies of

2. Characteristics of C₃ rain forest and C₃ savanna plant wax lipids

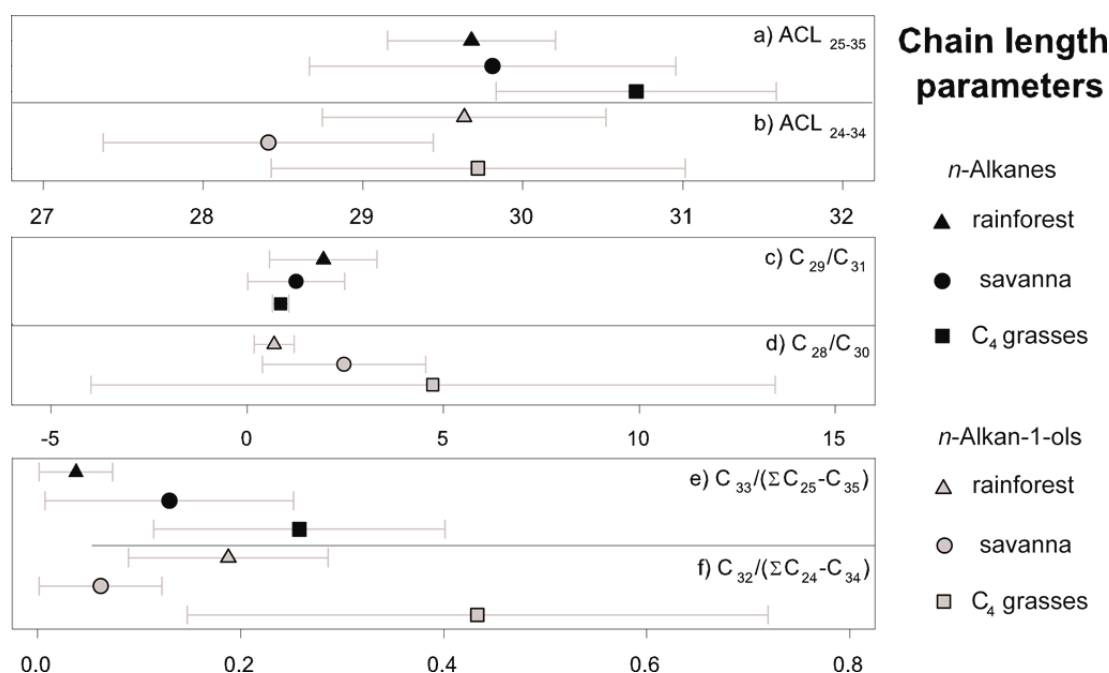


Fig. 2.7 Averaged values and standard deviation for chain length parameters of *n*-alkanes (black) and *n*-alkan-1-ols (grey) for rain forest species (triangles), savanna plants (circles) and C₄ grasses (squares). Displayed are average chain length of a) *n*-C₂₅ to *n*-C₃₅ alkanes (ACL₂₅₋₃₅), and b) of *n*-C₂₄ to *n*-C₃₄ alkanols (ACL₂₄₋₃₄), ratio of c) *n*-C₂₉ to *n*-C₃₁ alkane (C₂₉/C₃₁), and d) of *n*-C₂₈ to *n*-C₃₀ alkanols C₂₈/C₃₀ as well as relative abundance of the e) *n*-C₃₃ alkanes and f) *n*-C₃₂ alkanols. Data for C₄ grasses adopted from Rommerskirchen et al., 2006b. Data of graphical presentations is compiled in Table 7.4.

sediments from the southwest African continental margin. Such studies showed a similar trend of *n*-alkanes and *n*-alkanols to shorter chain homologues in sediment sampled off the rain forest compared to sediment sampled off savanna regions (Rommerskirchen et al., 2003; Rommerskirchen et al., 2006a). A similar discrepancy for a rain forest region was also observed by Huang et al. (2000) who found a higher abundance of shorter chain *n*-alkanols in sediments of the northeast Atlantic Ocean compared to dust sampled in the same region. This suggests that there may be additional sources for shorter chain *n*-alkanols. One possible source may be marine organisms because *n*-alkanols, mainly even carbon numbered *n*-C₂₂ to *n*-C₂₈ homologues, were identified in marine tropical sea grass (Nichols and Johns, 1985). Also marine microalgae were described to contain long chain saturated *n*-alkanols (*n*-C₂₀ to *n*-C₃₂) but microalgae were quoted to be only a

2. Characteristics of C₃ rain forest and C₃ savanna plant wax lipids

minor source of these lipids in most sediments (Volkman et al., 1998). Another possible source for *n*-C₂₀ to *n*-C₂₈ alkanols in sediments may be alkanols released from wax esters. The combined acids and alkanols of wax esters are often different in chain length from those in the corresponding free compounds (Kolattukudy, 1976). Fukushima and Ishiwatari (1984) found high contributions of *n*-C₂₀ to *n*-C₂₈ alkanols bound in wax esters of lacustrine and marine sediments.

The tendencies in chain length of *n*-alkanes described in this study are paralleled by a trend to less negative $\delta^{13}\text{C}_{\text{WMA25-35}}$ and $\delta^{13}\text{C}_{\text{WMA24-34}}$ ratios from rain forest over savanna to grassland vegetation (Fig. 2.6). Whereas the differences among the C₃ species have been discussed above, the difference between C₃ and C₄ species is caused by the different metabolic pathways.

The studied biomes were reported to have been well established in Africa at the end of the Miocene, and it was suggested that many present day plant lineages of Africa may date from the Miocene and since then increased in diversity whereas only few lines went extinct (Plana, 2004). Fossil ancestors of *Acacia* and *Ziziphus* species which are part of this study were identified in clay deposits from Fort Ternan (Kenya) dated to the Middle Miocene (Retallack, 1992). Therefore, we assume the data of biomarker distributions and compound specific stable carbon isotope composition presented here to be useful proxies for studies not only for the recent vegetation but also for expansion and contraction of tropical and subtropical vegetation zones since the Late Miocene.

2.6 Conclusions

In this paper we have shown differences in the bulk carbon isotopic composition as well as in the distribution pattern and molecular carbon isotopic composition of *n*-alkanes and *n*-alkan-1-ols for 45 savanna species and 24 rain forest plants native to Africa and sampled in their natural habitats. The plants display considerable variation in the content, distribution patterns and stable carbon isotopic composition of their lipids, but do not give a clear indication for a chemotaxonomic significance of these compounds.

2. Characteristics of C₃ rain forest and C₃ savanna plant wax lipids

For rain forest and savanna species the variation of the analysed parameters among different growth forms (herb, shrub, liana, and tree) are small. Characteristic similarities were observed for lipids and carbon isotopic signatures of plants from the same vegetation zone even though edaphic characteristics, sampling seasons, daily sun exposure as well as the age of the plant material were largely unknown and may have influenced the results. Therefore, we presented averaged histogram representations for C₃ rain forest plants, C₃ savanna plants and previously analysed C₄ grasses (Rommerskirchen et al., 2006b) which may roughly be representative for C₃ rain forest, C₃ savanna and C₄ grassland vegetation. The observed characteristics of plant waxes from these vegetation types are

- a shift to less negative carbon isotopic composition of whole plant material as well as for the *n*-alkanes and a trend to longer chain *n*-alkanes from C₃ rain forest over C₃ savanna to C₄ grassland vegetation;
- a distribution pattern maximum for *n*-alkanols of C₃ rain forest species laying between those of C₃ savanna plants and C₄ grasses.

These characteristics have implications for the use of wax compositions as biomarker proxies in geological records. For the *n*-alkanes we assume ACL values and the ratio of the *n*-C₂₉ to the *n*-C₃₁ alkane, which was already used in other environmental settings (e.g. Jansen et al., 2008), to be a suitable proxy to evaluate the changing contribution of savanna and rain forest vegetation to geological records of tropical and subtropical Africa. A similar trend was not found for *n*-alkanols but focussing on C₃ savanna species and C₄ grasses ACL values are a suitable parameter. Furthermore, the relative abundance of the *n*-C₃₃ alkane and/or the *n*-C₃₂ alkanol may be an indicator for the contribution of lipids derived from C₄ grasses as previously found by Rommerskirchen et al. (2006a), but the *n*-C₃₂ alkanol may be of limited use due to its abundance in rain forest plant waxes.

Our study also indicates the stable carbon isotopic compositions of land plant *n*-alkanes and *n*-alkan-1-ols to be powerful proxies for vegetation composition. Until now studies analysing stable carbon isotopic compositions of these components in geological archives in most cases only distinguished between contributions of C₃ and C₄ plants without considering a difference in

2. Characteristics of C₃ rain forest and C₃ savanna plant wax lipids

the signal of C₃ plants of different vegetation zones. But the different carbon isotopic composition of lipids from C₃ plants of savanna and rain forest habitats described in this study has to be taken into consideration in order to attain proper results.

3. *n*-Alkane parameters derived from a deep-sea sediment transect off southwest Africa reflect continental vegetation and climate conditions

Angela Vogts, Enno Schefuß, Tanja Badewien, Jürgen Rullkötter

This chapter was submitted to Organic Geochemistry.

3.1 Abstract

An isobathic transect of marine surface sediments from 1°N to 28°S off southwest Africa was used to further evaluate the potential of the abundance, chain length distribution and stable carbon isotope composition of long chain, land plant-derived *n*-alkanes as proxies for continental vegetation type and climate conditions. The results reveal a southward trend to longer chain length and less negative stable carbon isotope composition, reflecting the changing contribution of plants employing different photosynthetic pathways (C_3 and C_4). Both the stable carbon isotope composition and the average chain length distribution were found to be suitable for estimating the relative C_4 plant contribution to the sediments. The calculated C_4 plant proportion correlated reasonably well with the C_4 plant abundance in the postulated continental catchment areas if non-latitudinal eolian transport was taken into account. Furthermore, the calculated C_4 contribution to the sediments correlated significantly with the mean annual precipitation and aridity in the postulated catchment areas. Since (i) the sedimentary *n*-alkane parameters mirrored the continental vegetation and (ii) *n*-alkane-derived C_4 plant abundances may constitute a proxy for continental aridity, the study corroborates and expands the potential of *n*-alkanes in continental margin sediments for the reconstruction of recent and ancient environmental conditions on the adjacent continent.

3.2 Introduction

Land plant-derived biomarkers in sedimentary archives provide useful information concerning past vegetation and its climate-dependent variation. Valuable archives for such palaeoenvironmental studies are ocean margin sediments where long, undisturbed depositional sequences can occur. Land plant-derived biomarkers for such studies comprise constituents of epicuticular waxes and are employed in combination with their isotopic signatures (e.g. Rommerskirchen et al., 2003, 2006a; Schefuß et al., 2003a, 2005; Zhao et al., 2003; McDuffee et al., 2004; Feakins et al., 2005; Weijers et al., 2007; Niedermeyer et al., 2010; Tierney et al., 2010a,b). Epicuticular waxes cover all aerially exposed organs of higher land plants and in virtually all cases contain long chain *n*-alkanes, which are the focus of this study. After plant decay, the *n*-alkanes can persist in soils or are transported by wind and rivers to become incorporated into lake or ocean sediments. In such sedimentary archives the biomarkers constitute an integrated signal of the plant wax composition of the plant species within the catchment area.

Land plant-derived *n*-alkanes typically occur in the C_{25} to C_{35} range (Chibnall et al., 1934) with characteristic odd/even carbon number predominance (Eglinton and Hamilton, 1967). It was suggested that plants from arid tropical and subtropical climates biosynthesise longer chain wax components than those from habitats in the temperate regions (Gagosian and Peltzer, 1986) which would make their chain length distribution a potentially useful proxy for climate-dependent vegetation changes.

The stable carbon isotope composition of *n*-alkanes is another valuable feature and is related to the plant-specific CO_2 fixation pathways. Nearly 90% of the estimated 250,000 land plant species use the C_3 photosynthetic pathway (CBB Cycle; Bassham et al., 1954), i.e. almost all woody species of temperate and wet tropical regions (Sage, 2001). Another principal CO_2 fixation pathway, the C_4 metabolism (Hatch-Slack Cycle; Hatch and Slack, 1966), is an elaboration of the CBB Cycle and pre-concentrates CO_2 by way of a complex biochemical process (Hatch, 1987). This CO_2 concentrating mechanism prevents ineffective photorespiration and leads to improved water use efficiency under stressful environmental conditions, notably high tem-

3. Sediment transect I: *n*-Alkane chain length and $\delta^{13}\text{C}$ ratios

perature, high light intensity, high salinity, limited water supply and/or low CO_2 concentration (Downes, 1969; Björkmann, 1976). Since extra energy is needed for the advantageous two step process, C_4 plants can only successfully outcompete C_3 plants in regions like the sunny subtropical and tropical savanna and desert areas (Sage, 2004). The different CO_2 fixation pathways cause characteristic differences in the stable carbon isotope composition of leaf wax lipids of -29‰ to -39‰ in C_3 and -14‰ to -26‰ in C_4 plants, respectively (Bi et al., 2005 and references therein). A third metabolic pathway, the Crassulacean Acid Metabolism (CAM), is a less common elaboration of the CBB Cycle (Winter et al., 2005) and is commonly used by plants populating environmental niches, such as desert succulents and tropical epiphytes (Keeley and Rundel, 2003). As this metabolic pathway is generally a strategy for stress survival and not for high productivity, the contribution of CAM-utilising plants to biomass production, and thus geological archives, is negligible (Lüttge, 2004).

The goal of this study was to characterise how *n*-alkane characteristics in modern southeast Atlantic ocean margin sediments reflect the contribution of plants with different metabolic pathways (C_3 and C_4) from the adjacent African continent. Furthermore, we were interested in finding out if the abundance of C_4 plants is correlated with mean annual precipitation and/or aridity. The information is essential for reliable palaeo-vegetation reconstruction and palaeo-climatic interpretation. We analysed a transect of sediments off southwest Africa (1°N to 28°S) for their *n*-alkane distribution patterns and the molecular carbon stable isotope compositions of these biomarkers. Based on problems experienced in previous transect studies (Rommerskirchen et al., 2003), samples were collected from locations with similar water depth to minimise possible effects of different transport distances from the continent or water column height.

3.3 Material and methods

3.3.1 Sediment material

We analysed 13 marine sediment surface samples that constitute an isobathic (ca. 1300 m water depth) north to south transect (1°N to 28°S) along the southwestern African continental margin. The samples were retrieved during cruises M34/2 and M41/1 of the research vessel Meteor in 1996 and 1998, respectively, and recovered by way of multi-corer to obtain undisturbed surface sediment. Sampling locations are displayed in Fig. 3.1 and general sample information is compiled in Table 3.1. The multicores were separated into depth intervals, sealed in polyethylene plastic bags and stored at -20°C on board and afterwards at the University of Bremen. Material from the top-most available sediment layers (different intervals of 0 to 3.5 cm length; Table 3.1) was freeze dried and finely ground prior to analysis.

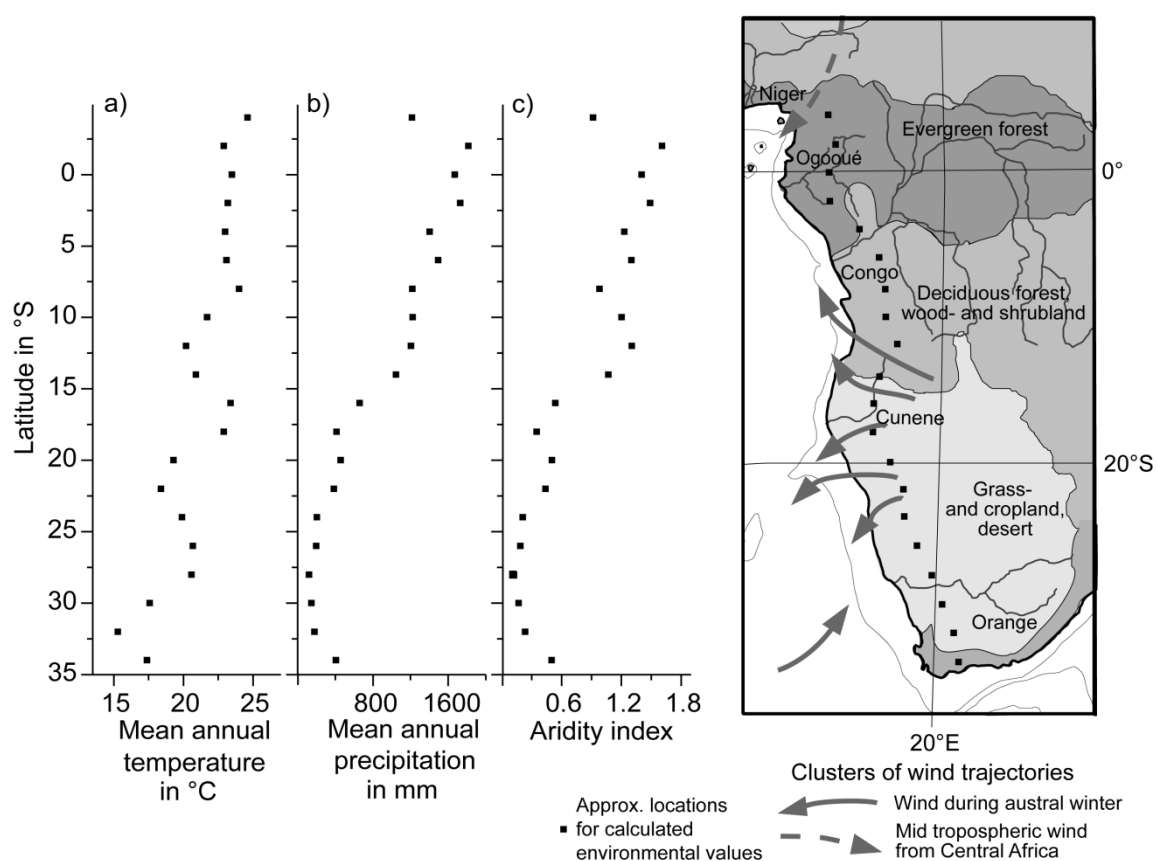


Fig. 3.1 Map of southern Africa and presentations of continental environmental conditions. Simplified present-day land cover based on Mayaux et al. (2004) and generalised wind directions according to Dupont and Wyputta (2003). Mean annual precipitation (a), mean annual temperature (b), and aridity index (UNEP, 1992); c) calculated for locations ca. 350 km distance to coast with WebWIMP modelling program (Matsuura et al., 2003). Exact locations and values of environmental parameters are given in Table 7.5.

Table 3.1 Sample information and analytical data for bulk material.

No.	GeoB No.	Latitude	Longitude	Water depth (m)	Cruise	Interval (cm bsf) ^a	TOC (%)	TIC (%)	$\delta^{13}\text{C}_{\text{OM}}$ (‰)
1	4904-6	0.962°N	8.88°E	1349	M41/1	0.5 - 2	2.65	0.91	-20.3
2	4906-4	0.69°S	8.378°E	1272	M41/1	1 - 2	3.04	0.34	-22.0
3	4909-3	2.068°S	8.625°E	1305	M41/1	0 - 1.5	2.27	1.53	-20.5
4	4912-3	3.73°S	09.785°E	1298	M41/1	0 - 1	2.33	1.39	-20.3
5	4913-3	5.503°S	11.072°E	1296	M41/1	0 - 2.5	3.33	0.02	-22.4
6	4915-2	7.75°S	11.873°E	1306	M41/1	0.5 - 2	2.94	0.11	-20.8
7	4916-3	10.173°S	12.687°E	1294	M41/1	0 - 1	4.08	0.21	-20.8
8	4917-4	11.903°S	13.073°E	1300	M41/1	0.5 - 2.5	3.85	0.39	-20.6
9	3713-1	15.628°S	11.58°E	1330	M34/2	1.5 - 2.5	1.51	0.55	-19.6
10	3715-2	18.955°S	11.057°E	1203	M34/2	1 - 3.5	4.52	3.12	-19.7
11	3706-3	22.717°S	12.602°E	1313	M34/2	0.5 - 1.5	4.05	8.02	-20.5
12	3705-3	24.303°S	12.997°E	1308	M34/2	0.5 - 2	4.24	8.40	-20.9
13	3701-1	27.952°S	14.003°E	1488	M34/2	0.5 - 1.5	1.13	9.38	-19.5

^aAnalysed sediment interval in cm below sea floor (bsf).

3.3.2 Analytical Methods

Bulk Parameters

Total organic carbon (TOC) content was determined as the difference between total carbon measured with a Vario EL Cube combustion instrument and inorganic carbon analysed via a UIC CO₂-coulometer. For stable carbon isotope analysis of bulk organic material, carbonate was dissolved by repeated addition of HCl (2 mol l⁻¹) and drying of the samples at 50°C. For isotope analysis a Carlo Erba Elemental Analyser 1108 was attached to a Finnigan MAT 252 isotope ratio mass spectrometer. Isotope compositions are expressed as $\delta^{13}\text{C}$ values in per mil relative to V-PDB. Samples were run at least in duplicate, with an absolute difference between measurements of <0.35‰. Results for bulk parameters are given in Table 3.1 for information.

Sample extraction and compound isolation

Marine surface sediments (9 to 23 g, depending on TOC content; Table 3.1), were extracted using an Accelerated Solvent Extractor (ASE 200, Dionex) with CH₂Cl₂ and MeOH (9/1, v/v; 3 x 5 min, 70 bar, 100°C). Completeness of extraction was checked by way of repeated extraction. Squalane was added to the extracts as internal standard. After removal of solvent, the extracts were redissolved in *n*-hexane and insoluble components removed by filtration over NaSO₄. The aliphatic/alicyclic hydrocarbons were separated from the *n*-hexane-soluble fraction by way of medium pressure liquid chromatography (Radke et al., 1980). Prior to analysis, behenic acid methyl ester was added to the hydrocarbon fraction as injection standard.

Gas chromatography (GC)

The hydrocarbon fractions were analysed using an Agilent 6890 GC instrument equipped with a cold injection system Gerstel KAS 4, high-temperature column J&W, DB-5HT, 30 m x 0.25 mm i.d., 0.1 µm film thickness and FID. The injector temperature was programmed from 60°C (5 s) to 350°C (60 s) at 10°C s⁻¹. Helium was used as carrier gas and the GC oven was programmed from 60°C (2 min) to 350°C (held 15 min) at 3°C min⁻¹. The *n*-alkanes were

3. Sediment transect I: *n*-Alkane chain length and $\delta^{13}\text{C}$ ratios

identified by comparison of retention times with standard mixtures and abundances calculated as $\mu\text{g g}^{-1}$ sediment dry weight on the basis of signal intensity and internal standard (squalane) in the GC-FID traces. Recovery was 85% or better. The differences in response between homologues of different chain length and internal standard were negligible (coefficient of variation $<6\%$), and no trend of response factors with chain length was observed.

Stable carbon isotope composition

The *n*-alkanes were separated from the branched and cyclic saturated hydrocarbons by way of urea adduction. Stable carbon isotope compositions were determined using a GC instrument (HP 5990) coupled to a Finnigan MAT 252 irm-MS via a combustion interface (GCC-II). The GC conditions were similar to those for quantification with the exception that the injector temperature was programmed from 60°C (5 s) to 325°C (120 s) at 10°C s^{-1} and the GC oven from 60°C (2 min) to 325°C (held 41 min) at 3°C min^{-1} .

Calibration was performed by injecting several pulses of CO_2 reference gas at the beginning and at the end of each run and by measurement of certified standard substances between sample runs. Additionally, docosanoic acid methyl ester of known stable carbon isotope composition was added to the samples and used for quality control. The standard deviation of docosanoic acid methyl ester was $<0.5\text{‰}$, with an averaged absolute error of 0.2‰ ($n = 40$). Samples were run at least in duplicate, with an absolute difference between measurements $<0.5\text{‰}$.

3.4 Regional setting

3.4.1 Environmental conditions in southwest Africa

Southwest Africa is characterised by a distinct topography. From the equatorial Congo Basin (usually <500 m) the elevation increases towards the South African Plateau, reaching an average altitude of 1000 m at about 10°S. Lower elevations occur in a narrow strip along the coast separated from the plateau by a steep slope.

In order to depict the climatic conditions in the study area, the Web-WIMP modelling program (Matsuura et al., 2003) was used to calculate annual mean temperature, precipitation and potential evapotranspiration for locations from 4°N to 34°S (2° steps) at ca. 350 km distance to the coast. This distance was chosen to depict the continental climate characteristic for the wind and river catchment areas and to avoid an influence of coastal climate, such as cold coastal temperatures in regions of coastal upwelling. From the calculated values the aridity index was calculated according to UNEP (1992) as a quotient of mean annual precipitation and potential evapotranspiration. At a large scale, mean annual temperature, precipitation and aridity index decrease from the equator to the south (Fig. 3.1a-c). Only at the southernmost part of the continent do temperature, precipitation and aridity index increase as a result of the equatorwards displacement of the mid-latitude Westerlies during austral winter.

3.4.2 Vegetation in southwest Africa

In Africa there is a clear gradient from dense evergreen biomes to dry open land cover from the equator to the subtropics, corresponding to the mean annual rainfall gradient (Mayaux et al., 2004). From the equator to the south, the vegetation of southwest Africa changes from evergreen rain forest through dry evergreen and deciduous forests, wood- and shrublands, grass- and croplands, to desert (Fig. 3.1). Because of winter precipitation on the higher latitude southern African coast woody vegetation is abundant again.

Rain forest vegetation is characterised by woody C_3 plants as the major representatives of the flora (Richards, 1996). The evergreen rain forest extends to about 9°S and is increasingly confined to river valleys towards its

3. Sediment transect I: *n*-Alkane chain length and $\delta^{13}\text{C}$ ratios

limits. Then, dry evergreen forests and further forests with deciduous plants gain importance. The closed forest (no grass cover) often abruptly passes into a wide zone of savanna, wood- and shrubland (Richards, 1996). In these savanna regions, deciduous woody species can cover up to 60% of the area (Cole, 1986) but the amount of woody C_3 vegetation decreases with increasing aridity, accompanied by increasing C_4 grass abundance. In the semi-deserts on the African Plateau (Kalahari and Nama Karoo) C_4 grasses dominate the vegetation, while in the dry coastal Namib Desert, the vegetation is very sparse and in the Succulent Karoo succulent plants dominate. Towards the Cape region woody C_3 vegetation becomes abundant again, forming the unique Fynbos vegetation.

3.4.3 Transport pathways for plant wax lipids

Eolian transport

Eolian transport pathways of terrestrial components were calculated by Dupont and Wyputta (2003) for wind born material reaching sediments off southwest Africa (6°S to 30°S , implemented in Fig. 3.1). They estimated the origin of the transported material by backward modelled trajectories and found a good latitudinal correspondence between the distribution patterns of pollen in marine surface sediments, the wind trajectories and the occurrence of the source plants on the continent. During austral summer, wind blows from the Atlantic towards the continent or parallel to the coast. Thus, there is little transport of terrestrial material to the sediments during this season. Only for the equatorial sites might there be some mid-tropospheric transport by Harmattan winds from north-central Africa. The main seawards transport from the continent occurs during austral fall and winter when easterly and southeasterly winds prevail. South of 25°S , wind blows mostly from the west and southwest, so eolian supply of terrigenous material is very low. There may be some potential for long range transport from South America but neither mid- nor low-tropospheric trajectories calculated by Dupont and Wyputta (2003) pass over parts of the South American continent.

3. Sediment transect I: *n*-Alkane chain length and $\delta^{13}\text{C}$ ratios

Riverine transport

In contrast to the coverage of wide ocean areas by wind, the majority of fluvial transported material is deposited in sediments near river mouths (Burdige, 2005). Rivers transport large amounts of dissolved and particulate organic matter to the oceans, and it has been shown that *n*-alkanes in marine sediments off rivers reflect the vegetation in adjacent river catchment areas (Bird et al., 1995; Schefuß et al., 2004; Weijers et al., 2009). In our study area, the Congo River system is the largest and also the second biggest in the world regarding the outflow at the mouth (Dai and Trenbeth, 2002). The outflow of other river systems in the study area is lower by a factor of ca. 10 for Ogooué (ca. 1°S) and Orange (28.5°S) and by a factor of 50 or more for other rivers (e.g. Kunene, 17°S; Heyns, 2003; Nilsson et al., 2005). However, the river outflow data only reflect the quantity of water and not the amount of *n*-alkanes transported. Direct quantification of the contribution of *n*-alkanes to deep sea sediments by these rivers is not available.

3.5 Results and discussion

3.5.1 *n*-Alkane abundance

Absolute abundance

Land plant-derived long chain *n*-alkanes in the range C_{25} to C_{35} had a summed abundance of 0.9 to 4.7 mg kg⁻¹ sediment dry weight (Table 3.2). The lowest abundance was observed for the southernmost site, likely a result of the low contribution of terrestrial material because of the prevailing westerly winds, in agreement with findings by Rommerskirchen et al. (2003). The abundances were highest off the Ogooué and Congo River mouths, reflecting the massive transport of terrestrial material by these river systems, as observed by Schefuß et al. (2004).

Carbon preference index

The C_{27} to C_{33} *n*-alkanes showed a strong odd/even predominance of 3.1 or higher (CPI_{27-33} ; Table 3.2) typical for their origin from higher land plant waxes and similar to the values found by Rommerskirchen et al. (2003) and

Table 3.2 Data for major terrestrial *n*-alkanes.

No.	<i>n</i> -Alkane content ($\mu\text{g kg}^{-1}$ dry weight) ^a											Σ_{25-35} (mg kg^{-1} DM)	CPI ₂₇₋₃₃	ACL ₂₇₋₃₃
	25	26	27	28	29	30	31	32	33	34	35			
1	142	109	296	159	1034	188	939	138	452	55	120	3.6	4.8	30.14
2	161	114	337	203	1444	266	1228	210	510	94	161	4.7	4.5	30.09
3	99	74	193	115	775	140	673	108	302	48	95	2.6	4.6	30.12
4	85	66	170	106	606	123	546	96	272	42	86	2.2	4.2	30.15
5	229	145	370	213	1167	245	1007	186	486	67	169	4.3	4.1	30.06
6	128	96	227	145	686	142	575	102	292	37	96	2.5	3.9	30.05
7	148	89	265	133	843	145	766	119	441	48	153	3.2	5.0	30.19
8	114	64	203	91	621	93	596	85	377	37	123	2.4	5.6	30.28
9	75	43	133	55	340	55	524	57	356	24	87	1.7	6.7	30.63
10	125	61	210	86	504	96	915	92	568	38	125	2.8	6.8	30.68
11	68	42	94	43	231	50	494	47	278	23	62	1.4	6.4	30.74
12	76	47	101	57	254	60	575	56	310	26	67	1.6	5.9	30.76
13	47	29	57	35	119	39	327	37	159	26	40	0.9	4.8	30.77

^a Bold values for individual *n*-alkanes refer to distribution pattern maxima.

3. Sediment transect I: *n*-Alkane chain length and $\delta^{13}\text{C}$ ratios

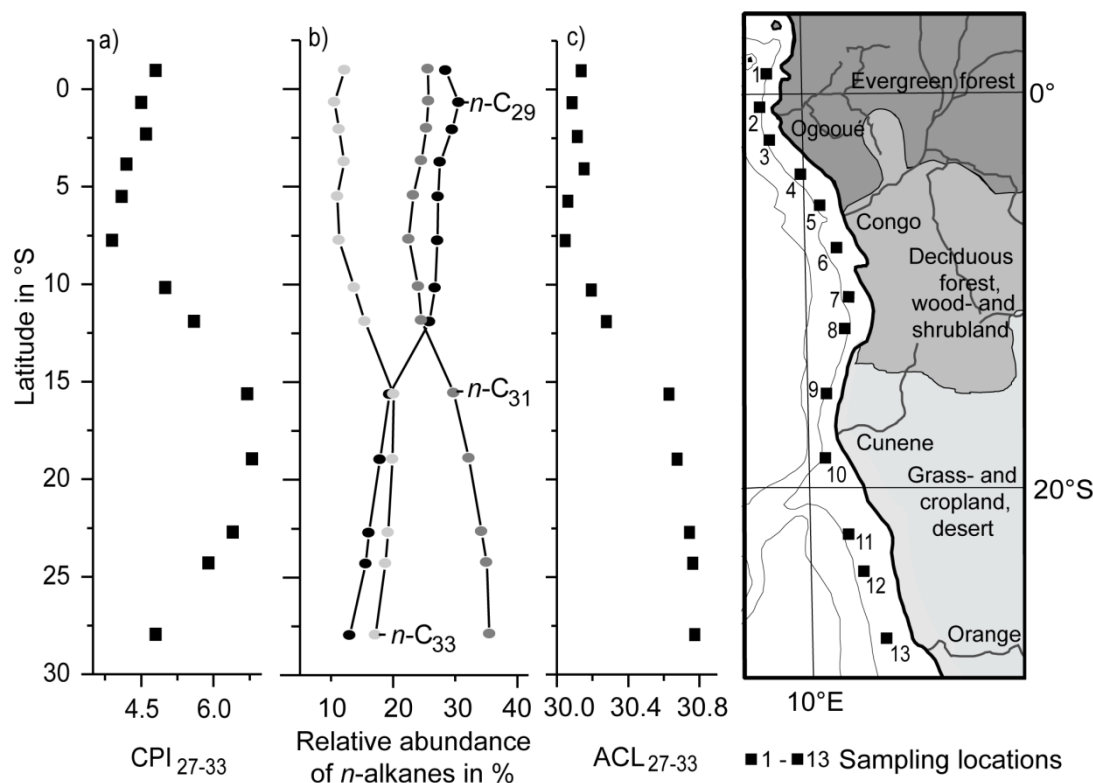


Fig. 3.2 Simplified present-day land cover on map based on Mayaux et al. (2004) with sampling locations of the north to south transect and graphs of sediment analysis results with a) CPI for *n*-alkanes with 27 to 33 carbons (CPI₂₇₋₃₃), b) relative abundance of individual *n*-alkanes, and c) ACL for *n*-C₂₇ to *n*-C₃₃ alkanes (ACL₂₇₋₃₃). Values of the relative abundance of the *n*-alkanes are given in Table 7.6.

Schefeuß et al. (2004) in the same area. In contrast, McDuffee et al. (2004) found lower CPI values of 1.3 to 2.7 for *n*-alkanes in sediments from the same or very similar locations and depth intervals, with the differences possibly related to a different work-up procedure.

A distinct trend in CPI values of ca. 4 in the north to values reaching nearly 7 off savanna regions was observed (Fig. 3.2a). Decreasing contamination with natural petroleum or refinery products from north to south, contributing homologous series of *n*-alkanes with low CPI values (ca.1) would explain the observed trend. Mass spectral analysis showed the presence of minor amounts of 17 α -hopane biomarkers, indicating a contribution of fossil material, but the 17 α -hopane abundance was similar for the samples with lowest and highest CPI values. The occurrence of small amounts of mature polycyclic hydrocarbon biomarkers in ocean surface sediments without cor-

3. Sediment transect I: *n*-Alkane chain length and $\delta^{13}\text{C}$ ratios

responding oil-like *n*-alkanes is quite common and has been attributed to an admixture of eroded material from land (e.g. Rullkötter et al., 1984). Alternatively, the trend in CPI values may be caused by plant sources showing different *n*-alkane CPI values. Analyses of rain forest and savanna C_3 plants showed, however, no significant differences of *n*-alkane CPI (Chapter 2).

The most likely cause for the observed trend of CPI ratios is the extent of degradation taking place after decay of plants and/or their wax-containing parts and incorporation of this material into soils. For eastern China, Rao et al. (2009) observed higher *n*-alkane CPI values in colder and drier areas compared to wetter and warmer tropical soils. This corresponds to our observation that higher values were observed off drier regions than off the moist rain forests. Even though the *n*-alkanes may have spent some time in the soil at their production site, the contribution of old material is assumed to be low and thus, not the cause for the observed CPI trends, because previous studies showed that dust and sediment samples off southwest Africa predominantly mirror recent continental vegetation (Rommerskirchen et al., 2003; Schefuß et al., 2003b, 2004). Furthermore, the leaf wax signal of contemporary vegetation or sub-recent soil organic matter rapidly overprints any contributions from ancient lipid material, e.g. from dried lakes, or anthropogenic components (Simoneit et al., 1988; Simoneit, 1997; Schefuß et al., 2003b).

There may be an additional effect on CPI based on transport pathways. In particular, the southern sites receive mainly eolian-transported material which became airborne via abrasion of the plant surface by e.g. sand blasting during storm events or via evaporation from the plants as a result of wood fires (Simoneit et al., 1977). The *n*-alkane distributions of this origin are assumed to remain relatively unchanged, i.e. close to the plant wax composition.

Chain length distribution

The *n*-alkanes with 29, 31, and 33 carbons had the highest abundance in all the transect samples. Distinct trends in their relative abundance are displayed in Fig. 3.2b. Near the equator, the *n*- C_{29} alkane (C_{29} hereafter) dominated the distribution patterns. This corresponds well to lipid data for rain for-

3. Sediment transect I: *n*-Alkane chain length and $\delta^{13}\text{C}$ ratios

est plants, in which it is the most abundant homologue (Vogts et al., 2009). Southwards, its relative abundance decreased and at 12°S the abundance of C_{29} and C_{31} was almost identical. The increasing contribution of C_{31} mirrored the continental transition zone between closed forest and open woodland because it is the dominant homologue in plant waxes of open savanna regions (Rommerskirchen et al., 2006b; Vogts et al., 2009). At 15°S and further south, C_{33} became the second most abundant homologue, while the abundance of C_{29} decreased even more. This is consistent with the fact that the importance of closed forest areas and woody vegetation further decreases, accompanied by an increase in C_4 grasses, in which C_{33} is more abundant than in woody vegetation (Rommerskirchen et al., 2006b; Vogts et al., 2009). The changing abundance of individual *n*-alkanes is numerically displayed by an increase in ACL. Near the equator ACL_{27-33} was around 30.1 (Table 3.2; Fig. 3.2c). At 10°S, the ratio started to increase and reached values of 30.8 at the sites south of 15°S. ACL_{27-33} ratios presented by Rommerskirchen et al. (2003) are in the same range.

For comparison with ACL ratios of other sediment and plant studies, we calculated values for the specific *n*-alkane ranges used in those studies (indicated by subscript numbers, values not displayed). ACL_{25-33} values calculated by McDuffee et al. (2004) for samples from similar sampling locations were 0.8 to 1.6 lower than ours, and the trend to higher values for the southern samples was less pronounced. As mentioned above, this may result from the different work-up method. Schefuß et al. (2003b) also found lower ACL_{25-35} values of 26 to 29.3 in dust samples and no correlation with continental vegetation.

Compared to plant samples, ACL_{25-35} values for the northern sediments of this study were higher than calculated for C_3 rain forest plant material presented by Vogts et al., 2009. This discrepancy may be due to the limited plant database but some contribution of C_4 grass waxes with longer chain *n*-alkanes to the northern sites also appears possible. As postulated by previous studies (Rommerskirchen et al., 2003, 2006a; Schefuß et al., 2004) such C_4 plant-derived material can reach the northern sites via long range eolian transport or may originate from rain forest swamps where C_4 grasses,

3. Sediment transect I: *n*-Alkane chain length and $\delta^{13}\text{C}$ ratios

e.g. from the genus *Cyperus* (like papyrus), dominate. However, since the overall *n*-alkane characteristics of tropical swamp C_4 grasses are unknown, their influence on the ACL remains speculative. At the southern sampling sites, the sedimentary ACL_{25-35} ratios resembled those of C_4 grasses presented by Rommerskirchen et al. (2006b), indicating an overwhelming C_4 plant contribution.

3.5.2 Stable carbon isotope composition of *n*-Alkanes

The dominant *n*-alkanes had stable carbon isotope ratio values from -34 to -25‰ (Table 3.3; Fig. 3.3a). As these long chain alkanes are not common in marine organisms (Chikaraishi and Naraoka, 2003; Mead et al., 2005) and hopane and CPI analysis indicated only a very minor contamination from petroleum *n*-alkanes, if at all, we are confident that the observed trends for the *n*-alkane carbon stable isotope composition are related to a nearly exclusive terrestrial origin of the compounds.

Most obvious is a trend to less negative stable carbon isotope composition from north to south, which runs virtually parallel for the three individual *n*-alkanes depicted (Fig. 3a). This is caused by a dominant contribution of C_3 plant derived material by the forest vegetation in the north and an increasing contribution of C_4 plant material from arid grassland further south. The most negative values were observed off the Ogooué and Congo River mouths, with the values being 1.1 to 3.3‰ (2‰ on average) lower than for the other locations off the rain forest. These low values may be related to either one of two phenomena or a combination of both. First, there may be a more pronounced dominance of C_3 plant contribution off the river mouths, reflecting the vegetation in the catchment area. For the other locations off the rain forest area, the C_3 plant signal may be slightly overprinted by an eolian C_4 plant signal from savanna regions. Another possible explanation may be the heterogeneity in stable carbon isotope signature of the rain forest plants. Plant parts growing under the canopy show more negative $\delta^{13}\text{C}$ values than those of the tree crowns. Thus, rivers may predominantly transport the more negative signal of the understory rain forest, whereas the wind contribution

3. Sediment transect I: *n*-Alkane chain length and $\delta^{13}\text{C}$ ratios

Table 3.3 Stable carbon isotope composition of major terrestrial *n*-alkanes with standard deviation (SD) of measurements as well as the weighted mean average (WMA).

No.	<i>n</i> -C ₂₉ alkane		<i>n</i> -C ₃₁ alkane		<i>n</i> -C ₃₃ alkane		$\delta^{13}\text{C}_{\text{WMA29-33}}$
	$\delta^{13}\text{C}$	SD	$\delta^{13}\text{C}$	SD	$\delta^{13}\text{C}$	SD	
1	-31.6	0.2	-30.2	0.0	-27.6	0.1	-30.3
2	-34.1	0.4	-33.2	0.2	-30.6	0.2	-33.2
3	-32.3	0.1	-31.6	0.1	-28.9	0.2	-31.4
4	-32.0	0.3	-30.6	0.2	-27.9	0.3	-30.7
5	-33.0	0.0	-32.3	0.2	-29.6	0.4	-32.1
6	-31.8	0.2	-31.2	0.3	-27.7	0.3	-30.8
7	-30.8	0.1	-29.8	0.1	-26.3	0.2	-29.4
8	-29.6	0.2	-28.3	0.1	-26.0	0.1	-28.3
9	-27.9	0.2	-27.0	0.2	-25.6	0.3	-26.9
10	-28.2	0.1	-26.8	0.3	-25.8	0.2	-26.9
11	-27.1	0.2	-25.2	0.1	-24.7	0.2	-25.5
12	-28.2	0.3	-25.6	0.1	-24.9	0.2	-26.0
13	-28.6	0.0	-26.1	0.1	-24.9	0.2	-26.3

(more strongly inherited at locations away from river deltas) reflects the abrasion of isotopically less negative plant constituents of the upper canopy. The assumed C₃ “river signal” for the stable carbon isotope composition was not, however, paralleled by the ACL values. The reason for this discrepancy is unknown.

At all locations, the $\delta^{13}\text{C}$ values increased from C₂₉ to the longer homologues, since C₄ plants produce higher proportions of longer *n*-alkanes than C₃ species (Rommerskirchen et al., 2006b; Vogts et al. 2009). At the northern sites, the $\delta^{13}\text{C}$ values of C₃₁ were closer to those of C₂₉, whereas they resembled more the values for C₃₃ at the southern sites (Fig. 3.3a). The trend to less negative values from equatorial to southern sites was even more pronounced for C₃₁. This shift relative to the other homologues reflected the predominant C₃ plant-derived origin at the northern sites and the increasing contribution of C₄ plant material in the south. Not only for C₂₉, but also for the other *n*-alkanes, are our $\delta^{13}\text{C}$ values similar to those in the other available datasets (Rommerskirchen et al., 2003; Schefuß et al., 2004).

A combined plot of our results for C₂₉ together with literature data from the same region (Huang et al., 2000; Rommerskirchen et al., 2003; McDuffee

3. Sediment transect I: *n*-Alkane chain length and $\delta^{13}\text{C}$ ratios

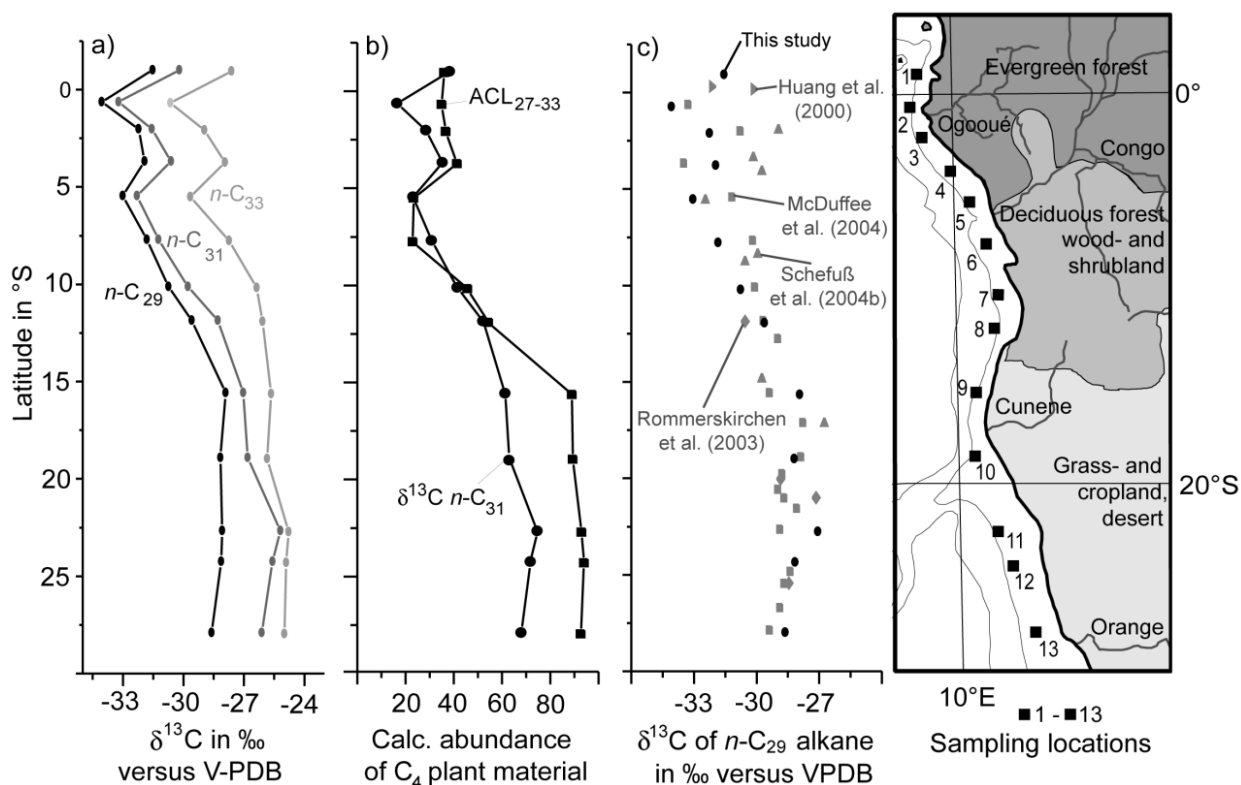


Fig. 3.3 Results of sediment analysis for the north to south transect with a) stable carbon isotope composition of dominating *n*-alkanes (‰) b) calculated C₄ plant abundance based on ACL of *n*-C₂₇ to *n*-C₃₃ alkanes (ACL₂₇₋₃₃, black squares) as well as on stable carbon isotope composition of *n*-C₃₁ alkane (black circles), and c) comparison of results for the stable carbon isotope composition of the *n*-C₂₉ alkane for our study (black circles) with literature data (grey symbols).

et al., 2004; Schefuß et al., 2004) is shown in Fig. 3.3c. This comparison is restricted to sediments derived from water depths between 500 and 2500 m in order to minimize possible effects of water column height or length of transport pathway with increasing distance from the coast. Even though there is some variation in the combined dataset, the general trend to less negative stable carbon isotope composition from the equator to the south is recognizable and mirrors the increasing abundance of C₄ plant dominated grassland on the continent. The largest variation in $\delta^{13}\text{C}_{29}$ values at a given latitude was observed for the northern part of the study area. This may be related to the sampling locations being specifically influenced by their proximity to the river mouths and river plumes, where the amounts of riverine and eolian material (and accordingly the abundance of C₄ derived material) may vary significantly

3. Sediment transect I: *n*-Alkane chain length and $\delta^{13}\text{C}$ ratios

over short distances. Despite the variation near the equatorial river sites, our results corroborate the great potential of the stable carbon isotope composition of individual *n*-alkanes for reconstructing the photosynthetic plant types of the source vegetation.

3.6 Reconstructing C_4 plant contribution

3.6.1 Calculations based on $\delta^{13}\text{C}$ values

On the basis of *n*-alkane parameters, binary mixing models can be used to calculate the abundance of C_4 plant material in sediments. A crucial part of such calculations is the availability of proper plant end member data. While Rommerskirchen et al. (2006b) presented such data for C_4 grasses, C_3 plant values are more heterogeneous and differ between rain forest and savanna plants (Vogts et al. 2009). As an approximation we chose end member values for C_3 plants which constitute an averaged value of rain forest and savanna plant weighted ratios and which lie between the $\delta^{13}\text{C}$ values employed in other studies (Rommerskirchen et al., 2003; Schefuß et al., 2004). End member values and results are compiled in Table 3.4.

The parameter most commonly employed for the calculation of C_4 plant abundance is the stable carbon isotope composition. The results of our calculations based on the dominant *n*-alkanes largely depend on the *n*-alkane used (Table 3.4). For instance, results obtained from calculations based upon C_{29} and C_{31} alkanes differ by up to 19%. But, if the results of the two most abundant homologues are compared (boldface values in Table 3.4) the differences in C_4 plant calculation do not exceed 10% in our data set. Despite these variations, our results based on stable carbon isotope data resemble those based on pollen abundances and stable carbon isotope compositions of *n*-alkanes and *n*-alkan-1-ols presented by Rommerskirchen et al. (2003) and Schefuß et al. (2004).

Based on C_{31} , a C_4 abundance of ca. 30% was calculated for the equatorial locations with lower C_4 plant abundance (20%) off the major rivers (Fig. 3.3b). This means that at none of the locations do the sediments exhibit an exclusive C_3 rain forest signal and that C_4 plant material was transported

3. Sediment transect I: *n*-Alkane chain length and $\delta^{13}\text{C}$ ratios

Table 3.4 End member data and results for calculations of abundance of C_4 plant derived material at the sample locations.

End member data	Calculation based on				
	$\delta^{13}\text{C}_{29}$	$\delta^{13}\text{C}_{31}$	$\delta^{13}\text{C}_{33}$	$\delta^{13}\text{C}_{\text{WMA29-33}}$	ACL_{25-35}
C_3 plants ^a	-35.4	-35.7	-35.3	-35.6	29.74
C_4 grasses ^b	-21.6	-22.1	-22.2	-22.0	30.71
No.	Calculated C_4 plant abundance (%) ^c				
1	29	38	57	39	36
2	10	17	36	18	35
3	24	29	48	31	37
4	26	35	55	36	41
5	18	23	43	26	23
6	26	31	57	35	23
7	34	41	66	45	46
8	43	52	69	54	54
9	55	61	72	64	89
10	53	63	70	64	89
11	61	75	78	74	93
12	53	72	77	71	94
13	50	68	76	69	93

^a Averaged values of rainforest and savanna plant average (Vogts et al., 2009).

^b Averaged values of C_4 grasses (Rommerskirchen et al., 2006b).

^c Boldface values refer to the two most abundant homologues.

to all of the sites, either by eolian transport or from C_4 plants growing in the rain forest region (e.g. swamps with papyrus). For the southern sites, a C_4 plant abundance of ca. 70% was calculated (Fig. 3.3b).

As some studies also employed weighted mean averages of stable carbon isotope ratio values for the calculation of C_4 plant abundance, we applied this method to the C_{27} to C_{35} range (not displayed) as well as C_{29} to C_{33} alkane range (Table 3.4). The results closely resemble those obtained from calculations based on C_{31} . Thus, at least for the present dataset, no additional benefit of weighted mean average calculations was observed.

3.6.2 Calculations based on ACL

Studies of the *n*-alkane characteristics of African plants have shown that not only the $\delta^{13}\text{C}$ values, but also ACL_{25-35} values differ significantly between C_3 and C_4 plants (Rommerskirchen et al., 2006b; Chapter 2). Thus, we also em-

3. Sediment transect I: *n*-Alkane chain length and $\delta^{13}\text{C}$ ratios

ployed this parameter for the calculation of C_4 plant abundance in order to elucidate if it can be used for the estimation of C_4 plant contribution (Table 3.4). Fig. 3.3b shows that for the samples from the northern locations the results resemble those based upon the stable carbon isotope composition. In contrast, for the southern sites abundances of >90% C_4 material were calculated from ACL_{25-35} values, compared to a value of 75% derived from stable carbon isotope compositions.

This discrepancy may partly be caused by limitations of the used end member data. The approach of this study did not take into account that the plant database shows a wide range of ACL_{25-35} values of C_3 plants and that some species can dominate the vegetation in a region and thus also the contribution to the continental margin sediment. For instance, the biome of the Mopane Woodlands is dominated by *Colophospermum mopane* which exhibits ACL_{25-35} values >31 (Vogts et al., 2009). Furthermore, shrubs and herbs become more abundant towards the south. Plants of these growth forms also synthesise *n*-alkanes with longer chains than do trees (Vogts et al., 2009). Despite these limitations, changes in C_4 grass contribution to the sediments in this region can be addressed not only by $\delta^{13}\text{C}$ ratios but to some extent also from ACL_{25-35} values.

3.6.3. Discussion of the calculated C_4 plant contribution

In order to evaluate how the abundance of the C_4 signal in the sediments can be explained by contributions from continental vegetation, the calculated values based on C_{31} were correlated with a map based on satellite-derived land cover maps which presents the proportion (%) of continental vegetation that uses the C_4 plant pathway (Still and Powell, 2010; Fig 3.4). The contribution of rivers, as well as the wind trajectories (Dupont and Wyputta, 2003), were taken into account. Postulated origins and the amount of contributions leading to the observed values are compiled in Table 3.5.

C_4 plant abundance of 17 to 38% calculated for locations one to four do not reflect the C_4 plant abundance in the rain forest area of the same latitude, where the C_4 plants maximally form 10% of the vegetation along the equator, increasing to 20% further south. Thus, an additional long range transport of

3. Sediment transect I: *n*-Alkane chain length and $\delta^{13}\text{C}$ ratios

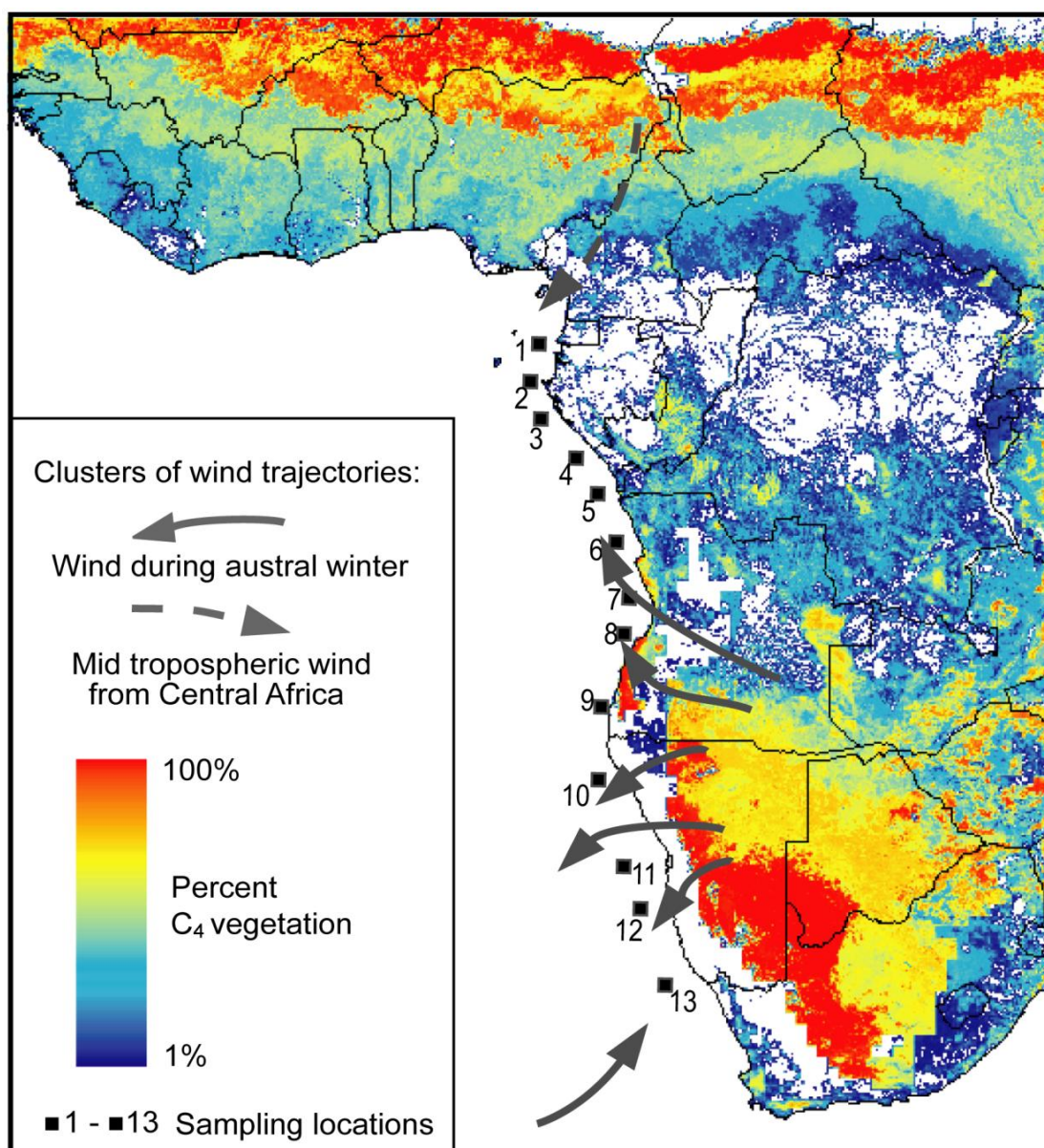


Fig. 3.4 Colour-coded map of proportion (%) of continental vegetation using C₄ pathway (Still and Powell, 2010) with wind trajectories (Dupont and Wypytta, 2003) and sampling locations. White areas represent either 100% C₃ vegetation (e.g. Central African rain forest) or absence of vegetation (Namib Desert).

eolian material by, e.g. Harmattan winds from northern central Africa, needs to be taken into account and which may contribute material with 80% C₄ signature. This effect should be highest for the northern site (40%), decrease further south (20%) but should no more be of significance off the Ogooué river (10%), where the fluvial signal dominates the sediment material. The C₄ abundance calculated from the sediment (23%) at location five

Table 3.5 Tentative scenarios for calculation of C_4 plant contribution to sediments from data for river discharge, wind trajectories (Dupont and Wyputta, 2003) and map of the proportion (%) of continental vegetation using the C_4 pathway (Still and Powell, 2010).

No.	Calculated C_4 plant contribution to location based on $\delta^{13}\text{C}_{31}$	Postulated contribution	Contribution to location	C_4 plant abundance contribution	Calculated C_4 plant contribution to location based postulated contribution
1	38	Continental vegetation signal of rain forest	60	10	38
		Long range transport by e.g. Harmattan winds	40	80	
2	17	Ogooue river outflow	90	10	17
		Long range transport by e.g. Harmattan winds	10	80	
3	29	Continental vegetation signal of rain forest	80	20	32
		Long range transport by e.g. Harmattan wind	20	80	
4	35	Continental vegetation signal of rain forest	80	20	32
		Long range transport by e.g. Harmattan wind	20	80	
5	23	Congo river outflow	100	20	20
6	31	ESE wind trajectories passing over area with abundant C_4	20	70	30
		ESE wind trajectories passing over area with abundant C_3	80	20	
7	41	ESE wind trajectories passing over area with abundant C_4	40	70	40
		ESE wind trajectories passing over area with abundant C_3	60	20	
8	52	ESE wind trajectories passing over C_3/C_4 transition zone	100	50	50
9	61	E wind trajectories passing C_4 dominated areas	80	80	68
		E wind trajectories passing C_3 dominated coastal areas	20	20	
10	63	E Wind trajectories passing C_4 dominated areas	80	80	68
		E Wind trajectories passing C_3 dominated coastal areas	20	20	
11	75	E Wind trajectories passing C_4 dominated areas	100	80	80
12	72	ENE Wind trajectories passing C_4 dominated areas	100	80	80
13	68	Low contribution by wind from cape flora and grassland	30	60	67
		Orange river signal transported by Benguela Current	70	70	

3. Sediment transect I: *n*-Alkane chain length and $\delta^{13}\text{C}$ ratios

off the Congo River corresponds well with the C_4 plant abundance in the catchment area (20%). Apparently, the intense river drainage overprints any contribution of windblown material of different origin.

For locations six to eight the calculated C_4 plant contribution (30 to 50%) does not resemble the continental abundance of C_4 plants in the area of the same latitude of maximal 20%. However, an eolian contribution from east-southeast explains the observed values, as the wind trajectories pass partly over areas with greater C_4 plant abundance. Further south, corresponding to ocean margin sites nine and ten, vegetation was divided into a more C_3 dominated region closer to the coast and a high C_4 plant abundance further inland. The latitudinally blowing wind transported this mixture of plant material to the sediments, leading to the observed values of about 60%.

Locations eleven and twelve revealed the highest abundances of C_4 material in the sediments, with values of >70%. This reflects the high abundance of C_4 plants transported from the continent to the sediments by nearly latitudinal winds for location eleven and wind blowing from east-northeast for location twelve, respectively. The southernmost site 13 showed slightly lower C_4 plant abundance, which did not reflect the still high abundance of C_4 material on the inner continent. Instead, a contribution by the Orange River plume may have caused a lower C_4 abundance for this site because along rivers C_3 plants are relatively more abundant. Furthermore, wind contributions from the C_3 -dominated Cape flora may add additional C_3 material but eolian contribution in the region is not a dominant factor as winds mainly blow towards the continent.

The explanations presented are tentative and, for instance, do not take into account the possibility that a higher amount of material from coastal vegetation compared to plants from inland areas may reach the sediments. Furthermore, due to limitations of the remote sensing approach, the map of continental vegetation that uses the C_4 plant pathway (Still and Powell, 2010) slightly overestimates the C_4 plant abundance in some regions and does not take into account the land cover density. However, reasonable explanations and quantifications for the calculated abundance of C_4 plant material in the sediments were obtained especially for sampling locations where the calcu-

lated C_4 plant contributions exceeded the abundance of these plants on the continental area of the same latitude.

3.6.4 Influence of environmental factors on C_4 plant abundance

The C_4 plant abundance is the result of a complex interplay of several parameters of which temperature and light are primary needs of C_4 plants (Sage, 2001). In the study area these parameters are not the limiting factors and secondary aspects like aridity, seasonality of rainfall, edaphic characteristics, fire and grazing stress are also important. In order to elucidate if the C_4 plant contribution to the sediments correlated with environmental conditions like mean annual precipitation or aridity in the continental catchment areas, the environmental parameters were determined for various locations on the continent (Table 7.7). The aridity index was calculated according to UNEP (1992) as a quotient of mean annual precipitation and potential annual evapotranspiration in order to elucidate not only the actual precipitation but the dryness the plants have to tolerate. Climatic parameters were calculated with the WebWIMP modelling program (Matsuura et al., 2003) with a resolution of 0.5° , which corresponds to roughly 50 km distance. For sampling sites one to five, nine to eleven and 13 the continental locations were at the same latitude as the sampling locations, whereas for sites six to eight locations in an east-southeast direction and for site twelve locations in east-northeast direction corresponding to the wind trajectories were used.

Climatic parameters were calculated for locations from 150 km to 400 km inland (every 50 km, Table 7.7). A minimum distance of 150 km was employed to avoid the influence of coastal climate, such as low precipitation due to cold coastal temperatures in regions of coastal upwelling. As the environmental parameters for material transported over very long distances are difficult to assess, these contributions were not taken into account, which may bias the correlations. Pearson correlation factors from these calculations are compiled in Table 3.6. For all parameters, high negative correlation factors were obtained for all distance intervals. Correlations are significant at the

3. Sediment transect I: *n*-Alkane chain length and $\delta^{13}\text{C}$ ratios

Table 3.6 Pearson correlation coefficients (r)^a of C_4 material abundance in sediments calculated from the stable carbon isotope composition of the $n\text{-C}_{31}$ alkane with mean annual precipitation and aridity index in postulated punctual catchment areas on the continent (Table 7.7).

	Distance to coast					
	150 km	200 km	250 km	300 km	350 km	400 km
Mean annual precipitation	-0.83	-0.88	-0.91	-0.92	-0.94	-0.94
Aridity index ^b	-0.69	-0.78	-0.86	-0.89	-0.92	-0.91

^a Bold values are significant at 99.9% level ($p < 0.001$), others are at 99% level ($p < 0.01$).

^b Calculated according to UNEP (1992) as quotient of mean annual precipitation and potential evapotranspiration.

99.9% level ($p < 0.001$) for nearly all locations. An approximate distance of 350 km from the coast afforded the highest correlation coefficients, indicating that the main catchment area may be this region. For this distance interval scatter plots are displayed in Fig. 3.5.

The significant correlations of mean annual precipitation and aridity indices with calculated C_4 plant contribution suggests that, at least in this re-

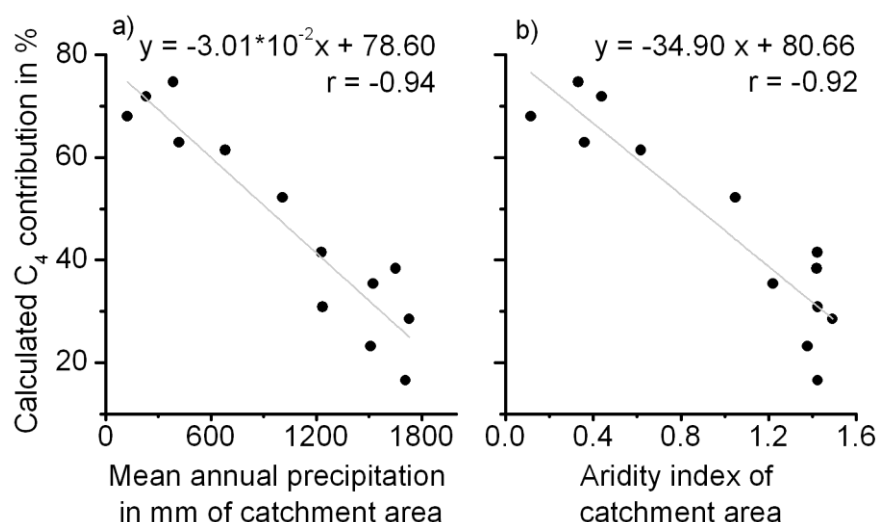


Fig. 3.5 Correlation of contribution of C_4 plant material calculated from stable carbon isotope composition of the $n\text{-C}_{31}$ alkane with a) mean annual precipitation and b) aridity index of catchment area. Climatic parameters are compiled in Table 7.7 and based on calculations for continental locations of ca. 350 km distance to coast with WebWIMP modelling program (Matsuura et al., 2003). Correlations are significant at 99.9% level ($p < 0.001$).

3. Sediment transect I: *n*-Alkane chain length and $\delta^{13}\text{C}$ ratios

gion, precipitation is a major factor influencing the C_4 plant abundance. The observed correlation may be useful for inferring ancient precipitation amounts and/or assessing the changing aridity of continental regions from calculated C_4 abundances if the other factors (temperature, light, seasonality of rainfall, edaphic characteristics, grazing and fire intensity as well as atmospheric CO_2 concentration) were similar to recent conditions.

3.7 Conclusions

This study corroborates the potential of long chain *n*-alkanes for the reconstruction of continental vegetation. From the equator to the south characteristic trends to longer chain length and less negative stable carbon isotope ratios were observed in ocean margin sediments along the southwest African continent. Both characteristics can be used to assess the contribution of C_4 material to the sediments because stable carbon isotope compositions as well as chain lengths distinguish C_3 from C_4 plant wax *n*-alkanes. The calculated values for C_4 plant contribution show reasonable correlations with C_4 abundance of postulated continental catchment areas if non-latitudinal eolian transport is taken into account.

The C_4 contribution to the sediments correlates significantly with the mean annual precipitation and the aridity indices in the catchment areas. Thus, the *n*-alkane characteristics may constitute useful indirect proxies for reconstructing the aridity on the continent via the determination of the C_4 plant abundance.

4. Stable hydrogen isotopic compositions of land plant-derived *n*-alkanes in marine sediments reflect δ D values of continental precipitation

Angela Vogts, Tanja Badewien, Jürgen Rullkötter, Enno Schefuß

This chapter was prepared for submission to *Geochimica et Cosmochimica Acta*.

4.1 Abstract

In order to explore the potential of the hydrogen isotope compositions of terrestrial biomarkers preserved in ocean sediments as proxies for continental hydrological conditions, a transect of marine surface sediment samples from 1°N to 28°S off southwest Africa was analysed. The conditions on the adjacent continent range from humid evergreen forest over deciduous forests, wood- and shrubland to arid grasslands and deserts. The hydrogen isotope ratios of the dominant *n*-alkanes (C_{29} , C_{31} and C_{33}) vary from -123 to -141‰. Despite the huge gradient of continental conditions and vegetation characteristics the hydrogen isotope ratios correlate with the modelled hydrogen isotope composition of mean annual, growing-season and end of growing-season precipitation of continental source areas along postulated transport pathways. For mean annual precipitation values best correlations were obtained for continental source areas at 250 km distance from the coast and the *n*- C_{31} alkane. Neglecting potential inconsistencies in catchment area definitions the apparent fractionations especially between the *n*- C_{29} and *n*- C_{31} alkanes and mean annual precipitation are remarkably uniform along the transect (-109 ± 3 and -115 ± 3 ‰, respectively) despite the significant differences of environmental conditions and vegetation. Thus, this study extends the potential of hydrogen isotope ratios of leaf wax *n*-alkanes preserved in sediments for palaeo-climatic studies towards biomarkers preserved in ocean margins. Their hydrogen isotope ratios can directly be converted to δ D ratios of ancient precipitation to elucidate changes of the hydrogen isotope composition of precipitation on the adjacent continent and their climatic control.

4.2 Introduction

Ocean margin sediments are most valuable archives for palaeo-climatic studies as they can provide long, undisturbed records of climate-dependent changes in sediment characteristics like, e.g., the molecular chemical composition of its constituents. But before ancient climate conditions can be assessed from sediment cores the way present-day conditions are reflected in recent sediments needs to be evaluated. Reliable and widespread molecular biomarkers with a good potential for palaeo-environmental studies are land plant-derived wax constituents. Plant waxes cover all aerially exposed organs of higher land plants, and in virtually all plant waxes *n*-alkanes, which are in the focus of this study, are abundant (Tulloch, 1976). After the decay of plants the wax components can be stored in intermediate reservoirs or directly transported by wind and rivers to lake or ocean sediments. In these archives the *n*-alkanes can be preserved over geological time scales and may constitute an integrated signal of the plant wax composition in the catchment area.

The hydrogen isotope ratios of biomarkers from land plant waxes have been considered a proxy for the corresponding composition of precipitation and the hydrologic conditions (e.g. Xie et al., 2000; Yang and Huang, 2003; Dawson et al., 2004; Liu and Huang, 2005; Schefuß et al., 2005; Sachse et al., 2006; Shuman et al., 2006; Aichner et al., 2010). Hydrogen atoms introduced to plant wax molecules during photosynthesis derive from plant water and plant water in turn is controlled by soil water, which is the only source for water in most plants and originates from precipitation. The hydrogen isotope signature of soil and plant water is, however, also influenced by evaporation and evapotranspiration (Sternberg, 1988). Additionally, it has been inferred that the δD values of plant water can be influenced to different extents by the plant characteristics like ecological life form (tree, shrub, grass; Liu et al., 2006; Liu and Yang, 2008) and the metabolic pathway employed ($C_3/C_4/CAM$; Chikaraishi and Naraoka, 2003; Bi et al., 2005; Smith and Freeman, 2006; Feakins and Sessions, 2010b). Despite these potentially obscuring multiple effects, the stable hydrogen isotope compositions of plant lipids in lake sediments exhibited a linear or nearly linear relationship to the

4. Sediment transect II: *n*-Alkane stable hydrogen isotope composition

δD ratios of source waters corroborating the idea that fossil lipids may serve as a direct proxy for source water hydrogen isotope characteristics (Sachse et al., 2004; Hou et al., 2008).

In order to explore the potential of the hydrogen isotope composition of *n*-alkanes preserved in ocean margin sediments as a proxy for continental hydrological conditions, a transect of marine surface sediment samples from 1°N to 28°S off southwest Africa was analysed. Africa, especially the western part with its distinct latitudinal distribution of vegetation zones and climatic conditions, constitutes an ideal test case for such a study. Sediment samples recovered from similar water depths (ca. 1300 m) were used to minimise possible effects of different transport distances from the continent or water column height. The hydrogen isotope composition of the three dominant *n*-alkanes (*n*-C₂₉, *n*-C₃₁, and *n*-C₃₃) was measured and compared to that of continental precipitation derived from modelling approaches (Bowen and Revenaugh, 2003; Bowen et al., 2005). To our knowledge this is the first marine sediment transect evaluating how the hydrogen isotope composition of *n*-alkanes preserved in ocean margin sediments mirrors the corresponding composition of continental precipitation. This information is essential for reliable reconstructions of the stable isotope composition of ancient precipitation and its climatic control.

4.3 Material and Methods

4.3.1 Sediment material

We analysed 13 marine surface sediment samples that constitute an isobathic (ca. 1300 m) north to south transect (1°N to 28°S) along the southwestern African continental margin. The samples were retrieved during cruises M34/2 and M41/1 of the German research vessel Meteor in 1996 and 1998, respectively, and recovered by multicorer to receive the undisturbed surface layers. The multi-cores were separated into depth intervals, the sections sealed in polyethylene bags and stored at -20°C on board and afterwards at the University of Bremen. Sampling locations are displayed in Fig. 4.1, and more detailed sample information is compiled in Table 4.1.

4. Sediment transect II: *n*-Alkane stable hydrogen isotope composition

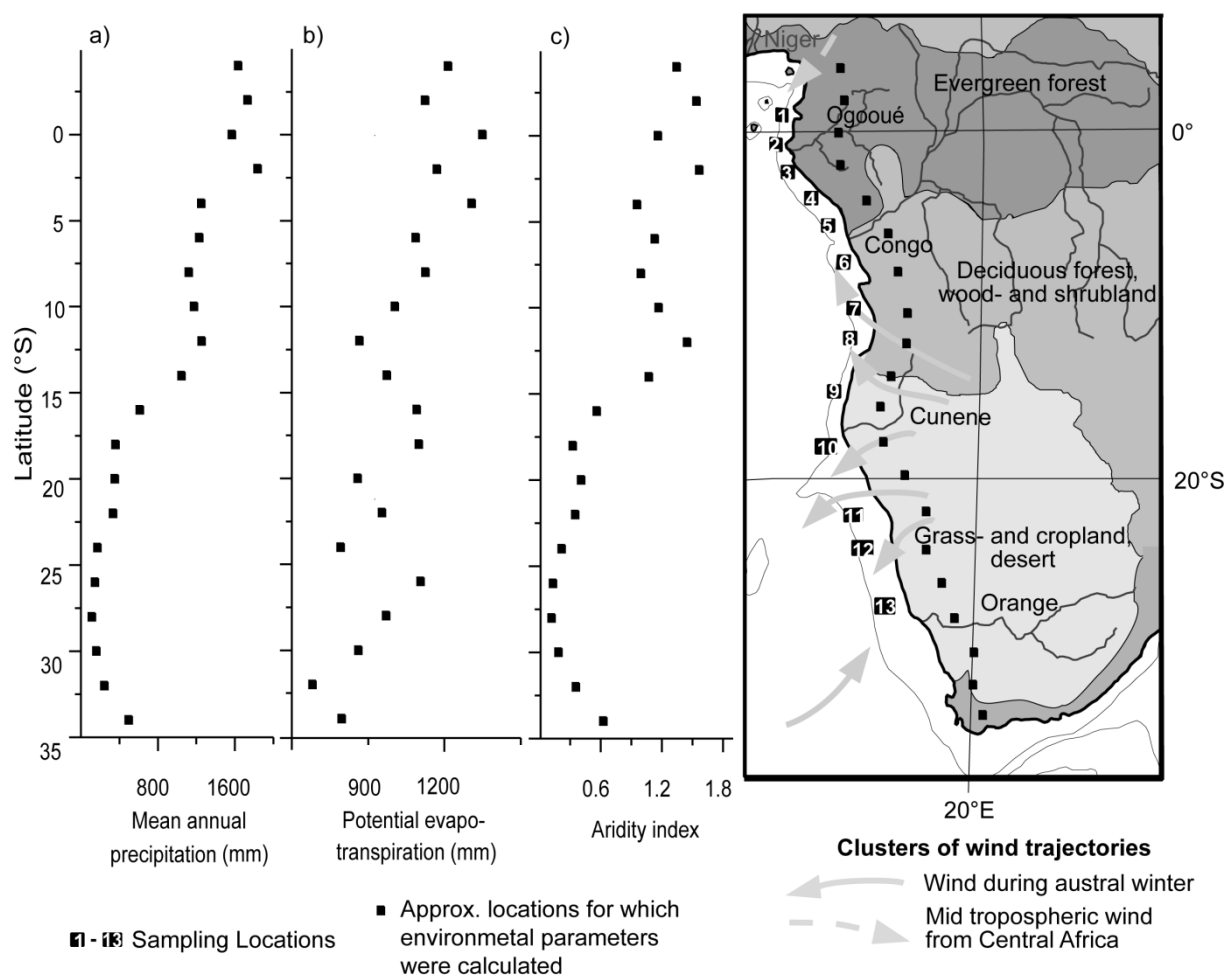


Fig. 4.1 Simplified present-day land cover map based on Mayaux et al. (2004) with sampling locations, clusters of wind trajectories based on Dupont and Wyputta (2003), and graphs of environmental parameters calculated for locations with 250 km distance to the coast with the WebWIMP modelling program (Matsuura et al., 2003). Latitude and longitude of locations as well as values for environmental parameters are compiled in Table 7.8.

4.3.2 Analytical methods

The procedures for the isolation of aliphatic/alicyclic hydrocarbons from the marine sediments are described in Chapter 3.3.2. Branched compounds were separated from the straight-chain hydrocarbons by urea adduction. Stable hydrogen isotope compositions of the *n*-alkanes were analysed by gas chromatography (GC, Agilent 6890) coupled to a Thermo Scientific MAT 253 ir-MS via a combustion interface (GCC-III). The GC instrument was equipped with a 30 m capillary column (J&W, DB-5, 0.25 mm i.d., 0.25 µm film

4. Sediment transect II: *n*-Alkane stable hydrogen isotope composition

Table 4.1 Compilation of sample information.

No.	GeoB No.	Latitude	Longitude	Water depth (m)	Cruise	Interval (cm bsf) ¹
1	4904-6	0.962°N	8.88°E	1349	M41/1	0.5 - 2
2	4906-4	0.69°S	8.378°E	1272	M41/1	1 - 2
3	4909-3	2.068°S	8.625°E	1305	M41/1	0 - 1.5
4	4912-3	3.73°S	09.785°E	1298	M41/1	0 - 1
5	4913-3	5.503°S	11.072°E	1296	M41/1	0 - 2.5
6	4915-2	7.75°S	11.873°E	1306	M41/1	0.5 - 2
7	4916-3	10.173°S	12.687°E	1294	M41/1	0 - 1
8	4917-4	11.903°S	13.073°E	1300	M41/1	0.5 - 2.5
9	3713-1	15.628°S	11.58°E	1330	M34/2	1.5 - 2.5
10	3715-2	18.955°S	11.057°E	1203	M34/2	1 - 3.5
11	3706-3	22.717°S	12.602°E	1313	M34/2	0.5 - 1.5
12	3705-3	24.303°S	12.997°E	1308	M34/2	0.5 - 2
13	3701-1	27.952°S	14.003°E	1488	M34/2	0.5 - 1.5

¹ Analysed sediment interval in cm below sea floor.

thickness), the injector temperature was programmed from 60°C (5 s) to 305°C (120 s) at 10°C s⁻¹ and the GC oven was programmed from 60°C (2 min) to 300°C at a rate of 3°C min⁻¹, followed by an isothermal phase of 36 min. Isotope ratios are expressed as δD values in per mil (‰) relative to Vienna Standard Mean Ocean Water (V-SMOW).

Calibration of isotope analysis was performed by injecting several pulses of reference gas (H₂) at the beginning and at the end of each run and by measurement of a standard mixture between sample runs. The standard mixture contained lab standards and certified standard substances which together span a range of -50‰ to -250‰ (normalised to the V-SMOW/SLAP isotope scale). For eleven standard substances (fatty acid methyl esters and alkanes) in the retention time interval of the target compounds the precision for replicate analyses expressed as averaged standard deviation was 3.5‰, and the averaged absolute error was 2.1‰ (n = 33). Analyses of samples were run at least in triplicate with standard deviations better than 3.5‰ (2.1‰ on average, n = 60). Eicosanoic acid methyl ester (certified) and docosanoic acid methyl ester (lab standard) of known hydrogen isotope composition were added to the samples and used for quality control, but standard deviations for these internal standards were higher (7.6 and 6.7‰, respectively). This is attributed to coelution of sample components with the standards.

4.4 Regional setting

4.4.1 Hydrological conditions in southwest Africa

To depict environmental conditions in the study area Fig. 4.1 provides values for mean annual precipitation amount, potential evapotranspiration (both calculated with the WebWIMP modelling program; <http://climate.geog.udel.edu/~wimp/>) as well as aridity index (calculated according to UNEP, 1992). The tropical climate is governed by the seasonal migration of the ITCZ in response to changes in the latitudinal maximum of solar heating. Along the equator a humid zone without definite dry periods and mean annual rainfall of 1500 mm and more prevails (Fig. 4.1a). Further south, mean annual precipitation decreases gradually and the climate is monsoonal, with austral summer rains and winter drought. Subtropical deserts follow where precipitation is scarce. For instance, parts of the Namib Desert receive less than 100 mm precipitation per year (Richard and Pocard, 1998). South of 32°S mean annual precipitation increases again due to the equatorward displacement of the mid-latitude Westerlies during austral winter causing highest precipitation during winter and dry summers.

The hydrogen isotope composition of the precipitation varies with moisture source, altitude, amount of precipitation and degree of continentality (Gat, 1996). The model-based map of mean annual δD_P (hydrogen isotope composition of precipitation) mirrors the interplay of these factors leading to ratios ranging from relatively positive values in the rain forest region over more negative values south of the Congo River to more positive ratios south of 20°S (Bowen and Revenaugh, 2003; Fig. 4.2). The δD_P in Africa varies with season by up to 60‰ but for the postulated catchment areas relevant to this study the difference of growing season or end of growing season δD_P and mean annual δD_P does not exceed 11‰ (Fig. 4.2a).

4. Sediment transect II: *n*-Alkane stable hydrogen isotope composition

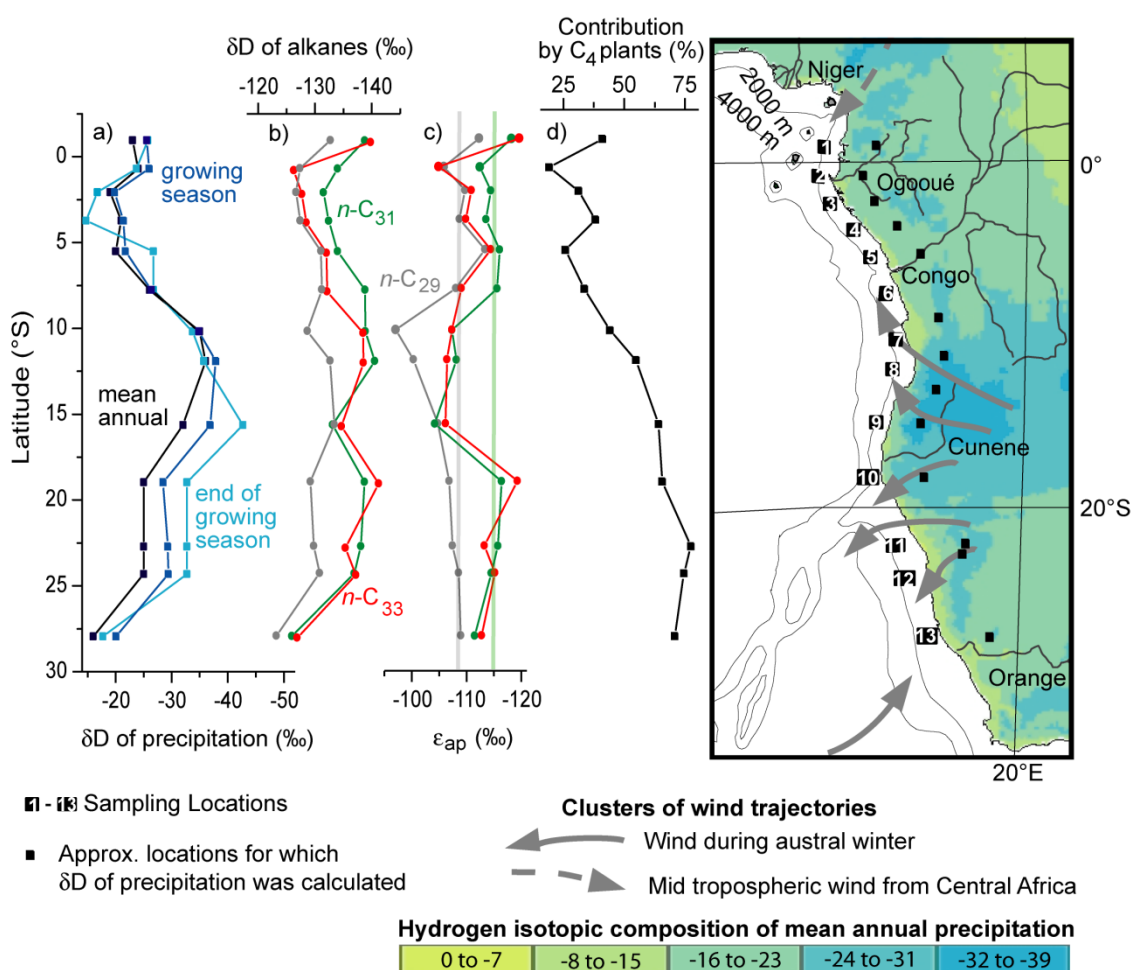


Fig. 4.2 Stable hydrogen isotope composition of (a) precipitation at 250 km distance from the coast in postulated catchment areas indicated by black squares in the map, latitude and longitude are compiled in Table 7.7, (b) *n*-alkanes dominating the aliphatic fraction of the sediment samples as well as (c) apparent fractionation between *n*-alkanes and mean annual precipitation, vertical lines represent ϵ_a of -109 (grey) and -115‰ (green), (d) contribution by C_4 plants to the sediments calculated from the weighted mean averaged stable carbon isotopic composition of *n*-alkanes (Table 3.3, Chapter 3), and map of southwest Africa showing sampling locations as well as hydrogen isotope composition of mean annual precipitation (Bowen and Revenaugh, 2003). Clusters of wind trajectories based on Dupont and Wyputta (2003).

4.4.2 Vegetation of southwest Africa

In general, there is a clear gradient from dense evergreen biomes to dry open land-cover from the equator to the subtropics, corresponding to the mean annual rainfall gradient (Mayaux et al., 2004). Looking southwards from the equator, the vegetation of southwest Africa ranges from evergreen

4. Sediment transect II: *n*-Alkane stable hydrogen isotope composition

rain forest through dry evergreen and deciduous forests, wood- and shrublands, grass- and croplands to deserts (simplified map: Fig. 4.1). At the high latitude southern African coast woody species become abundant again forming the unique Fynbos vegetation.

Rain forest vegetation is characterised by woody C₃ plants as major representatives of the flora (Richards, 1996). The evergreen rain forest extends to about 9° S and is increasingly confined to river valleys towards its limits. Then, dry evergreen forests and further on forests with deciduous plants gain importance. The closed forest (no grass cover on the ground) often abruptly passes into a wide zone of savanna wood- and shrub-land (Richards, 1996). In these savanna regions deciduous woody species can cover up to 60% of the area (Cole, 1986) but the amount of woody C₃ vegetation decreases with increasing aridity, accompanied by increasing C₄ grass abundance. In the semi-deserts on the African Plateau (Kalahari and Nama Karoo) C₄ grasses dominate the vegetation while in the dry coastal Namib Desert the vegetation is very sparse. In the Succulent Karoo succulent plants employing the Crassulacean Acid Metabolism (CAM) dominate but as CAM is generally a strategy for stress survival and not for high productivity, the contribution of CAM-utilising plants to biomass production, and thus also to geological archives, is negligible (Lüttge, 2004).

4.4.3. Transport pathways and catchment areas for plant wax lipids

Modelled eolian transport pathways of terrestrial components were presented by Dupont and Wyputta (2003) for wind-born material reaching sediments off southwest Africa (6°S to 30°S, implemented in Figs. 4.1 and 4.2). The main transport away from the continent occurs during austral fall and winter when south-easterly to north-easterly winds prevail. For the equatorial sites there may be some mid-tropospheric transport by Harmattan winds from north-central Africa. South of 25°S, wind blows mostly from the west and southwest and thus, eolian supply of terrigenous material is very small (Dupont and Wyputta, 2003).

Also rivers transport large amounts of dissolved and particulate organic matter to ocean sediments near river mouths, and it has been shown that

4. Sediment transect II: *n*-Alkane stable hydrogen isotope composition

n-alkanes in marine sediments off rivers reflect the vegetation in adjacent river catchments (Bird et al., 1995; Schefuß et al., 2004; Weijers et al., 2009). In the study area the Congo River system is the largest and also the second biggest in the world regarding the outflow at the mouth (Dai and Trenbeth, 2002). The outflows of the Ogooué (ca. 1°S) and the Orange (28.5°S) are lower by a factor of ca. ten, and even lower by a factor of 50 or more for other rivers (e.g. Kunene; 17°S; Heyns, 2003; Nilsson et al., 2005). However, the river outflow data only reflect the quantity of water and not the amount of *n*-alkanes transported. Quantitative data on the contribution of *n*-alkanes to deep sea sediments by these rivers are not available.

4.5. Results and Discussion

4.5.1 Hydrogen isotope composition of *n*-alkanes

In all samples, the *n*-C₂₉, *n*-C₃₁, and *n*-C₃₃ alkanes (hereafter abbreviated C₂₉, C₃₁ and C₃₃) are the most abundant homologues (Chapter 3.5.1). The stable hydrogen isotope composition of these compounds varies from -123 to -141‰ (Table 4.2, Fig. 4.2b). The observed values are slightly more positive than ratios for C₂₉ in core-top material of a sediment core recovered off the Congo River mouth (ca. -145 ‰, Schefuß et al., 2005). As studies of marine organisms do not show any significant abundances of these long-chain alkanes (Chikaraishi and Naraoka, 2003; Mead et al., 2005) and hopane and carbon preference index analyses indicate the presence of constant but only very small amounts of petroleum *n*-alkanes (Chapter 3.5.1), the observed variations of the *n*-alkane stable hydrogen isotope compositions are nearly exclusively related to the source land plants.

The δD ratios of C₂₉ (δD_{29}) vary by only 10‰ but the variations of δD_{31} and δD_{33} are higher (15‰). A slight trend was observed from negative values at the northernmost site to more positive values for the sites off the rain forest to again more negative values south of the Congo River mouth whereas the highest values for all homologues were measured for the samples from the southernmost site (Fig. 4.2b). Among the *n*-alkanes of a given sampling

4. Sediment transect II: *n*-Alkane stable hydrogen isotope composition

Table 4.2 Stable hydrogen isotope composition of major terrestrial *n*-alkanes and weighted mean averaged stable hydrogen isotope composition (WMA) with standard deviation (SD).

No.	<i>n</i> -C ₂₉ Alkane		<i>n</i> -C ₃₁ Alkane		<i>n</i> -C ₃₃ Alkane		WMA ₂₉₋₃₃	
	δD (‰) ¹	SD (‰)	δD (‰) ¹	SD (‰)	δD (‰) ¹	SD (‰)	δD (‰)	SD (‰)
1	-133	2	-139	2	-140	3	-136	2
2	-127	2	-134	2	-127	3	-130	2
3	-127	2	-131	3	-128	3	-129	2
4	-127	2	-132	1	-129	1	-130	2
5	-131	2	-134	2	-132	3	-132	2
6	-131	2	-139	1	-132	2	-134	2
7	-129	0	-139	2	-139	1	-135	1
8	-133	1	-140	1	-139	3	-137	2
9	-133	3	-133	2	-135	2	-134	2
10	-129	2	-139	2	-141	2	-137	2
11	-130	2	-138	3	-136	1	-135	2
12	-131	2	-137	1	-137	3	-136	2
13	-123	2	-126	2	-127	3	-126	2

¹ **Boldface values** refer to the two most abundant homologues.

location δD₂₉ is most positive in the majority of cases and δD₃₁ is 5‰ more negative on average. δD₃₃ resembles δD₃₁ except for locations 2 to 5 where the values are similar to those of C₂₉.

4.5.2 Correlation with the δD signal of precipitation

To elucidate possible correlations of the δD ratios of the sedimentary *n*-alkanes with those of precipitation (δD_P) the online isotopes-in-precipitation calculator (OIPC 2.2, Bowen and Revenaugh, 2003) was employed to determine the δD values of mean annual precipitation (Table 4.3). Calculations were made for equidistant locations along postulated main contribution pathways (Table 7.7), which are based on wind trajectories presented by Dupont and Wyputta (2003). Thus, locations of the same latitude as the marine sampling sites (sites 1 to 5, 9 to 11, and 13), along east-southeast trajectories (sites 6 to 8), or along east-northeast trajectories (site 12), respectively, were selected. The sites on the continent had a distance to each other of 0.5° (ca. 50 km) starting at approximately 100 km from the coast to exclude possible effects of coastal climate. Previous analyses of continental margin sediments

4. Sediment transect II: *n*-Alkane stable hydrogen isotope composition

Table 4.3 Hydrogen isotope composition of mean annual and growing-season precipitation for continental locations (Table 7.7) and Pearson correlation coefficients for linear correlation with *n*-alkane stable hydrogen isotope composition.

No.	Approximate distance from shore (km)								Growing season	Last month of growing season
	100	150	200	250	300	350	400	250		
	Hydrogen isotope composition of precipitation (95 % confidence interval) in ‰ ¹									
	Annual mean	Annual mean	Annual mean	Annual mean	Annual mean	Annual mean	Annual mean	Annual mean		
1	-24 (4)	-23 (4)	-23 (4)	-23 (4)	-23 (4)	-22 (6)	-23 (6)	-23 (6)	-26	-26
2	-17 (4)	-16 (4)	-17 (4)	-24 (4)	-22 (4)	-21 (6)	-21 (6)	-21 (6)	-26	-24
3	-16 (3)	-18 (4)	-17 (4)	-19 (4)	-25 (4)	-27 (5)	-25 (5)	-25 (5)	-20	-17
4	-25 (4)	-21 (4)	-16 (4)	-21 (4)	-22 (4)	-24 (4)	-24 (4)	-24 (4)	-22	-15
5	-17 (3)	-21 (3)	-17 (3)	-20 (3)	-23 (3)	-21 (3)	-23 (3)	-23 (3)	-22	-27
6	-11 (4)	-13 (3)	-16 (3)	-26 (3)	-24 (3)	-30 (3)	-25 (3)	-25 (3)	-27	-27
7	-28 (3)	-30 (3)	-30 (3)	-35 (2)	-35 (2)	-36 (2)	-37 (3)	-37 (3)	-35	-34
8	-30 (2)	-41 (3)	-41 (3)	-36 (2)	-38 (4)	-37 (4)	-37 (4)	-37 (4)	-38	-36
9	-18 (2)	-31 (3)	-31 (2)	-32 (2)	-30 (2)	-30 (2)	-32 (1)	-32 (1)	-37	-43
10	-21 (6)	-28 (5)	-26 (5)	-25 (5)	-24 (5)	-24 (5)	-24 (5)	-24 (5)	-29	-33
11	-17 (4)	-20 (3)	-25 (3)	-25 (3)	-25 (3)	-25 (3)	-24 (3)	-24 (3)	-30	-33
12	-10 (5)	-17 (4)	-20 (4)	-25 (4)	-22 (4)	-28 (4)	-26 (5)	-26 (5)	-30	-33
13	-12 (4)	-15 (4)	-16 (4)	-16 (4)	-19 (4)	-18 (4)	-17 (4)	-17 (4)	-20	-18
$r(n\text{-C}_{29}\text{ alkane})^2$	0.24	<i>0.49</i>	<i>0.54</i>	<i>0.60</i>	0.46	0.47	<i>0.53</i>	0.63	0.72	
$r(n\text{-C}_{31}\text{ alkane})^2$	0.42	0.45	<i>0.56</i>	0.67	0.53	<i>0.59</i>	<i>0.55</i>	0.62	0.58	
$r(n\text{-C}_{33}\text{ alkane})^2$	0.43	<i>0.62</i>	0.68	<i>0.61</i>	<i>0.49</i>	0.47	<i>0.53</i>	0.65	0.72	
$r(\delta D_{\text{WMA29-33}})^2$	0.35	<i>0.54</i>	0.64	0.66	<i>0.49</i>	<i>0.52</i>	<i>0.54</i>	0.69	0.75	

¹ Confidence intervals not available for monthly values.

² **Bold italic numbers:** Correlation significant at the 99 % level. *Italic numbers:* Correlation significant at the 95 % level.

4. Sediment transect II: *n*-Alkane stable hydrogen isotope composition

revealed a reasonable correspondence between the C₄ species abundance in the postulated catchment areas and the contribution of C₄ plant derived components to the sediments (Chapter 3.6.3). The calculated hydrogen isotope ratios of mean annual continental precipitation show a good correlation with the δD ratios of the individual and weighted mean *n*-alkane ratios (Table 4.3). The range of δD_P for the continental locations (max. 28‰) is higher than the range of hydrogen isotope ratios for sedimentous alkanes (max. 15‰). This may be related to the simplified assumption regarding the catchment areas as averaging effects over bigger catchment areas can smoothen δD_P differences. However, except for 100 km distance from the coast, the correlation coefficients are above 0.45 with a significance of correlation above 95% in most cases. The highest correlation coefficients were observed for the distances of 200 and 250 km from the coast. Previous analyses of the same samples revealed significant correlations ($p > 99.9\%$) between the C₄ contribution to the sediments and environmental parameters for the same postulated catchment locations of 200 to 400 km distance from the coast (Chapter 3). Thus, this area may represent a major source region contributing to the sediments even though this is only a simplified approach which does not take into account that the sediments may receive a mixture of material from this area with and potentially significant amounts of material from coastal or river-side vegetation. Also, long-range transport like, e.g., contribution by Harmattan winds from north central Africa was not taken into account, because the δD ratios of contributions from such wide catchment areas are difficult to assess.

As the precipitation is unevenly distributed across Africa in terms of amount and stable hydrogen isotope composition, monthly δD_P was calculated for locations at approximately 250 km distance from the coast (OIPC 2.2, Bowen et al., 2005). To assess the aspect of seasonality, δD values for growing-season precipitation were calculated by averaging monthly values with respect to rainfall amounts (Table 4.3). Months were attributed to growing season if the amount of precipitation was higher than potential evapotranspiration (Table 7.9). Precipitation amount and potential

4. Sediment transect II: *n*-Alkane stable hydrogen isotope composition

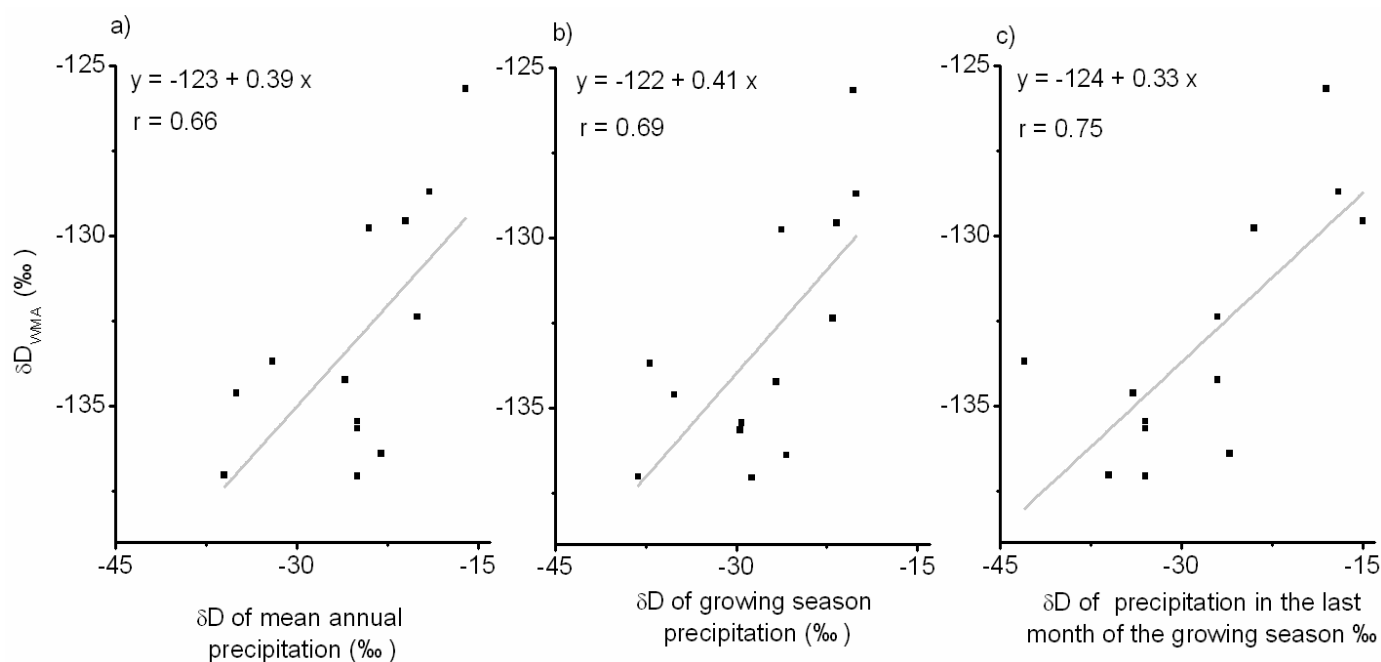


Fig. 4.3 Linear correlation of weighted mean averaged δD ratios of the sedimentary *n*-alkanes with hydrogen isotope composition of (a) mean annual, (b) growing-season, and (c) last month of growing-season precipitation for locations with 250 km distance from the coast in postulated catchment areas.

evapotranspiration were calculated with the WebWIMP modelling program (Matsuura et al., 2003). For locations with precipitation lower than potential evapotranspiration in most or all months the three months with the highest precipitation were taken. The resulting δD ratios for growing-season precipitation are up to 5 ‰ (3 ‰ on average) more negative than those of mean annual precipitation (Fig. 4.2b). The correlation of δD_{29} , δD_{33} and δD_{WMA} with hydrogen isotope composition of the growing-season precipitation is slightly better but lower for δD_{31} compared to the correlation with mean annual precipitation ratios (Table 4.3, Fig. 4.3).

As Sachse et al. (2009) found the *n*-alkane signal preserved in soils to be representative of the weeks before leaf senescence, also correlations with the last month of the growing season were tested and similar or better correlations were obtained except for C_{31} (Fig. 4.3c, Table 4.3). This is consistent with studies indicating that leaf waxes are continuously produced during the lifespan of a plant due to the need of replacing wax components abraded by mechanical stress (Richardson et al., 2005). In contrast, other studies indicate that the bulk of *n*-alkanes are synthesized during leaf formation

4. Sediment transect II: *n*-Alkane stable hydrogen isotope composition

(Jetter et al., 2006), and for field-grown barley Sachse et al. (2010) showed that the hydrogen isotope signature of *n*-alkanes reflects leaf water δD at the time of leaf development. Thus, also correlations of the δD ratios of the sediment-derived *n*-alkanes with the δD_P ratios for the first and second month of the growing season were tested but yielded lower Pearson correlation coefficients (data not displayed). However, it must be taken into account that the strength of correlation with growing-season precipitation may also be influenced by the seasonality of the prevailing winds which mainly blow towards the ocean during austral winter (Dupont and Wyputta, 2003).

4.5.3 Apparent fractionation

To further evaluate influences on the correlations described before, the apparent stable hydrogen isotope fractionation (ϵ_a) between δD_P and δD_L (stable hydrogen isotope composition of lipids) was calculated using the following equation:

$$\epsilon_a = 1000[(\delta D_L + 1000)/(\delta D_P + 1000) - 1]$$

Calculations were made using mean annual δD_P at 250 km distance from the coast in postulated catchment areas, because the improvement of correlations by employing growing-season δD_P was not consistent for all homologues. The calculated values from -97 to -120‰ (Table 4.4) for this ocean sediment transect are in the range observed for plants and lake sediments (e.g., Chikaraishi and Naraoka, 2003; Bi et al., 2005; Polissar and Freeman, 2010). The graphical presentation of ϵ_a ratios of the alkanes (Fig. 4.2c) exhibits similar general trends for C_{29} and C_{31} with low variation from sites 1 to 6, more positive values for locations 7 to 9 and more negative and constant ratios again from locations 10 to 13. The positive ϵ_a for locations 7 to 9 may be related to the limitations of the punctual catchment area assessment because the postulated catchment areas for locations 7 to 9 are within the continental region of most negative δD_P as displayed in the map in Fig. 4.2. Long-range transport and/or slight changes of wind directories would contribute material from areas with less negative δD_P which leads to ϵ_a ratios

4. Sediment transect II: *n*-Alkane stable hydrogen isotope composition

Table 4.4 Apparent hydrogen isotope fractionation (ϵ_a) for hydrogen isotope composition of *n*-alkanes and mean annual precipitation with standard deviation (SD) for continental locations at 250 km distance from the coast in postulated catchment areas.

No.	$\epsilon_{aC_{29}}$ (‰)	SD (‰)	$\epsilon_{aC_{31}}$ (‰)	SD (‰)	$\epsilon_{aC_{33}}$ (‰)	SD (‰)	$\epsilon_{aWMA_{29-33}}$ (‰)	SD (‰)
1	-112	4	-118	4	-120	4	-116	4
2	-106	3	-113	4	-105	4	-108	3
3	-110	3	-115	4	-111	4	-112	4
4	-109	4	-114	3	-110	3	-111	3
5	-113	3	-116	3	-115	4	-115	3
6	-108	3	-116	3	-109	3	-111	3
7	-97	2	-108	3	-107	2	-103	2
8	-100	2	-108	2	-107	3	-105	3
9	-105	4	-104	3	-106	3	-105	3
10	-107	4	-117	4	-119	4	-115	4
11	-107	3	-116	4	-113	2	-113	3
12	-109	4	-115	3	-115	4	-113	3
13	-109	3	-112	3	-113	4	-111	4

[†] **Boldface values** refer to the two most abundant homologues.

in the range of other samples. Neglecting locations 7 to 9 ϵ_a is fairly constant for C_{29} and for C_{31} with average ratios of $-109 \pm 3\text{‰}$ and $-115 \pm 3\text{‰}$, respectively (indicated by vertical lines in Fig. 4.2c). The ϵ_a for C_{33} resembles ϵ_a of C_{31} for locations 1 and 7 to 13 whereas it is similar to C_{29} for locations 2 to 6 (Fig. 4.2c). This indicates that there are different vegetation areas contributing to the abundance of this alkane in the course of the sediment transect. As C_{33} is not abundant in trees, shrubs and lianas in the rain forest (Vogts et al., 2009) it may be derived from other plants of this habitat like, e.g., epiphytes or grasses in tropical swamps. Analytical data for such plants from the study region are not available yet but studies for other locations revealed a systematic difference of apparent fractionations for different ecological life forms in the sense that for grasses more negative ratios were observed than for woody vegetation (Liu et al., 2006; Hou et al., 2007). However, the ϵ_a of C_{33} is not more negative but more positive than ϵ_a of C_{31} for these sites seems to contradict an origin of C_{33} from rain forest swamp grasses. Another or an additional explanation may be the contribution of long-range transported mate-

4. Sediment transect II: *n*-Alkane stable hydrogen isotope composition

rial (e.g., by Harmattan winds) with different isotope composition. Based on stable carbon isotope composition, previous results postulated a long-range contribution of up to 40% to explain the high abundance of C₄-plant-derived alkanes at locations 1 to 4 (Chapter 3.6.3).

The calculated ϵ_a values incorporate the effects of soil evaporation, transpiration and biosynthesis whereas it was hypothesised that the fractionation of hydrogen during biosynthesis of *n*-alkanes is constant (Sessions et al., 1999; Sachse et al., 2004; Feakins and Sessions, 2010a). Therefore, evaporation of soil water and evapotranspiration from the plant are the main factors influencing the apparent fractionation. As vapour-phase water is depleted in the heavy isotopes relative to the liquid from which it is derived, strong evaporation at the arid sites leads to higher δD ratios of soil and plant water and a lower apparent fractionation between precipitation and *n*-alkane ratios. For instance, Aichner et al. (2010) and Smith and Freeman (2006) found lower fractionation at sites receiving less precipitation. For our continental locations with 250 km distance from the coast mean annual precipitation decreases from nearly 2000 mm near the equator towards less than 200 mm for the southernmost site. Despite this huge gradient in environmental conditions ϵ_a is fairly constant and, thus, Pearson correlation coefficients of ϵ_a and environmental factors are low (Table 4.5). This corresponds well to studies of soils in China (Rao et al., 2009) and lake sediments in Europe (Sachse et al., 2004) which also found relatively constant fractionations over large latitudinal ranges but in these cases ϵ_a was more negative with, -130‰ for C₂₉ in European lakes. Also lake sediments from evergreen

Table 4.5 Pearson correlation coefficients for apparent fractionation and environmental parameters (Table 7.7) for locations in postulated catchment areas at 250 km distance from the coast.

	Mean annual precipitation	Potential Evapotranspiration	Aridity Index
ϵ_{aC29}^1	-0.10	-0.37	0.06
ϵ_{aC31}^1	-0.12	-0.10	-0.05
ϵ_{aC33}^1	<i>0.29</i>	0.08	<i>0.36</i>
$\epsilon_{aWMA29-33}^1$	0.10	-0.09	<i>0.21</i>

¹ *Italic numbers*: Correlation significant at the 75 % level.

4. Sediment transect II: *n*-Alkane stable hydrogen isotope composition

forests in America revealed relatively negative ratios of -117 to -128‰ but for lakes in the South American Páramo shrubland ratios of -94 to -122‰ for C₂₉ were observed (Polissar and Freeman, 2010) which resemble the values of this study.

A possible explanation for the lack of correlation of environmental parameters with ϵ_a are the vegetation characteristics of southwest Africa. Data for ϵ_a of plants from the study region are not available yet, but the different ϵ_a values for grasses and woody vegetation of other environments (Liu et al., 2006; Hou et al., 2007) are assumed to be applicable to Africa, too, as the factors causing the differences are also relevant for African plants. One possible explanation for less negative δD values of woody plants is the ability of woody plants to access deeper water (Asbjornsen et al., 2008) which exhibits higher δD ratios (Griewé et al., 2001). An additional factor is the different evapotranspiration of grasses and trees due to the dissimilar microhydraulic systems and thickness of the leaves leading to different water use efficiencies (Liu and Yang, 2008).

The change from woody vegetation to grasses in the study region is also a change from C₃ to C₄ plants (Fig. 4.2d) but the metabolic pathway is assumed to be of lower relevance for ϵ_a than the life form effect. For instance, McInerney et al. (2011) compiled ϵ_a ratios of several studies and the ϵ_a for C₄ grasses (-145‰) was between those for C₃ grasses (170‰) and dicotyledenous C₃ plants (herbs, shrubs, trees; -120‰). However, ϵ_a is not as constant as the averaged ratios suggest. For subhumid and arid sites in southern California (precipitation <800 mm a⁻¹) Feakins and Sessions (2010a) found a less negative ϵ_a of ca. -90‰ for mixed wood- and shrubland plants, excluding grasses. In contrast, ϵ_a of C₄ grasses of the North American Great Plains was above -140‰ for locations where precipitation exceeded 350 mm a⁻¹ (Smith and Freeman, 2006). This suggests, that there may be an influence of aridity on ϵ_a of C₃ plants also in our study region but the effect may be masked by the increasing abundance of C₄ grasses which are less influenced by aridity. This may partly explain the fairly uniform ϵ_a values in the studied transect.

4. Sediment transect II: *n*-Alkane stable hydrogen isotope composition

Table 4.6 Contribution of C₄ plants to the alkanes calculated from stable carbon isotope composition (Chapter 3) and Pearson correlation coefficients for correlation with apparent hydrogen isotope fractionation for these alkanes at every location.

No.	% C ₄ based on C ₂₉	% C ₄ based on C ₃₁	% C ₄ based on C ₃₃	r ¹
1	29	38	57	-0.86
2	10	17	36	0.38
3	24	29	48	0.08
4	26	35	55	-0.05
5	18	23	43	-0.10
6	26	31	57	0.25
7	34	41	66	-0.66
8	43	52	69	-0.63
9	55	61	72	-0.83
10	53	63	70	-0.98
11	61	75	78	-0.89
12	53	72	77	-0.99
13	50	68	76	-1.00

¹ *italic numbers*: significant at the 75% level

bold italic numbers: Significant at the 90 % level

For our samples the relative contribution of C₄ plants is different for every alkane (Chapter 3.6.1, Table 3.4) because they are produced in different amounts by these plants (Rommerskirchen et al., 2006b; Vogts et al., 2009). This C₄ contribution to the alkanes was correlated with the apparent fractionation for the homologues at every sampling location (Table 4.6). For most of the southern locations reasonable correlation was observed even though it has to be taken into account that the significance of the correlations are low due to only three data points for every location. However, the apparent correlation substantiates the theory of different ϵ_a for woody species and C₄ grasses. Furthermore, the low correlation for the northern sites may be another indication for possibly different sources for C₃₃ in this area as discussed before.

4.5.4 Implications for palaeo-climatic studies

The hydrogen isotope composition of fossil *n*-alkanes will not be altered over geological time scales (Schimmelmann et al., 2006; Wang et al., 2009). As

4. Sediment transect II: *n*-Alkane stable hydrogen isotope composition

our study indicates that δD ratios of sedimentary plant wax *n*-alkanes reflect continental rainfall δD ratios, we conclude that δD ratios of alkanes in ocean margin sediments can be related to the isotope composition of ancient precipitation. The apparent fractionations, especially for C_{29} and C_{31} , appear to be fairly constant (-109 ± 3 and $-115\pm 3\text{‰}$, respectively) even though the climatic conditions and vegetation composition change significantly. Under the current setting the change from woody vegetation to C_4 grasses appears to superimpose potential aridity effects. However, to exclude influences of vegetation composition changes on palaeo-environmental assessments, the contribution by these different ecological life forms should be addressed at the same time. Furthermore, the knowledge about potential catchment areas and their possible variation over time is essential to achieve reliable results. However, the δD ratios of alkanes in ocean margin sediments may be directly converted to δD ratios of ancient precipitation by the fractionation factors presented and, thus, are useful proxies for δD_P changes and their causal climatic variations.

4.6 Conclusions

The δD values of leaf wax *n*-alkanes (C_{29} , C_{31} , and C_{33}) in ocean margin sediments along southwest Africa vary from -123 to -141‰ . These ratios were compared to the modelled δD ratios for precipitation at continental locations along postulated transport pathways from land to ocean. The highest correlation coefficients were observed for mean annual precipitation values at locations with 250 km distance to the coast. If ratios for the growing season and the end of the growing season were applied, the correlation increased for C_{29} , C_{33} and weighted mean averaged values but decreased for C_{31} . The apparent fractionations between alkane and precipitation δD ratios appear to be fairly constant, especially for C_{29} and C_{31} (-109 ± 3 and $-115\pm 3\text{‰}$, respectively) despite the changing environmental conditions and varying abundance of plants of different ecological life forms (trees, grasses). Thus, hydrogen isotope ratios of leaf wax *n*-alkanes preserved in ocean sediments have a high potential for palaeo-climatic studies and may be directly converted into δD ratios of ancient precipitation.

5. Summary and perspectives

In this thesis, the applicability of plant wax-derived long-chain *n*-alkanes and *n*-alkan-1-ols as proxies for continental vegetation composition, hydrologic and climatic conditions was validated. Africa was chosen as study area due to its broad latitudinal vegetation zones, which largely mirror climate conditions, and the abundance of plants utilising different metabolic pathways. In a first step, the knowledge about biological endmembers was expanded by the analysis of rain forest and savanna C₃ species. Secondly, recent sediment samples from an isobathic north to south transect along the southwest African continental margin were analysed to evaluate how present-day continental conditions are mirrored by the characteristics of preserved lipids. The sediment transect parallels a distinctive continental gradient from humid habitats dominated by woody C₃ vegetation towards arid regions where C₄ grasses prevail.

During plant wax analyses 69 C₃ species grown in Africa under natural conditions were evaluated for their bulk and molecular stable carbon isotopic compositions as well as distribution patterns of long-chain *n*-alkanes (*n*-C₂₅ to *n*-C₃₅) and *n*-alkan-1-ols (*n*-C₂₄ to *n*-C₃₄). The plant species chosen represent rain forest plants (24) and savanna species (45) from different habits (herb, shrub, liana, and tree). The variation of the analysed parameters among different growth forms is small within the vegetation zones, but characteristic differences occur between the signatures of rain forest and savanna plants. Therefore, averaged histograms for rain forest and savanna C₃ plants were presented in combination with previously published data of tropical C₄ grasses (Rommerskirchen et al., 2006b). These histograms may roughly be representative for C₃ rain forest, C₃ savanna and C₄ grassland vegetation and reveal a trend to longer *n*-alkane chains and less negative stable carbon isotope ratios of *n*-alkanes and *n*-alkanols in the course of these biomes. Isotopic composition, ACL values and the ratio of the *n*-C₂₉ to the *n*-C₃₁ alkane were postulated to be suitable proxies to evaluate the changing contribution of rain forest, savanna and grassland vegetation to geological records of tropical and subtropical Africa. For the *n*-alkanols, however, the maximum of the averaged distribution pattern of C₃ rain forest plants is between those of

C₃ savanna plants and C₄ grasses. However, focussing on savannas and grasslands ACL values of *n*-alkanols may be a suitable parameter to judge the changing contributions of these biomes to sediments. Furthermore, the relative abundance of the *n*-C₃₃ alkane and/or the *n*-C₃₂ alkanol may be used as indicator for the contribution of lipids derived from C₄ grasses. This was previously postulated by Rommerskirchen et al. (2006a), because the *n*-C₃₃ alkane and the *n*-C₃₂ alkanol are not abundant in C₃ species of the adjacent savanna biome.

For the second part of the study 13 recent marine sediments constituting an isobathic transect along the southwest African continent from 1°N to 28°S were analysed. The compound-specific stable carbon and hydrogen isotope signatures as well as the chain-length distributions of long-chain *n*-alkanes were evaluated. The odd-carbon-numbered homologues in the C₂₇ to C₃₃ range dominated the distribution patterns. Near the equator chain-length distribution as well as carbon isotope composition indicated a high contribution by C₃ plants from the rain forest on the adjacent continent. But especially at sampling locations not dominated by fluvial organic material a significant contribution of C₄-plant-derived material, possibly introduced by long range eolian transport, was evident. Further south, longer-chain *n*-alkanes with less negative stable carbon isotope composition became abundant, which reflects the increasing contribution of C₄ grasses. By employing the endmember dataset evaluated in the first part of this thesis, the stable carbon isotope composition and the average chain-length distribution were found suitable to estimate the relative C₄-plant contribution to the sediments. The calculated C₄-plant proportion corresponds to the C₄-plant abundance in postulated continental catchment areas if non-latitudinal and long-range eolian contributions are taken into account. Furthermore, the calculated C₄ contribution to the sediments significantly correlates with the amount of mean annual precipitation and the aridity in the postulated catchment areas. This indicates that the water supply can be an important factor for C₄ plant abundance/C₃ plant absence if primary requirements (light intensity and temperature) are fulfilled.

The evaluation of the hydrogen isotope ratios of the *n*-alkanes derived from the same isobathic sediment transect was the third part of this study. The values for the C₂₉, C₃₁ and C₃₃ *n*-alkanes correlated with modelled hydrogen isotope compositions of mean annual precipitation in the postulated catchment areas. Calculations based on growing-season and end of growing-season precipitation partly but not systematically improved this correlation. The apparent fractionation, especially between the *n*-C₂₉ and *n*-C₃₁ alkanes and mean annual precipitation, is fairly constant if three locations are not taken into account. For these locations the hydrogen isotope composition of the precipitation is assumed to be biased by the limitations of the punctual catchment area definition. The apparent fractionation shows no significant correlation with the amount of precipitation and does not depend on vegetation composition. Even though the C₃-plant abundance decreases towards the south and C₃ plants are possibly affected by aridity, too, these effects may be superimposed by an increasing abundance of C₄ grasses showing higher isotopic fractionations and lower susceptibility to aridity effects. This could explain the observed constant apparent fractionation between the *n*-C₂₉ and *n*-C₃₁ alkanes and mean annual precipitation.

Despite the expanded knowledge provided by this study, uncertainties remain which may bias the correlations. For instance, the dataset especially for rain forest plants is small and does not include epiphytes (partly CAM species), swamp C₄ grasses, plant material from the upper canopy or submerged plants growing on river banks. Thus, subsequent investigations should elaborate on the knowledge about the variation of the plant wax signatures of source organisms contributing to geological archives. Regarding the transect samples the contribution of *n*-alkan-1-ols and their characteristics should also be addressed because these compounds can serve as proxies for continental vegetation if *n*-alkane characteristics are masked by e.g., contribution from oil seeps. Furthermore, assumptions about the eolian and fluvial contribution as well as the catchment areas are tentative and may be substantiated by analyses of organic material transported by wind and rivers as well as modelling approaches employing, e.g., more detailed wind trajectories and/or catchment area vegetation and precipitation composition

models. As our study also substantiated assumptions about the variation of the characteristics of plant wax biomarkers with distance from the continent these effects need further elucidation, too.

However, despite the remaining uncertainties the results of the plant and sediment studies corroborate the potential of plant wax-derived long-chain organic compounds for palaeo-vegetational studies. Above this, it was demonstrated which parameters are most useful to represent the vegetation characteristics and how these parameters correlate with environmental parameters. The presented correlations and hydrogen isotope fractionations can be employed by palaeo-orientated studies to deduce climatic conditions from analyses of the characteristics of plant-wax derived long-chain organic compounds in geological archives.

6. References

- Aichner, B., Herzs Schuh, U., Wilkes, H., Vieth, A., Böhner, J., 2010. δD values of *n*-alkanes in Tibetan lake sediments and aquatic macrophytes - A surface sediment study and application to a 16 ka record from Lake Koucha. *Organic Geochemistry* 41, 779-790.
- Ali, H.A.M., Mayes, R.W., Hector, B.L., Orskov, E.R., 2005. Assessment of *n*-alkanes, long-chain fatty alcohols and long-chain fatty acids as diet composition markers: The concentrations of these compounds in range-land species from Sudan. *Animal Feed Science and Technology* 121, 257-271.
- Arens, N.C., Jahren, A.H., Amundson, R., 2000. Can C_3 plants faithfully record the carbon isotopic composition of atmospheric carbon dioxide? *Paleobiology* 26, 137-164.
- Asbjornsen, H., Shepherd, G., Helmers, M., Mora, G., 2008. Seasonal patterns in depth of water uptake under contrasting annual and perennial systems in the Corn Belt Region of the Midwestern U.S. *Plant and Soil* 308, 69-92.
- ASTER GDEM Validation Team, 2009. ASTER Global DEM Validation, Summary Report, http://www.ersdac.or.jp/GDEM/E/image/ASTERGDEM_ValidationSummaryReport_Ver1.pdf, last accessed 13.1.2011.
- Avato, P., Bianchi, G., Pogna, N., 1990. Chemosystematics of surface lipids from Maize and some related species. *Phytochemistry* 29, 1571-1576.
- Baker, E.A., 1982. Chemistry and morphology of plant epicuticular waxes. In: Cutler, D.F., Alvin, K.L., Price, C.E. (Eds.), *The Plant Cuticle*, Linnean Society Symposium Series, No. 10. Academic Press, London, 139-165.
- Bassham, J.A., Benson, A.A., Kay, L.D., Harris, A.Z., Wilson, A.T., Calvin, M., 1954. The path of carbon in photosynthesis XXI - The cyclic regeneration of carbon dioxide acceptor. *Journal of the American Chemical Society* 76, 1760-1770.
- Bender, M.M., 1968. Mass spectrometric studies of ^{13}C variations in corn and other grasses. *Radiocarbon* 10, 468-472.

- van Bergen, P.F., Bull, I.D., Poulton, P.R., Evershed, R.P., 1997. Organic geochemical studies of soils from the Rothamsted Classical Experiments I. Total lipid extracts, solvent insoluble residues and humic acids from Broadbalk Wilderness. *Organic Geochemistry* 26, 117-135.
- Berner, R.A., 1993. Paleozoic atmospheric CO₂: Importance of solar radiation and plant evolution. *Science* 261, 66-70.
- Bi, X.H., Sheng, G.Y., Liu, X.H., Li, C., Fu, J.M., 2005. Molecular and carbon and hydrogen isotopic composition of *n*-alkanes in plant leaf waxes. *Organic Geochemistry* 36, 1405-1417.
- Bianchi, A., Bianchi, G., 1990. Surface lipid composition of C₃ and C₄ plants. *Biochemical Systematics and Ecology* 18, 533-537.
- Bird, M.I., Summons, R.E., Gagan, M.K., Roksandic, Z., Dowling, L., Head, J., Fifield, L.K., Cresswell, R.G., Johnson, D.P., 1995. Terrestrial vegetation change inferred from *n*-alkane $\delta^{13}\text{C}$ analysis in the marine environment. *Geochimica et Cosmochimica Acta* 59, 2853-2857.
- Björkmann, O., 1976. Adaptive and genetic aspects of C₄ photosynthesis. In: Bunns, R.H., Block, C.C. (Eds.), *CO₂ Metabolism and Plant Productivity*. University Park Press, Baltimore, 287-309.
- Björkmann, O., Berry, J., 1973. High-efficiency photosynthesis. *Scientific American* 279 (4), 80-93.
- Boom, A., 2004. A geochemical study of lacustrine sediments: Towards palaeo-climatic reconstructions of high Andean biomes in Colombia, PhD thesis. University of Amsterdam, Amsterdam.
- Bortz, J.T., Wertz, P.W., Downing, D.T., 1989. The origin of alkanes found in human-skin surface-lipids. *Journal of Investigative Dermatology* 93, 723-727.
- Bowen, G.J., Revenaugh, J., 2003. Interpolating the isotopic composition of modern meteoric precipitation. *Water Resources Research* 39, 1299, doi:10.1029/2003WR002086.
- Bowen, G.J., Wassenaar, L.I., Hobson, K.A., 2005. Global application of stable hydrogen and oxygen isotopes to wildlife forensics. *Oecologia* 143, 337-348.

- Bray, E.E., Evans, E.D., 1961. Distribution of *n*-paraffins as a clue to recognition of source beds. *Geochimica et Cosmochimica Acta* 22, 2-15.
- Buchmann, N., Guehl, J.M., Barigah, T.S., Ehleringer, J.R., 1997. Interseasonal comparison of CO₂ concentrations, isotopic composition, and carbon dynamics in an Amazonian rainforest (French Guiana). *Oecologia* 110, 120-131.
- Burdige, D.J., 2005. Burial of terrestrial organic matter in marine sediments: A reassessment. *Global Biogeochemical Cycles* 19, GB4010, doi:10.1029/2004GB002368.
- Chibnall, A.C., Piper, S.H., Pollard, A., Williams, E.F., Sahai, P.N., 1934. The constitution of the primary alcohols, fatty acids and paraffins present in plant and insect waxes. *Biochemical Journal* 28, 2189-2208.
- Chikaraishi, Y., Naraoka, H., 2003. Compound specific δD and $\delta^{13}C$ analyses of *n*-alkanes extracted from terrestrial and aquatic plants. *Phytochemistry* 63, 361-371.
- Chikaraishi, Y., Naraoka, H., Poulson, S.R., 2004. Hydrogen and carbon isotopic fractionations of lipid biosynthesis among terrestrial (C₃, C₄ and CAM) and aquatic plants. *Phytochemistry* 65, 1369-1381.
- Cole, M.M., 1986. *The Savannas: Biogeography and Geobotany*. Academic Press, London.
- Collatz, G.J., Berry, J.A., Clark, J.S., 1998. Effects of climate and atmospheric CO₂ partial pressure on the global distribution of C₄ grasses: Present, past, and future. *Oecologia* 114, 441-454.
- Conte, M.H., Weber, J.C., 2002. Long-range atmospheric transport of terrestrial biomarkers to the western North Atlantic. *Global Biogeochemical Cycles* 16, 1142, doi:10.1029/2002GB001922.
- Dai, A., Trenbeth, K.E., 2002. Estimates of freshwater discharge from continents: Latitudinal and seasonal variations. *Journal of Hydrometeorology* 3, 660-687.
- Dawson, D., Grice, K., Wang, S.X., Alexander, R., Radke, J., 2004. Stable hydrogen isotopic composition of hydrocarbons in torbanites (Late Carboniferous to Late Permian) deposited under various climatic conditions. *Organic Geochemistry* 35, 189-197.

- Dodd, R.S., Rafii, Z.A., Power, A.B., 1998. Ecotypic adaptation in *Austrocedrus chilensis* in cuticular hydrocarbon composition. *New Phytologist* 138, 699-708.
- Dodd, R.S., Afzal-Rafii, Z., 2000. Habitat-related adaptive properties of plant cuticular lipids. *Evolution* 54, 1438-1444.
- Donovan, L.A., Ehleringer, J.R., 1991. Ecophysiological differences among juvenile and reproductive plants of several woody species. *Oecologia* 86, 594-597.
- Dove, H., Mayes, R.W., 1991. The use of plant wax alkanes as marker substances in studies of the nutrition of herbivores: A review. *Australian Journal of Agricultural Research* 42, 913-952.
- Dove, H., Mayes, R.W., Freer, M., 1996. Effects of species, plant part, and plant age on the *n*-alkane concentrations in the cuticular wax of pasture plants. *Australian Journal of Agricultural Research* 47, 1333-1347.
- Downes, R.W., 1969. Differences in transpiration rates between tropical and temperate grasses under controlled conditions. *Planta* 88, 261-273.
- Dupont, L.M., Wyputta, U., 2003. Reconstructing pathways of aeolian pollen transport to the marine sediments along the coastline of SW Africa. *Quaternary Science Reviews* 22, 157-174.
- Edwards, G.E., Nakamoto, H., Burnell, J.N., Hatch, M.D., 1985. Pyruvate, P_i dikinase and NADP-malate dehydrogenase in C₄ photosynthesis: Properties and mechanism of light/dark regulation. *Annual Review of Plant Physiology* 36, 255-286.
- Eglinton, G., Hamilton, R.J., 1967. Leaf epicuticular waxes. *Science* 156, 1322-1334.
- Ehleringer, J.R., Field, C.B., Lin, Z.-F., Kuo, C.-Y., 1986. Leaf carbon isotope and mineral composition in subtropical plants along an irradiance cline. *Oecologia* 70, 520-526.
- Ehleringer, J.R., Cerling, T.E., Helliker, B.R., 1997. C₄ photosynthesis, atmospheric CO₂, and climate. *Oecologia* 112, 285-299.
- Farquar, G.D., 1983. On the nature of carbon isotope discrimination in C₄ species. *Australian Journal of Plant Physiology* 10, 205-226.

- Farquar, G.D., O'Leary, M.H., Berry, J.A., 1982. On the relationship between carbon isotope discrimination and the intercellular carbon dioxide concentration in leaves. *Australian Journal of Plant Physiology* 9, 121-137.
- Farquar, G.D., Ehleringer, J.R., Hubick, K.T., 1989. Carbon isotope discrimination and photosynthesis. *Annual Review of Plant Physiology and Plant Molecular Biology* 40, 503-537.
- Feakins, S.J., Sessions, A.L., 2010a. Controls on the D/H ratios of plant leaf waxes in an arid ecosystem. *Geochimica et Cosmochimica Acta* 74, 2128-2141.
- Feakins, S.J., Sessions, A.L., 2010b. Crassulacean acid metabolism influences D/H ratio of leaf wax in succulent plants. *Organic Geochemistry* 41, 1269-1276.
- Feakins, S.J., deMenocal, P.B., Eglinton, T.I., 2005. Biomarker records of late Neogene changes in northeast African vegetation. *Geology* 33, 977-980.
- Fukushima, K., Ishiwatari, R., 1984. Acid and alcohol compositions of wax esters in sediments from different environments. *Chemical Geology* 47, 41-56.
- Gagosian, R.B., Peltzer, E.T., 1986. The importance of atmospheric input of terrestrial organic material to deep-sea sediments. *Organic Geochemistry* 10, 661-669.
- Gat, J.R., 1996. Oxygen and hydrogen isotopes in the hydrologic cycle. *Annual Review of Earth and Planetary Sciences* 24, 225-262.
- Geiger, R., 1950. *The Climate Near the Ground*. Harvard University Press, Cambridge.
- Grieu, P., Lucero, D.W., Ardiani, R., Ehleringer, J.R., 2001. The mean depth of soil water uptake by two temperate grassland species over time subjected to mild soil water deficit and competitive association. *Plant and Soil* 230, 197-209.
- de la Harpe, A.C., Visser, J.H., Grobbelaar, N., 1981. Photosynthetic characteristics of some African parasitic flowering plants. *International Journal of Plant Physiology* 103, 265-275.

- Hatch, M.D., 1987. C₄ photosynthesis: A unique blend of modified biochemistry, anatomy and ultrastructure. *Biochimica et Biophysica Acta* 895, 81-106.
- Hatch, M.D., Slack, C.R., 1966. Photosynthesis by sugar-cane leaves - a new carboxylation reaction and pathway of sugar formation. *Biochemical Journal* 101, 103-111.
- Hattersley, P.W., 1982. $\delta^{13}\text{C}$ values of C₄ types of grasses. *Australian Journal of Agriculture Research* 9, 139-154.
- Hayes, J.M., 1993. Factors controlling ^{13}C contents of sedimentary organic compounds - principles and evidence. *Marine Geology* 113, 111-125.
- Heyns, P., 2003. Water-resources management in Southern Africa. In: Nakayama, M. (Ed.), *International Waters in Southern Africa*. United Nations University Press, Hong Kong, 5-37.
- Hoefs, J., 1997. *Stable Isotope Geochemistry*. Springer-Verlag, Berlin.
- Hou, J.Z., D'Andrea, W.J., MacDonald, D., Huang, Y.S., 2007. Hydrogen isotopic variability in leaf waxes among terrestrial and aquatic plants around Blood Pond, Massachusetts (USA). *Organic Geochemistry* 38, 977-984.
- Hou, J., D'Andrea, W., Huang, Y., 2008. Can sedimentary leaf waxes record D/H ratios of continental precipitation? *Geochimica et Cosmochimica Acta* 72, 3503-3517.
- Huang, Y.S., Dupont, L., Sarnthein, M., Hayes, J.M., Eglinton, G., 2000. Mapping of C₄ plant input from North West Africa into North East Atlantic sediments. *Geochimica et Cosmochimica Acta* 64, 3505-3513.
- Jansen, B., Nierop, K.G.J., Hagemann, J.A., Cleef, A.M., Verstraten, J.M., 2006. The straight-chain lipid biomarker composition of plant species responsible for the dominant biomass production along two altitudinal transects in the Ecuadorian Andes. *Organic Geochemistry* 37, 1514-1536.
- Jansen, B., Haussmann, N.S., Tonneijck, F.H., Verstraten, J.M., de Voogt, P., 2008. Characteristic straight-chain lipid ratios as a quick method to assess past forest-páramo transitions in the Ecuadorian Andes. *Palaeogeography, Palaeoclimatology, Palaeoecology* 262, 129-139.

- Jetter, R., Kunst, L., Samuels, A.L., 2006. Composition of plant cuticular waxes. In: Riederer, M., Müller, C. (Eds.), *Annual Plant Reviews 23: Biology of the Plant Cuticle*. Blackwell, Oxford, 145-181.
- Jones, M.B., 1987. The photosynthetic characteristics of papyrus in a tropical swamp. *Oecologia* 71, 335-359.
- Karar, R.O., Mohamed, B.F., Marrs, R.H., 2005. Factors influencing the weed flora in the Gezira Scheme, Sudan. *Weed Research* 45, 121-129.
- Keeley, J.E., Rundel, P.P., 2003. Evolution of CAM and C₄ carbon-concentrating mechanism. *International Journal of Plant Sciences* 164, 55-77.
- Koch, P.L., Behrensmeyer, A.K., Fogel, M.L., 1991. The isotopic ecology of plants and animals in Amboseli National Park, Kenya. *Annual Report of the Director of the Geophysical Laboratory, Carnegie Institution*, 163-171.
- Kolattukudy, P.E., 1976. *Chemistry and Biochemistry of Natural Waxes*. Elsevier, Amsterdam.
- Lauer, W., Frankenberg, P., 1985. Versuch einer geo-ökologischen Klassifikation der Klimate. *Geographische Rundschau* 37, 359-365.
- Leegood, R.C., 1999a. Photosynthesis in C₃ plants: The Benson-Calvin Cycle and photorespiration. In: Lea, P.J., Leegood, R.C. (Eds.), *Plant Biochemistry and Molecular Biology*. John Wiley & Sons Ltd., Chichester, 29-50.
- Leegood, R.C., 1999b. Carbon dioxide concentrating mechanisms: C₄ photosynthesis and Crassulacean Acid Metabolism. In: Lea, P.J., Leegood, R.C. (Eds.), *Plant Biochemistry and Molecular Biology*. John Wiley & Sons Ltd., Chichester, 51-79.
- Lichtfouse, E., Derenne, S., Mariotti, A., Largeau, C., 1994. Possible algal origin of long-chain odd *n*-alkanes in immature sediments as revealed by distributions and carbon-isotope ratios. *Organic Geochemistry* 22, 1023-1027.
- Liu, W., Huang, Y., 2005. Compound specific D/H ratios and molecular distributions of higher plant leaf waxes as novel palaeoenvironmental indi-

- cators in the Chinese Loess Plateau. *Organic Geochemistry* 36, 851-860.
- Liu, W.G., Yang, H., 2008. Multiple controls for the variability of hydrogen isotopic compositions in higher plant *n*-alkanes from modern ecosystems. *Global Change Biology* 14, 2166-2177.
- Liu, W., Yang, H., Li, L., 2006. Hydrogen isotopic compositions of *n*-alkanes from terrestrial plants correlate with their ecological life forms. *Oecologia* 150, 330-338.
- Lüttge, U., 2002. CO₂-concentrating: Consequences in Crassulacean Acid Metabolism. *Journal of Experimental Botany* 53, 2131-2142.
- Lüttge, U., 2004. Ecophysiology of Crassulacean Acid Metabolism (CAM). *Annals of Botany* 93, 629-652, doi:10.1093/aob/mch087.
- Matsuura, K., Willmott, C., Legates, D., 2003. WebWIMP: The web-based water-budget interactive modelling program.
<http://climate.geog.udel.edu/~wimp/>. Last accessed: 02.11.2010.
- Maffei, M., 1996. Chemotaxonomic significance of leaf wax alkanes in the *Gramineae*. *Biochemical Systematics and Ecology* 24, 53-64.
- Mayaux, P., Bartholome, E., Fritz, S., Belward, A., 2004. A new land-cover map of Africa for the year 2000. *Journal of Biogeography* 31, 861-877.
- McDuffee, K.E., Eglinton, T.I., Sessions, A.L., Sylva, S., Wagner, T., Hayes, J.M., 2004. Rapid analysis of ¹³C in plant-wax *n*-alkanes for reconstruction of terrestrial vegetation signals from aquatic sediments. *Geochemistry Geophysics Geosystems* 5, Q10004, doi:10.1029/2004GC00772.
- McInerney, F.A., Helliker, B.R., Freeman, K.H., 2011. Hydrogen isotope ratios of leaf wax *n*-alkanes in grasses are insensitive to transpiration. *Geochimica et Cosmochimica Acta* 75, 541-554.
- Mead, R., Xu, Y., Chong, J., Jaffé, R., 2005. Sediment and soil organic matter source assessment as revealed by the molecular distribution and carbon isotopic composition of *n*-alkanes. *Organic Geochemistry* 36, 363-370.
- Medina, E., Minchin, P., 1980. Stratification on $\delta^{13}\text{C}$ values of leaves in Amazonian rain forests. *Oecologia* 45, 377-378.

- Mook, W.G., Bommerson, J.C., Staverman, W.H., 1974. Carbon isotope fractionation between dissolved bicarbonate and gaseous carbon dioxide. *Earth and Planetary Science Letters* 22, 169-176.
- Muzuka, A.N.N., 1999. Isotopic compositions of tropical east African flora and their potential as source indicators of organic matter in coastal marine sediments. *Journal of African Earth Sciences* 28, 757-766.
- Nichols, P.D., Johns, R.B., 1985. Lipids of the tropical seagrass *Thalassia hemprichii*. *Phytochemistry* 24, 81-84.
- Niedermeyer, E.M., Schefuß, E., Sessions, A.L., Mulitza, S., Mollenhauer, G., Schulz, M., Wefer, G., 2010. Orbital- and millennial-scale changes in the hydrologic cycle and vegetation in the western African Sahel: Insights from individual plant wax δD and $\delta^{13}C$. *Quaternary Science Reviews* 29, 2996-3005.
- Nilsson, C., Reidy, C.A., Dynesius, M., Revenga, C., 2005. Fragmentation and flow regulation of the world's large river systems. *Science* 308, 405-408.
- O'Leary, M.H., 1981. Carbon isotope fractionation in plants. *Phytochemistry* 20, 553-567.
- O'Leary, M.H., 1988. Carbon isotopes in photosynthesis. *Bioscience* 38, 328-336.
- Osmond, C.B., Winter, K., Ziegler, H., 1980. Functional significance of different pathways of CO₂ fixation of photosynthesis. In: Lange, O.L., Nobel, P.S., Osmond, C.B., Ziegler, H. (Eds.), *Encyclopedia of Plant Physiology* 12A. Springer, Berlin, 480-547.
- Pancost, R.D., Boot, C.S., 2004. The palaeoclimatic utility of terrestrial biomarkers in marine sediments. *Marine Chemistry* 92, 239-261.
- Pierce, S., Winter, K., Griffiths, H., 2002. Carbon isotope ratio and the extent of daily CAM use by *Bromeliaceae*. *New Phytologist* 156, 75-83.
- Plana, V., 2004. Mechanisms and tempo of evolution in the African Guineo-Congolian rainforest. *Philosophical Transactions of the Royal Society of London, Series B - Biological Sciences* 359, 1585-1594.

- Polissar, P.J., Freeman, K.H., 2010. Effects of aridity and vegetation on plant-wax δD in modern lake sediments. *Geochimica et Cosmochimica Acta* 74, 5785-5797.
- Poynter, J., Eglinton, G., 1991. The biomarker concept - strengths and weaknesses. *Fresenius' Journal of Analytical Chemistry* 339, 725-731.
- Poynter, J.G., Farrimond, P., Robinson, A.L., Eglinton, G., 1989. Aeolian-derived higher land plant lipids in the marine sedimentary record: Links with palaeoclimate. In: Leinen, M., Sarnthein, M. (Eds.), *Palaeoclimatology and Palaeometeorology: Modern and Past Patterns of Global Atmospheric Transport*. Kluwer Academic, Norwell, 435-462.
- Proksch, P., Sternburg, C., Rodriguez, E., 1981. Epicuticular alkanes from desert plants of Baja California. *Biochemical Systematics and Ecology* 9, 205-206.
- Radke, M., Willsch, H., Welte, D.H., 1980. Preparative hydrocarbon group type determination by automated medium pressure liquid chromatography. *Analytical Chemistry* 52, 406-411.
- Rao, Z., Zhu, Z., Wang, S., Jia, G., Qiang, M., Wu, Y., 2009a. CPI values of terrestrial higher plant derived long-chain *n*-alkanes: A potential paleoclimatic proxy. *Frontiers of Earth Science in China* 3, 226-272.
- Rao, Z., Zhu, Z., Jia, G., Henderson, A.C.G., Xue, Q., Wang, S., 2009b. Compound specific δD values of long chain *n*-alkanes derived from terrestrial higher plants are indicative of the δD of meteoric waters: Evidence from surface soils in eastern China. *Organic Geochemistry* 40, 922-930.
- Retallack, G.J., 1992. Middle Miocene fossil plants from Fort Ternan (Kenya) and evolution of African grasslands. *Paleobiology* 18, 383-400.
- Richard, Y., Pocard, I., 1998. A statistical study of NDVI sensitivity to seasonal and interannual rainfall variations in Southern Africa. *International Journal of Remote Sensing* 19, 2907-2920.
- Richards, P.W., 1996. *The Tropical Rain Forest*. Cambridge University Press, Cambridge.
- Richardson, A., Franke, R., Kerstiens, G., Jarvis, M., Schreiber, L., Fricke, W., 2005. Cuticular wax deposition in growing barley (*Hordeum vul-*

- gare*) leaves commences in relation to the point of emergence of epidermal cells from the sheaths of older leaves. *Planta* 222, 472-483.
- Ries, S.K., Wert, V., Sweeley, C.C., Leavitt, R.A., 1977. Triacontanol: A new naturally occurring plant growth regulator. *Science* 195, 1339-1341.
- Rommerskirchen, F., Eglinton, G., Dupont, L., Güntner, U., Wenzel, C., Rullkötter, J., 2003. A north to south transect of Holocene southeast Atlantic continental margin sediments: Relationship between aerosol transport and compound specific $\delta^{13}\text{C}$ land plant biomarker and pollen records. *Geochemistry Geophysics Geosystems* 4, 1101, doi:10.1029/2003GC000541
- Rommerskirchen, F., Eglinton, G., Dupont, L., Rullkötter, J., 2006a. Glacial/interglacial changes in southern Africa: Compound-specific $\delta^{13}\text{C}$ land plant biomarker and pollen records from southeast Atlantic continental margin sediments. *Geochemistry Geophysics Geosystems* 7, Q08010, doi:10.1029/2005GC001223.
- Rommerskirchen, F., Plader, A., Eglinton, G., Chikaraishi, Y., Rullkötter, J., 2006b. Chemotaxonomic significance of distribution and stable carbon isotopic composition of long-chain alkanes and alkan-1-ols in C_4 grass waxes. *Organic Geochemistry* 37, 1303-1332.
- Rullkötter, J., Mukhopadhyay, P.K., Schaefer, R.G., Welte, D.H., 1984. Geochemistry and petrography of organic matter in sediments from Deep Sea Drilling Project Sites 545 and 547, Mazagan Escarpment. In: Hinz, K., Winterer, E.L., et al. (Eds.), Initial Reports of the Deep Sea Drilling Project 79. U.S. Government Printing Office, Washington DC, 775-806.
- Sachse, D., Radke, J., Gleixner, G., 2004. Hydrogen isotope ratios of recent lacustrine sedimentary *n*-alkanes record modern climate variability. *Geochimica et Cosmochimica Acta* 68, 4877-4889.
- Sachse, D., Radke, J., Gleixner, G., 2006. δD values of individual *n*-alkanes from terrestrial plants along a climatic gradient - Implications for the sedimentary biomarker record. *Organic Geochemistry* 37, 469-483.
- Sachse, D., Kahmen, A., Gleixner, G., 2009. Significant seasonal variation in the hydrogen isotopic composition of leaf-wax lipids for two deciduous

- tree ecosystems (*Fagus sylvatica* and *Acer pseudoplatanus*). *Organic Geochemistry* 40, 732-742.
- Sachse, D., Gleixner, G., Wilkes, H., Kahmen, A., 2010. Leaf wax *n*-alkane δ D values of field-grown barley reflect leaf water δ D values at the time of leaf formation. *Geochimica et Cosmochimica Acta* 74, 6741-6750.
- Sage, R.F., 2001. C₄ Plants. In: Levin, S.A. (Ed.), *Encyclopedia of Biodiversity*. Academic Press, San Diego, 575-598.
- Sage, R.F., 2004. The evolution of C₄ photosynthesis. *New Phytologist* 161, 341-370.
- SAHRA - Sustainability of Semi-Arid Hydrology and Riparian Areas, 2010. Rainout effect on $\delta^2\text{H}$ and $\delta^{18}\text{O}$ values.
<http://www.sahra.arizona.edu/programs/isotopes/images/diagram13.gif>.
Last accessed: 05.01.2011.
- Schefeuf, E., Ratmeyer, V., Stuut, J.-B., Jansen, J.H.F., Sinninghe Damsté, J.S., 2003a. Carbon isotope analyses of *n*-alkanes in dust from the lower atmosphere over the central eastern Atlantic. *Geochimica et Cosmochimica Acta* 67, 1757-1767.
- Schefeuf, E., Schouten, S., Jansen, J.H.F., Sinninghe Damsté, J.S., 2003b. African vegetation controlled by tropical sea surface temperatures in the mid-Pleistocene period. *Nature* 422, 418-421.
- Schefeuf, E., Versteegh, G.J.M., Jansen, J.H.F., Sinninghe Damsté, J.S., 2004. Lipid biomarkers as major source and preservation indicators in SE Atlantic surface sediments. *Deep-Sea Research I* 51, 1199-1228.
- Schefeuf, E., Schouten, S., Schneider, R.R., 2005. Climatic controls on central African hydrology during the past 20,000 years. *Nature* 437, 1003-1006.
- Schidlowski, M., 1987. Application of stable isotopes to early biochemical evolution on earth. *Annual Review of Earth and Planetary Sciences* 15, 47-72.
- Schimmelmann, A., Sessions, A.L., Mastalerz, M., 2006. Hydrogen isotopic (D/H) composition of organic matter during diagenesis and thermal maturation. *Annual Review of Earth and Planetary Sciences* 34, 501-533.

- Schleser, G.H., Jayasekera, R., 1985. $\delta^{13}\text{C}$ -variations of leaves in forests as an indication of reassimilated CO_2 from the soil. *Oecologia* 65, 536-542.
- Scholes, R.J., Dowty, P.R., Caylor, K., Parsons, D.A.B., Frost, P.G.H., Shugart, H.H., 2002. Trends in savanna structure and composition along an aridity gradient in the Kalahari. *Journal of Vegetation Science* 13, 419-428.
- Schulze, E.-D., Ellis, R., Schulze, W., Trimborn, P., Ziegler, H., 1996. Diversity, metabolic types and $\delta^{13}\text{C}$ carbon isotope ratios in the grass flora of Namibia in relation to growth form, precipitation and habitat conditions. *Oecologia* 106, 352-369.
- Schwark, L., Zink, K., Lechterbeck, J., 2002. Reconstruction of postglacial to early Holocene vegetation history in terrestrial Central Europe via cuticular lipid biomarkers and pollen records from lake sediments. *Geology* 30, 463-466.
- Sessions, A.L., Burgoyne, T.W., Schimmelmann, A., Hayes, J.M., 1999. Fractionation of hydrogen isotopes in lipid biosynthesis. *Organic Geochemistry* 30, 1193-1200.
- Shakhidoyatov, K.M., Rashkes, A.M., Khidyrova, N.K., 1997. Components of cotton plant leaves, their functional role and biological activity. *Chemistry of Natural Compounds* 33, 605-616.
- Sharp, Z., 2007. The hydrosphere. In: Sharp, Z. (Ed.), *Principles of Stable Isotope Geochemistry*. Pearson Prentice Hall, Upper Saddle River, 64-102.
- Shepherd, T., 2003. Wax pathways. In: Thomas, B., Murphy, D.J. (Eds.), *Encyclopedia of Applied Plant Sciences*. Elsevier, Amsterdam, 1204-1225.
- Shepherd, T., Griffiths, D.W., 2006. The effects of stress on plant cuticular waxes. *New Phytologist* 171, 469-499.
- Shuman, B., Huang, Y., Newby, P., Wang, Y., 2006. Compound-specific isotopic analyses track changes in seasonal precipitation regimes in the Northeastern United States at ca 8200 cal yr BP. *Quaternary Science Reviews* 25, 2992-3002.

- Simoneit, B.R.T., 1997. Compound-specific carbon isotope analyses of individual long-chain alkanes and alkanolic acids in Harmattan aerosols. *Atmospheric Environment* 31, 2225-2233.
- Simoneit, B.R.T., Chester, R., Eglinton, G., 1977. Biogenic lipids in particulates from the lower atmosphere over the eastern Atlantic. *Nature* 267, 682-685.
- Simoneit, B.R.T., Cox, R.E., Standley, L.J., 1988. Organic matter of the troposphere IV. Lipids in Harmattan aerosols of Nigeria. *Atmospheric Environment* 22, 983-1004.
- Smith, B.N., Epstein, S., 1971. Two categories of $^{13}\text{C}/^{12}\text{C}$ ratios for higher plants. *Plant Physiology* 47, 380-384.
- Smith, D.G., Mayes, R.W., Raats, J.G., 2001. Effect of species, plant part, and season of harvest on *n*-alkane concentrations in the cuticular wax of common rangeland grasses from southern Africa. *Australian Journal of Agricultural Research* 52, 875-882.
- Smith, F.A., Freeman, K.H., 2006. Influence of physiology and climate on δD of leaf wax *n*-alkanes from C_3 and C_4 grasses. *Geochimica et Cosmochimica Acta* 70, 1172-1187.
- Still, C.J., Powell, R.L., 2010. Continental scale distribution of vegetation stable carbon isotope ratios. In: West, J.B., Bowen, G.J., Dawson, T.E., Tu, K.P. (Eds.), *Isoscapes - Understanding Movement, Pattern, and Progress on Earth Through Isotope Mapping*. Springer, New York, pp. 179-194.
- Sternberg, L.D.L., 1988. D/H ratios of environmental water recorded by D/H ratios of plant lipids from submerged plants. *Nature* 333, 59-61.
- Stránský, K., Streibl, M., 1969. On natural waxes XII - Composition of hydrocarbons in morphologically different plant parts. *Collection of Czechoslovak Chemical Communications* 34, 103-117.
- Tierney, J.E., Oppo, D.W., Rosenthal, Y., Russell, J.M., Linsley, B.K., 2010a. Coordinated hydrological regimes in the Indo-Pacific region during the past two millennia. *Paleoceanography* 25, PA1102, doi:10.1029/2009PA001871.

- Tierney, J.E., Russell, J.M., Huang, Y., 2010b. A molecular perspective on Late Quaternary climate and vegetation change in the Lake Tanganyika basin, East Africa. *Quaternary Science Reviews* 29, 787-800.
- Tipple, B.J., Pagani, M., 2010. A 35 Myr North American leaf-wax compound-specific carbon and hydrogen isotope record: Implications for C₄ grasslands and hydrologic cycle dynamics. *Earth and Planetary Science Letters* 299, 250-262.
- Tribe, I.S., Gaunt, J.K., Parry, D.W., 1968. Cuticular lipids in *Gramineae*. *Biochemical Journal* 109, 8-9.
- Tulloch, A.P., 1976. Chemistry of waxes of higher plants. In: Kolattukudy, P.E. (Ed.), *Chemistry and Biochemistry of Natural Waxes*. Elsevier, Amsterdam, 235-287.
- UNEP, 1992. *World Atlas of Desertification*. E. Arnold, London.
- Vogel, J.C., 1978. Recycling of carbon in a forest environment. *Ecologia Plantarum* 13, 89-94.
- Vogts, A., Moossen, H., Rommerskirchen, F., and Rullkötter, J., 2009. Distribution patterns and stable carbon isotopic composition of alkanes and alkan-1-ols from plant waxes of African rain forest and savanna C₃ species. *Organic Geochemistry* 40, 1037-1054.
- Volkman, J.K., Barrett, S.M., Blackburn, S.I., Mansour, M.P., Sikes, E.L., Gellin, F., 1998. Microalgal biomarkers: A review of recent research developments. *Organic Geochemistry* 29, 1163-1179.
- Wang, Y., Sessions, A.L., Nielsen, R.J., Goddard III, W.A., 2009. Equilibrium ²H/¹H fractionation in organic molecules. II: Linear alkanes, alkenes, ketones, carboxylic acids, esters, alcohols and ethers. *Geochimica et Cosmochimica Acta* 73, 7076-7086.
- Weijers, J.W.H., Schefuß, E., Schouten, S., Sinninghe Damsté, J.S., 2007. Coupled thermal and hydrological evolution of tropical Africa over the Last Deglaciation. *Science* 315, 1701-1704.
- Weijers, J.W.H., Schouten, S., Schefuß, E., Schneider, R.R., Sinninghe Damsté, J.S., 2009. Disentangling marine, soil and plant organic carbon contributions to continental margin sediments: A multi-proxy approach

- in a 20,000 year sediment record from the Congo deep-sea fan. *Geochimica et Cosmochimica Acta* 73, 119-132.
- Winslow, J.C., Hunt, J., E. Raymond, Piper, S.C., 2003. The influence of seasonal water availability on global C₃ versus C₄ grassland biomass and its implications for climate change research. *Ecological Modelling* 163, 153-173.
- White, F., 1983. *The Vegetation of Africa*. United Nations, Paris.
- Winter, K., Aranda, J., Holtum, J.A.M., 2005. Carbon isotope composition and water-use efficiency in plants with crassulacean acid metabolism. *Functional Plant Biology* 32, 381-388.
- Xie, S., Nott, C.J., Avsejs, L.A., Volders, F., Maddy, D., Chambers, F.M., Gledhill, A., Carter, J.F., Evershed, R.P., 2000. Palaeoclimate records in compound-specific δD values of a lipid biomarker in ombrotrophic peat. *Organic Geochemistry* 31, 1053-1057.
- Yang, H., Huang, Y.S., 2003. Preservation of lipid hydrogen isotope ratios in Miocene lacustrine sediments and plant fossils at Clarkia, northern Idaho, USA. *Organic Geochemistry* 34, 413-423.
- Zhao, M., Dupont, L., Eglinton, G., Teece, M., 2003. *n*-Alkane and pollen reconstruction of terrestrial climate and vegetation for NW Africa over the last 160 kyr. *Organic Geochemistry* 34, 131-142.

7. Appendix

Table 7.1 Data of averaged histogram representations of leaf wax *n*-alkanes of samples from rain forest and savanna plants with different growth forms (Fig. 2.3).

Chain length	Relative abundance of <i>n</i> -alkanes with standard deviation (SD)											
	Savanna herbs		Savanna shrubs		Savanna trees		Rain forest lianas		Rain forest shrubs		Rain forest trees	
	Relative abundance	SD	Relative abundance	SD	Relative abundance	SD	Relative abundance	SD	Relative abundance	SD	Relative abundance	SD
24	1.7	0.8	0.4	0.5	0.9	1.0	0.9	0.4	1.6	1.5	1.6	2.1
25	4.3	2.4	2.0	1.9	5.9	6.5	1.0	0.4	2.2	2.2	1.2	1.0
26	1.3	0.6	1.1	1.0	2.0	2.0	0.5	0.3	1.3	1.4	0.6	0.5
27	8.8	4.2	9.1	6.7	16.8	14.8	2.9	2.4	5.3	5.4	3.2	2.1
28	2.7	1.6	2.1	1.7	3.5	2.4	0.9	0.6	1.7	1.1	1.4	0.9
29	19.4	10.3	24.9	12.6	25.8	17.2	59.0	14.2	45.6	20.3	55.8	23.7
30	3.2	1.4	3.3	2.7	2.4	1.3	2.4	0.5	2.4	0.8	2.8	1.3
31	28.5	9.4	44.6	10.5	27.7	17.0	29.5	13.6	33.0	17.7	28.0	20.8
32	3.7	2.1	2.8	1.1	2.4	2.3	0.7	0.4	1.8	2.0	1.5	1.5
33	23.0	14.5	8.9	4.8	11.3	11.8	1.9	1.2	4.7	3.8	3.7	4.2
34	1.1	1.1	0.3	0.3	0.3	0.3	0.0	0.1	0.1	0.3	0.1	0.2
35	2.0	2.2	0.5	0.4	0.8	1.3	0.2	0.3	0.2	0.4	0.1	0.3
36	0.2	0.1	0.1	0.2	0.1	0.3	0.1	0.2	0.0	0.0	0.0	0.0
Chain length	Stable carbon isotope composition of <i>n</i> -alkanes ($\delta^{13}\text{C}$) with standard deviation (SD)											
	$\delta^{13}\text{C}$	SD	$\delta^{13}\text{C}$	SD	$\delta^{13}\text{C}$	SD	$\delta^{13}\text{C}$	SD	$\delta^{13}\text{C}$	SD	$\delta^{13}\text{C}$	SD
25	-32.4	0.2	-32.5	1.3	-32.0	1.3	n.d.	n.d.	n.d.	n.d.	n.d.	n.d.
27	-34.2	2.6	-32.9	1.9	-32.5	2.1	n.d.	n.d.	-33.1	1.3	n.d.	n.d.
29	-34.1	2.6	-34.3	1.4	-33.0	2.4	-37.9	1.6	-36.3	2.6	-38.3	3.6
31	-35.6	2.4	-34.4	1.5	-33.7	2.8	-37.4	1.5	-35.7	1.8	-39.1	4.6
33	-35.8	1.9	-33.7	1.5	-34.0	2.6	n.d.	n.d.	-36.2	1.7	n.d.	n.d.
35	n.d.	n.d.	n.d.	n.d.	-32.4	4.3	n.d.	n.d.	n.d.	n.d.	n.d.	n.d.

Table 7.2 Data of averaged histogram representations of leaf wax *n*-alkan-1-ols of samples from rain forest and savanna plants with different growth forms (Fig. 2.4).

Chain length	Relative abundance of <i>n</i> -alkan-1-ols with standard deviation (SD)											
	Savanna herbs		Savanna shrubs		Savanna trees		Rain forest lianas		Rain forest shrubs		Rain forest trees	
	Relative abundance	SD	Relative abundance	SD	Relative abundance	SD	Relative abundance	SD	Relative abundance	SD	Relative abundance	SD
23	1.5	2.6	0.4	0.4	0.3	0.5	0.6	0.5	0.2	0.2	0.2	0.1
24	4.6	3.2	3.6	6.7	5.5	8.3	4.5	4.0	3.4	2.4	3.4	2.3
25	1.2	0.7	1.3	2.2	1.6	2.8	0.4	0.2	0.5	0.4	0.7	0.7
26	19.9	13.9	11.9	4.3	12.5	13.2	8.6	9.3	10.6	12.2	12.9	11.3
27	3.2	2.0	3.1	2.3	2.0	1.4	0.6	0.4	1.0	1.0	1.1	0.9
28	37.8	13.1	43.3	11.1	36.7	16.4	18.1	10.8	16.2	9.5	17.3	7.1
29	3.0	2.3	3.3	2.6	2.9	2.2	3.3	1.7	2.6	1.2	4.5	2.7
30	18.7	9.1	21.2	10.7	29.9	19.0	34.3	19.1	35.9	19.0	33.7	20.1
31	1.6	2.8	2.0	2.3	1.0	1.3	2.4	1.3	1.4	1.2	2.0	1.5
32	6.7	5.6	7.8	5.8	5.5	6.3	19.1	9.3	20.4	10.0	15.7	10.6
33	0.2	0.3	0.6	0.9	0.4	0.9	1.5	1.8	0.7	0.7	1.3	1.4
34	1.6	2.3	1.4	2.0	1.4	2.4	6.5	7.4	7.1	5.4	7.2	6.6
35	0.1	0.2	0.1	0.2	0.0	0.1	0.2	0.4	0.0	0.1	0.1	0.2
Chain length	Stable carbon isotope composition of <i>n</i> -alkan-1-ols ($\delta^{13}\text{C}$) with standard deviation (SD)											
	$\delta^{13}\text{C}$	SD	$\delta^{13}\text{C}$	SD	$\delta^{13}\text{C}$	SD	$\delta^{13}\text{C}$	SD	$\delta^{13}\text{C}$	SD	$\delta^{13}\text{C}$	SD
24	n.d.	n.d.	n.d.	n.d.	-33.8	0.2	n.d.	n.d.	-32.3	n.d.	n.d.	n.d.
26	-36.7	1.8	-34.9	0.8	-32.8	1.4	n.d.	n.d.	-32.4	1.6	n.d.	n.d.
28	-37.3	2.6	-33.8	1.6	-33.1	1.9	n.d.	n.d.	-32.6	1.2	-37.4	n.d.
30	-34.2	2.5	-35.0	1.4	-33.0	2.5	n.d.	n.d.	-33.4	0.9	-36.7	n.d.
32	n.d.	n.d.	-35.0	1.0	-33.0	1.9	n.d.	n.d.	-33.5	n.d.	n.d.	n.d.
34	n.d.	n.d.	n.d.	n.d.	-34.8	2.1	n.d.	n.d.	n.d.	n.d.	n.d.	n.d.

Table 7.3 Data of averaged histogram representations of leaf wax *n*-alkanes and *n*-alkan-1-ols of samples from rain forest species, savanna plants and C₄ grasses (Fig. 2.6).

		Relative abundance of <i>n</i> -alkanes with standard deviation (SD)						Relative abundance of <i>n</i> -alkan-1-ols with standard deviation (SD)													
		Rain forest plants			Savanna plants			C ₄ grasses			Rain forest plants			Savanna plants			C ₄ grasses				
Chain length	Relative abundance	SD	Relative abundance	SD	Relative abundance	SD	Chain length	Relative abundance	SD	Relative abundance	SD	Chain length	Relative abundance	SD	Relative abundance	SD	Chain length	Relative abundance	SD	Relative abundance	SD
24	1.4	1.5	1.0	1.0	0.0	0.0	23	0.3	0.3	0.5	1.2	0.7	0.8								
25	1.6	1.7	4.8	5.5	0.0	0.0	24	3.6	2.8	5.0	7.3	3.8	3.7								
26	0.9	1.0	1.7	1.7	1.1	0.9	25	0.5	0.5	1.5	2.4	0.7	0.7								
27	4.1	4.0	13.8	12.7	13.4	5.7	26	10.8	10.9	13.7	12.2	10.0	12.3								
28	1.4	1.0	3.1	2.2	1.5	0.8	27	0.9	0.8	2.4	1.8	1.2	1.1								
29	51.9	20.2	24.5	15.3	19.0	5.9	28	17.0	8.8	38.2	14.9	24.7	25.5								
30	2.5	0.9	2.7	1.7	1.9	0.7	29	3.3	1.9	3.0	2.3	2.0	2.5								
31	30.7	17.1	31.2	16.1	38.1	13.5	30	34.8	18.5	26.2	16.8	13.0	12.4								
32	1.5	1.6	2.7	2.1	1.7	0.4	31	1.8	1.3	1.3	1.8	1.7	1.9								
33	3.7	3.5	12.9	12.1	27.2	14.9	32	18.7	9.8	6.2	6.0	45.1	25.4								
34	0.1	0.2	0.4	0.6	0.8	0.6	33	1.1	1.2	0.4	0.8	1.3	2.0								
35	0.2	0.4	1.0	1.5	5.3	5.2	34	7.0	6.0	1.4	2.3	0.0	0.0								
36	0.0	0.1	0.1	0.2	0.1	0.2	35	0.1	0.2	0.1	0.1	0.0	0.0								

		Stable carbon isotope composition of <i>n</i> -alkanes (δ ¹³ C)						Stable carbon isotope composition of <i>n</i> -alkan-1-ols (δ ¹³ C) with standard deviation (SD)													
		Rain forest plants			Savanna plants			C ₄ grasses			Rain forest plants			Savanna plants			C ₄ grasses				
Chain length	δ ¹³ C	SD	δ ¹³ C	SD	δ ¹³ C	SD	Chain length	δ ¹³ C	SD	δ ¹³ C	SD	Chain length	δ ¹³ C	SD	δ ¹³ C	SD	Chain length	δ ¹³ C	SD	δ ¹³ C	SD
25	n.d.	n.d.	-32.1	1.2	n.d.	n.d.	24	-32.3	n.d.	-33.8	0.2	-22.9	1.5								
27	-33.1	1.3	-32.9	2.2	-21.8	2.5	26	-32.4	n.d.	-34.6	2.3	-23.0	2.7								
29	-37.3	2.8	-33.5	2.3	-21.6	2.0	28	-33.8	2.6	-34.0	2.5	-23.1	2.1								
31	-37.1	3.0	-34.2	2.5	-22.1	2.1	30	-34.2	1.8	-33.5	2.4	n.d.	n.d.								
33	-36.1	1.5	-34.5	2.4	-22.2	1.8	32	-33.5	n.d.	-33.6	1.9	-21.0	2.1								
35	n.d.	n.d.	-31.0	3.9	-22.3	1.6	34	n.d.	n.d.	-34.8	2.1	n.d.	n.d.								

Table 7.4 Data of averaged values and their standard deviation (SD) for chain length parameters of *n*-alkanes and *n*-alkan-1-ols from C₃ rain forest species, C₃ savanna plants and C₄ grasses (Fig. 2.7).

Parameter	C ₃ rain forest plants		C ₃ savanna plants		C ₄ grasses	
	Average	SD	Average	SD	Average	SD
ACL ₂₅₋₃₅	29.68	0.53	29.81	1.15	30.71	0.88
ACL ₂₄₋₃₄	29.63	0.89	28.41	1.03	29.72	1.30
C ₂₉ /C ₃₁	3.1	3.1	1.5	2.8	0.6	0.5
C ₂₈ /C ₃₀	0.7	0.5	2.5	2.1	4.7	8.7
C ₃₃ /C ₂₅₋₃₅	0.04	0.04	0.13	0.12	0.26	0.14
C ₃₂ /C ₂₄₋₃₄	0.19	0.10	0.06	0.06	0.43	0.29

Table 7.5 Mean annual precipitation and temperature as well as aridity index (UNEP, 1992) calculated for locations at ca. 350 km distance from the coast with Web WIMP modeling program (Matsuura et al., 2003). Locations and values are implemented in Fig 3.1.

Latitude	Longitude at ca. 350 km from coast (°E)	Mean annual temperature (°C)	Mean annual precipitation (mm)	Potential evapotranspiration (mm)	Aridity index
4°N	12.5	24.6	1217.7	1326	0.92
2°N	13.0	22.9	1816.4	1129	1.61
0°	12.5	23.5	1671.2	1188	1.41
2°S	12.5	23.2	1730.6	1160	1.49
4°S	14.5	23.0	1403.0	1140	1.23
6°S	16.0	23.1	1495.6	1148	1.30
8°S	16.5	24.0	1220.3	1242	0.98
10°S	16.5	21.7	1223.7	1017	1.20
12°S	17.0	20.2	1207.1	923	1.31
14°S	15.5	20.9	1046.5	978	1.07
16°S	15.0	23.4	662.3	1233	0.54
18°S	15.0	22.9	415.2	1186	0.35
20°S	16.5	19.3	459.6	911	0.50
22°S	17.5	18.4	384.5	874	0.44
24°S	17.5	19.9	204.5	970	0.21
26°S	18.5	20.7	197.3	1045	0.19
28°S	19.0	20.6	122.8	1053	0.12
30°S	20.5	17.6	148.3	872	0.17
32°S	21.5	15.3	181.5	767	0.24
34°S	21.5	17.4	408.8	818	0.50

Table 7.6 Data of the relative abundance of the dominant *n*-alkanes in the sediments of the north to south transect (Fig 3.2b).

Location	Relative abundance in %		
	<i>n</i> -C ₂₉ alkane	<i>n</i> -C ₃₁ alkane	<i>n</i> -C ₃₃ alkane
1	28.5	25.9	12.4
2	30.5	26.0	10.8
3	29.5	25.6	11.5
4	27.6	24.8	12.4
5	27.2	23.5	11.3
6	27.1	22.8	11.6
7	26.8	24.3	14.0
8	25.8	24.8	15.7
9	19.4	30.0	20.3
10	17.9	32.4	20.1
11	16.1	34.5	19.4
12	15.6	35.3	19.0
13	13.0	35.8	17.4

Table 7.7 Data of locations employed as representatives of potential catchment areas. Values were used for the calculation of correlation coefficients (Tables 3.6, 4.5) and hydrogen isotope composition of precipitation (Table 4.3). Data of environmental conditions were derived from Web WIMP modeling program (Matsuura et al., 2003). Aridity index calculated according to UNEP (1992). Elevations were derived from ASTER digital elevation model (ASTER GDEM Validation Team, 2009).

	Distance to coast						
	100 km	150 km	200 km	250 km	300 km	350 km	400 km
Latitude (°N)	1	1	1	1	1	1	1
Longitude (°E)	10.5	11.0	11.5	12.0	12.5	13.0	13.5
Mean annual temperature (°C)	25.1	23.5	24.4	24.5	23.6	23.3	23.4
Mean annual precipitation (mm)	2451.8	2101.1	1835.2	1647.8	1665.9	1653	1591
Potential evapotranspiration (mm)	1184	1292	1305	1198	1150	1164	1177
Aridity index	2.1	1.6	1.4	1.4	1.4	1.4	1.4
Elevation (m)	592	491	544	526	474	518	520
Latitude (°S)	0.5	0.5	0.5	0.5	0.5	0.5	0.5
Longitude (°E)	9.5	10.0	10.5	11.0	11.5	12.0	12.5
Mean annual temperature (°C)	26.3	25.9	25.8	25.8	25.8	23.6	23.8
Mean annual precipitation (mm)	2054.8	1971.6	2027.5	2027.5	2027.5	1708.2	1734.6
Potential evapotranspiration (mm)	1567	1512	1500	1222	1130	1200	1213
Aridity index	1.3	1.3	1.4	1.7	1.8	1.4	1.4
Elevation (m)	94	12	45	560	403	339	358
Latitude (°S)	2	2	2	2	2	2	2
Longitude (°E)	10.0	10.5	11.0	11.5	12.0	12.5	13.0
Mean annual temperature (°C)	26.0	25.6	24.3	23.3	24.2	23.2	22.9
Mean annual precipitation (mm)	1870.1	1890.6	1872	1837.9	1738.9	1730.6	1816.4
Potential evapotranspiration (mm)	1525	1481	1290	1171	1276	1160	1129
Aridity index	1.2	1.3	1.5	1.6	1.4	1.5	1.6
Elevation (m)	37	187	113	273	676	775	629
Latitude (°S)	3.5	3.5	3.5	3.5	3.5	3.5	3.5
Longitude (°E)	11.5	12.0	12.5	13.0	13.5	14.0	14.5
Mean annual temperature (°C)	24.6	25.5	25.4	23.6	22.1	24.0	22.8
Mean annual precipitation (mm)	1304.8	1224.1	1261.2	1455.9	1416.8	1525.3	1697.6
Potential evapotranspiration (mm)	1327	1457	1439	1208	1056	1251	1115
Aridity index	1.0	0.8	0.9	1.2	1.3	1.2	1.5
Elevation (m)	704	391	97	380	480	604	498
Latitude (°S)	5.5	5.5	5.5	5.5	5.5	5.5	5.5
Longitude (°E)	13.0	13.5	14.0	14.5	15.0	15.5	16.0
Mean annual temperature (°C)	25.0	23.8	23.9	24.3	23.0	22.6	23.4
Mean annual precipitation (mm)	1026.2	1096.2	1222.6	1297.8	1311.4	1509.7	1531.9
Potential evapotranspiration (mm)	1398	1233	1240	1289	1140	1096	1181
Aridity index	0.7	0.9	1.0	1.0	1.2	1.4	1.3
Elevation (m)	216	512	228	413	605	520	661
Latitude (°S)	9	9.5	9.5	10	10	10.5	10.5
Longitude (°E)	14.0	14.5	15.0	15.5	16.0	16.0	16.5
Mean annual temperature (°C)	24.8	25.2	23.7	22.8	22.4	24.0	23.5
Mean annual precipitation (mm)	1019.4	1070.2	1036.7	1121	1185.1	1220.3	1209.7
Potential evapotranspiration (mm)	1367	1432	1218	1126	1083	1242	1189
Aridity index	0.7	0.7	0.9	1.0	1.1	1.0	1.0
Elevation (m)	37	199	468	1177	1051	1399	1075

Table 7.7 (continued)

Latitude (°S)	11	11.5	11.5	12	12	12.5	12.5
Longitude (°E)	14.5	15.0	15.5	16.0	16.0	16.5	17.0
Mean annual temperature (°C)	22.0	21.0	20.7	21.5	21.7	21.2	20.7
Mean annual precipitation (mm)	983.8	1080.9	1126.7	1175.5	1223.7	1244.2	1257.6
Potential evapotranspiration (mm)	1051	969	952	1005	1017	985	950
Aridity index	0.9	1.1	1.2	1.2	1.2	1.3	1.3
Elevation (m)	1258	1327	1344	1622	1622	1658	1714
Latitude (°S)	12.5	13	13	13.5	13.5	14	14
Longitude (°E)	12.5	13.0	13.0	13.5	13.5	14.0	14.0
Mean annual temperature (°C)	15.5	20.1	21.0	19.1	19.1	20.2	21.2
Mean annual precipitation (mm)	1143.8	1257.8	1289.4	1256.6	1239.8	1207.1	1242.1
Potential evapotranspiration (mm)	726	917	975	866	861	923	994
Aridity index	1.6	1.4	1.3	1.5	1.4	1.3	1.2
Elevation (m)	1286	1981	1981	1610	1716	1558	1554
Latitude (°S)	15.5	15.5	15.5	15.5	15.5	15.5	15.5
Longitude (°E)	13.0	13.5	14.0	14.5	15.0	15.5	16.0
Mean annual temperature (°C)	24.4	20.3	20.7	22.1	22.7	22.3	21.8
Mean annual precipitation (mm)	648.7	717.1	700.1	688.3	675.6	682.5	713.3
Potential evapotranspiration (mm)	1316	939	967	1085	1146	1106	1062
Aridity index	0.5	0.8	0.7	0.6	0.6	0.6	0.7
Elevation (m)	438	1283	1276	1327	1171	1164	1277
Latitude (°S)	19.0	19.0	19.0	19.0	19.0	19.0	19.0
Longitude (°E)	13.5	14.0	14.5	15.0	15.5	16.0	16.5
Mean annual temperature (°C)	16.9	16.8	19.1	21.1	22.0	22.6	22.7
Mean annual precipitation (mm)	160.2	284.3	313	331.5	373.7	417.5	483.8
Potential evapotranspiration (mm)	776	774	884	1021	1103	1158	1180
Aridity index	0.2	0.4	0.4	0.3	0.3	0.4	0.4
Elevation (m)	920	1338	1230	1155	1102	1086	1108
Latitude (°S)	22.5	22.5	22.5	22.5	22.5	22.5	22.5
Longitude (°E)	15.5	16.0	16.5	17.0	17.5	18.0	18.5
Mean annual temperature (°C)	12.0	15.5	17.7	17.9	19.1	19.5	19.7
Mean annual precipitation (mm)	154.9	236.3	268.8	357.5	329.8	313.8	333
Potential evapotranspiration (mm)	646	740	829	843	911	943	959
Aridity index	0.2	0.3	0.3	0.4	0.4	0.3	0.3
Elevation (m)	961	1200	1528	1568	1568	1514	1451
Latitude (°S)	23	23	22.5	22.5	22	22	21.5
Longitude (°E)	15.0	15.5	16.0	16.5	17.0	17.5	18.0
Mean annual temperature (°C)	16.5	12.3	16.7	18.5	20.4	20.0	20.4
Mean annual precipitation (mm)	167.5	170.8	176.5	192	195.1	229.7	249
Potential evapotranspiration (mm)	777	657	803	894	1023	989	1026
Aridity index	0.2	0.3	0.2	0.2	0.2	0.2	0.2
Elevation (m)	458	953	1200	1528	1374	1790	1603
Latitude (°S)	28	28	28	28	28	28	28
Longitude (°E)	16.5	17.0	17.5	18.0	18.5	19.0	19.5
Mean annual temperature (°C)	17.7	19.5	19.0	19.6	20.2	20.6	19.4
Mean annual precipitation (mm)	69.1	92.3	112.5	116	116.3	122.8	129
Potential evapotranspiration (mm)	820	922	914	971	1024	1053	974
Aridity index	0.1	0.1	0.1	0.1	0.1	0.1	0.1
Elevation (m)	432	613	699	707	945	858	799

Table 7.8 Data of environmental conditions in southwest Africa calculated for locations with ca. 250 km distance to the coast with Web WIMP modeling program (Matsuura et al., 2003). Aridity index calculated according to UNEP (1992). Locations and values are implemented in Fig 4.1.

Latitude	Longitude at ca. 250 to coast (°E)	Mean annual temperature (°C)	Mean annual precipitation (mm)	Potential evapotranspiration (mm)	Aridity index
4°N	11.5	23.8	1635.9	1214	1.35
2°N	12.0	22.9	1732.2	1124	1.54
0°	11.5	24.8	1570.2	1350	1.16
2°S	11.5	23.3	1837.9	1171	1.57
4°S	13.5	24.4	1253.1	1307	0.96
6°S	15.0	22.5	1230.6	1087	1.13
8°S	15.5	22.8	1121.0	1126	1.00
10°S	16.0	21.5	1175.4	1005	1.17
12°S	16.0	19.1	1256.6	866	1.45
14°S	14.5	20.8	1047.9	974	1.08
16°S	14.0	22.2	613.7	1091	0.56
18°S	14.0	22.1	360.1	1100	0.33
20°S	15.5	18.6	352.3	859	0.41
22°S	16.5	20.0	336.6	955	0.35
24°S	16.5	16.7	172.6	793	0.22
26°S	17.5	21.3	146.6	1106	0.13
28°S	18.0	19.6	116.0	971	0.12
30°S	19.5	17.7	162.7	862	0.19
32°S	20.5	12.6	243.9	682	0.36
34°S	20.5	16.8	499.3	796	0.63

Table 7.9 Monthly values of hydrologic parameters employed for the calculation of the hydrogen isotope composition of growing-season precipitation (Table 4.3). Monthly ratios of the hydrogen isotope composition of precipitation (δD_P) were derived from the online isotopes-in-precipitation calculator (OIPC 2.2, Bowen et al., 2005). Precipitation amount and potential evapotranspiration were calculated for locations at ca. 250 km distance from the coast with Web WIMP modeling program (Matsuura et al., 2003). For latitude, longitude and elevation of locations see Table 7.7.

Location		Jan	Feb	Mar	Apr	May	Jun	Jul	Aug	Sep	Oct	Nov	Dec
1	δD_P [†]	-18	-21	-30	-31	-26	-12	-5	-14	-14	-28	-24	-26
	Precipitation (mm)	83	101	202	202	186	53	17	28	142	310	233	110
	Pot. evapotransp. (mm)	107	100	114	112	110	91	81	84	94	102	100	103
2	δD_P [†]	-17	-20	-33	-33	-24	-10	0	-9	-10	-27	-25	-26
	Precipitation (mm)	152	141	224	229	212	22	6	10	76	330	363	185
	Pot. evapotransp. (mm)	111	104	122	116	113	87	76	81	94	106	103	109
3	δD_P [†]	-11	-11	-27	-28	-17	-6	7	-2	-3	-19	-21	-22
	Precipitation (mm)	173	199	220	223	150	11	5	5	34	224	346	248
	Pot. evapotransp. (mm)	109	103	116	112	106	80	71	76	87	104	102	105
4	δD_P [†]	-13	-9	-29	-30	-15	-8	9	0	0	-18	-24	-25
	Precipitation (mm)	156	152	191	219	122	6	1	2	13	117	275	202
	Pot. evapotransp. (mm)	114	108	122	116	111	80	68	73	87	108	109	112
5	δD_P [†]	-14	-9	-25	-27	-14	-8	12	4	3	-15	-23	-26
	Precipitation (mm)	131	119	163	237	105	5	1	3	22	110	217	184
	Pot. evapotransp. (mm)	122	113	130	122	117	87	70	77	94	118	118	121
6	δD_P [†]	-26	-28	-35	-27	-26	1	6	8	3	-12	-21	-36
	Precipitation (mm)	120	104	187	169	25	1	1	5	40	130	199	146
	Pot. evapotransp. (mm)	90	83	91	83	76	60	60	67	77	88	87	90
7	δD_P [†]	-34	-39	-48	-34	-33	5	2	5	-1	-15	-21	-44
	Precipitation (mm)	204	141	210	121	14	1	0	3	24	110	195	234
	Pot. evapotransp. (mm)	82	73	79	72	61	47	51	67	84	89	81	80
8	δD_P [†]	-34	-41	-50	-36	-34	8	2	4	-1	-12	-18	-44
	Precipitation (mm)	189.7	149	230	116	9.7	0.5	5.7	0.6	12	83	161	190
	Pot. evapotransp. (mm)	86	79	85	77	63	48	50	67	87	95	89	87
9	δD_P [†]	-30	-37	-43	-32	-29	13	4	4	1	-5	-12	-39
	Precipitation (mm)	128	145	162	56	2	0	0	0	2	29	76	88
	Pot. evapotransp. (mm)	115	96	100	89	65	43	45	66	96	125	124	121
10	δD_P [†]	-24	-29	-33	-23	-19	22	3	3	2	3	-6	-27
	Precipitation (mm)	73	86	75	21	2	0	1	0	1	10	24	38
	Pot. evapotransp. (mm)	119	99	101	86	59	37	36	52	84	110	118	120
11	δD_P [†]	-27	-29	-33	-21	-13	26	-5	-4	-2	3	-6	-23
	Precipitation (mm)	77	89	73	35	6	2	2	1	3	12	27	30
	Pot. evapotransp. (mm)	110	86	82	61	42	27	28	42	66	88	98	113
12	δD_P [†]	-27	-29	-33	-21	-13	26	-5	-4	-2	2	-6	-23
	Precipitation (mm)	54	74	59	20	5	2	1	1	2	8	20	22
	Pot. evapotransp. (mm)	105	85	82	61	44	29	30	43	64	85	93	108
13	δD_P [†]	-19	-21	-21	-18	-14	5	-10	-9	-5	-3	-8	-17
	Precipitation (mm)	11	20	27	14	5	6	6	2	3	7	6	9
	Pot. evapotransp. (mm)	147	125	114	74	42	25	23	33	51	82	109	146

[†] Bold face values were used for the calculation of growing season δD_P .

Danksagung

Die vorliegende Arbeit ist durch die Anleitung, Mitarbeit und Unterstützung vieler Menschen möglich geworden. An erster Stelle gilt mein Dank Prof. Dr. J. Rullkötter für die interessante Themenstellung, das mit entgegengebrachte Vertrauen und seine Unterstützung. Seine Fragen und Anregungen waren eine wertvolle Hilfe bei Tagungsbeiträgen, Publikationen und bei der Anfertigung dieser Arbeit. Prof. G. Englington, dem „Großvater“ der Alkanforschung, danke ich für seine Bereitschaft das Zweitgutachten zu übernehmen und für die fruchtbaren Diskussionen insbesondere im Rahmen der Zusammenarbeit bei der Vorbereitung des Plenarvortrages für die IPC3 Konferenz in London. Großer Dank geht auch an die „großen Brüder“ dieser Arbeit, Dr. F. Rommerskirchen und Dr. E. Schefuß, denen ich für ihre ständige Diskussionsbereitschaft und die Unterstützung bei den Publikationen danke. Auch den jüngeren Geschwistern der Alkanforscherfamilie T. Badewien und H. Moossen gilt mein Dank für die gute Zusammenarbeit.

A very big „THANK YOU“ to the whole alkane family!

Ich danke weiterhin Dr. R.W. Mayes (Macaulay Institute, Aberdeen, UK), Dr. L. Dupont (Universität Bremen), E. Marais (Nationalmuseum, Namibia) und Prof. M. Sosef, F. Aleva sowie Dr. J.J. Wieringa (Universität Wageningen, Niederlande) für die Hilfe bei der Auswahl und die Bereitstellung von Pflanzenmaterial. Danken möchte ich auch Dr. M. Zabel für die Unterstützung bei Auswahl und Auffinden der Sedimentproben sowie den Organisatoren und Fahrteilnehmern der Ausfahrten M34/2 und M41/1 des Forschungsschiffs Meteor. Weiterhin danke ich C. Still und R. Powell für die Bereitstellung der Abbildung über die Häufigkeit der C₄ Pflanzen in Afrika.

Weiterhin möchte ich mich herzlich bei den Mitgliedern der AG Organische Geochemie, insbesondere bei Dr. B. Scholz-Böttcher und Dr. J. Köster, und bei der Familia Geochimica für die vielen nützlichen Diskussionen bedanken. Ganz besonderer Dank geht an B. Kopke, A. Müllenmeister, R. Grundmann und C. Versteegen die stets Labore und Equipment in Schuss hielten und bei der Lösung praktischer Probleme halfen. Diese Arbeit wurde zudem in dankenswerter Weise unterstützt durch die praktischen Laborarbeiten der der Auszubildenden S. Einert, A. Beqiray, S. Schüler, I. Ulber und H. Haase. Dr. C. März und Dr. F. Rommerskirchen danke ich für die schnelle Bereitstellung von Fachliteratur, die mir ansonsten nur schwer zugänglich gewesen wäre.

Schließlich möchte ich mich bei der AG Organische Geochemie und der Familia Geochimica auch für das persönliche Arbeitsumfeld und die Zerstreuung durch Veranstaltungen außerhalb des üblichen Arbeitsalltags bedanken. Insbesondere danke ich den Kollegen Dr. M. Beck, Dr. P. Böning, Dr. J. Fichtel, Dr. A. Hetzel, S. Kohls und Dr. C. März, die aktiver Teil des zeitweise anoxischen aber stets netten Büroklimas waren.

Meiner Familie, insbesondere meinen Eltern, sowie meinem Michael danke ich für den Rückhalt und die Unterstützung. Ohne sie wäre es mir weitaus schwerer gefallen, diesen Weg zu gehen.

Der Deutschen Forschungsgemeinschaft gilt mein Dank für die finanzielle Förderung dieses Projektes.

Lebenslauf

Name: Angela Vogts
Geburtsdatum: 22. März 1978
Geburtsort: Westerstede
Staatsangehörigkeit: deutsch
Familienstand: ledig

Schulbildung:

1984 - 1988 Grundschule Wiefelstede
1988 - 1990 Orientierungsstufe Wiefelstede
1990 - 1997 Gymnasialzweig der Kooperativen Gesamtschule Rastede (Abitur)

Berufsausbildung:

1997-2000

Ausbildung zur Chemielaborantin, Fachrichtung Chemie, am Institut für Futtermitteluntersuchung der Landwirtschaftlichen Untersuchungs- und Forschungsanstalt Weser-Ems, Oldenburg

WiSe 2000 – SoSe 2006

Studium Chemie (Diplom) an der Carl von Ossietzky Universität Oldenburg

Vordiplom: 07.04.2003

Diplomarbeit am Institut für Chemie und Biologie des Meeres der Carl von Ossietzky Universität Oldenburg, Thema: Molekulare und Kohlenstoffisotopenzusammensetzung geochemisch bedeutsamer Pflanzenbestandteile

Diplom: 08.05.2006

Seit WiSe 2006

Promotionsstudentin an der Carl von Ossietzky Universität Oldenburg am Institut für Chemie und Biologie des Meeres im Rahmen des DFG-Projektes „Wachsalkane und -alkohole in Ozeansedimenten als Indikatoren kontinentaler Klimaveränderungen – Validierung eines molekularen Parameters“

Erklärung

Hiermit versichere ich, dass ich die vorliegende Arbeit selbstständig angefertigt und keine anderen als die angegebenen Quellen und Hilfsmittel verwendet habe. Zusätzlich erkläre ich, dass diese Dissertation weder in ihrer Gesamtheit noch in Teilen einer anderen wissenschaftlichen Hochschule zur Begutachtung in einem Promotionsverfahren vorliegt oder vorgelegen hat.

Oldenburg,

(Angela Vogts)